



Scalable Manufacturing of Energetic Materials for Integrated Systems

**Stephen Tse, Alberto Cuitino, Fernando Muzzio,
Assimina Pelegri, and Bernard Kear**

School of Engineering, Rutgers University
Piscataway, NJ 08854

Inaugural Meeting of the National Energetic Materials Consortium
Texas Tech University
13 October 2015

Outline

- **Nanowire Synthesis of NanoEnergetics**
- **Nanoparticle Synthesis of Cubic Boron Nitride**
- **In-situ Laser-Based Diagnostics**
- **Graphene Synthesis**
- **Characterization and Continuous Automation of an Environmentally Green Primer**

The image features a solid red background. In the top left corner, the word "RUTGERS" is written in a large, white, serif font. Below it, in a smaller, white, sans-serif font, are the words "THE STATE UNIVERSITY OF NEW JERSEY". A large, faint, circular seal of Rutgers University is visible in the background, centered behind the text. The seal contains the text "RUTGERS THE STATE UNIVERSITY" around its perimeter and a central emblem.

RUTGERS
THE STATE UNIVERSITY
OF NEW JERSEY

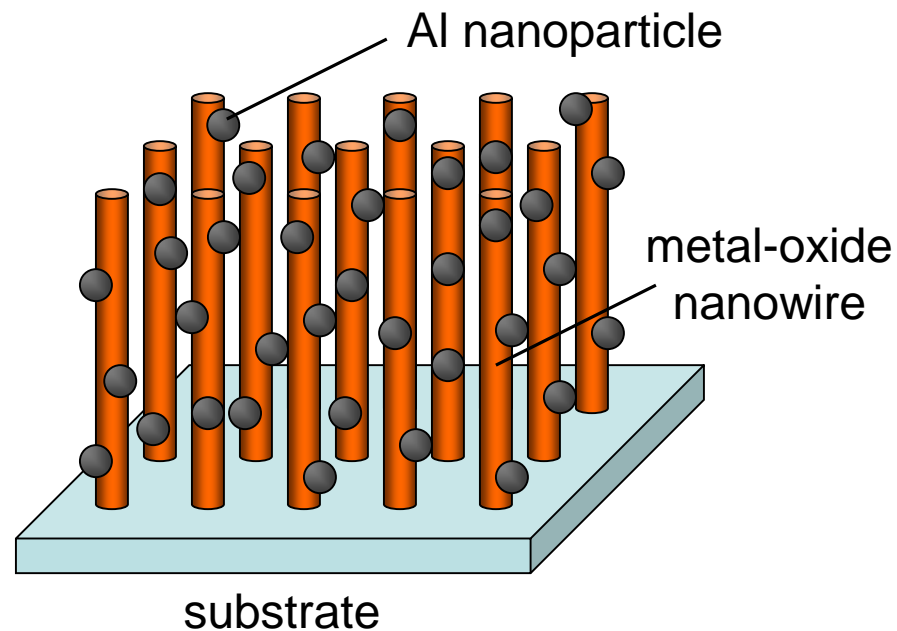
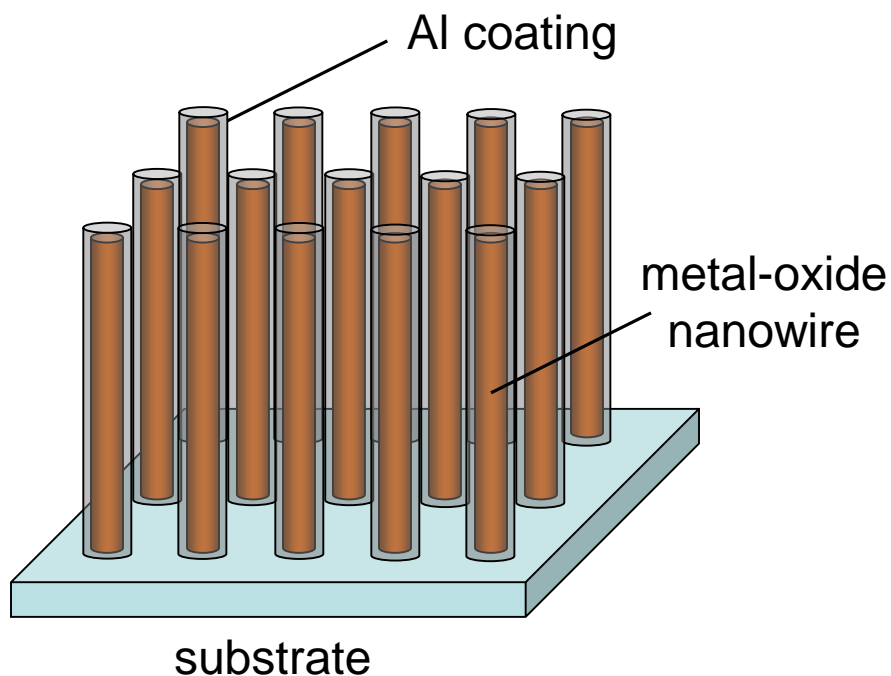
Nanowire Synthesis

Relevance -- Nanowires

- Robust materials with improved properties are needed for structural, functional, and device applications
- Of strong interest are functional one-dimensional nanostructures due to their unique and innovative applications in optics, optoelectronics, catalysis, and piezoelectricity
- Semiconducting oxide nanowires constitute a unique group of 1D nanomaterials, which have well-defined and uniform shapes, stable surfaces, and single-crystal volumes
- These properties are keys to nanoelectronic applications like use as field effect transistors, ultra-sensitive nano-size gas sensors, nanoresonators, and nanocantilevers

Relevance -- Nanowires

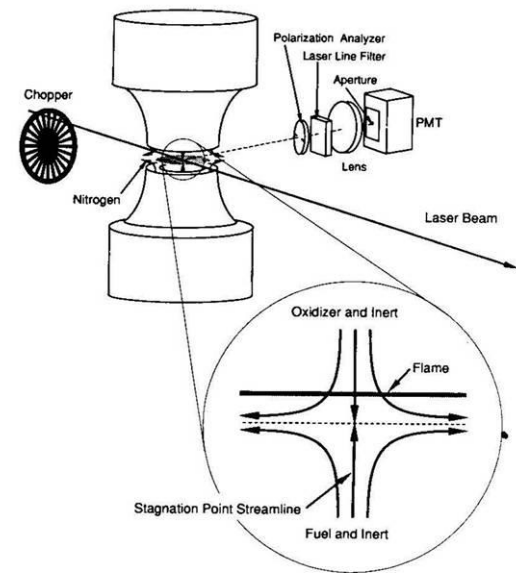
- Moreover, nanowires of MoO_3 , CuO , WO_3 , Fe_2O_3 , Bi_2O_3 , and MnO_2 can be exploited for tailored heat release in nano-energetic applications involving thermite reactions with nano-Al



Motivation

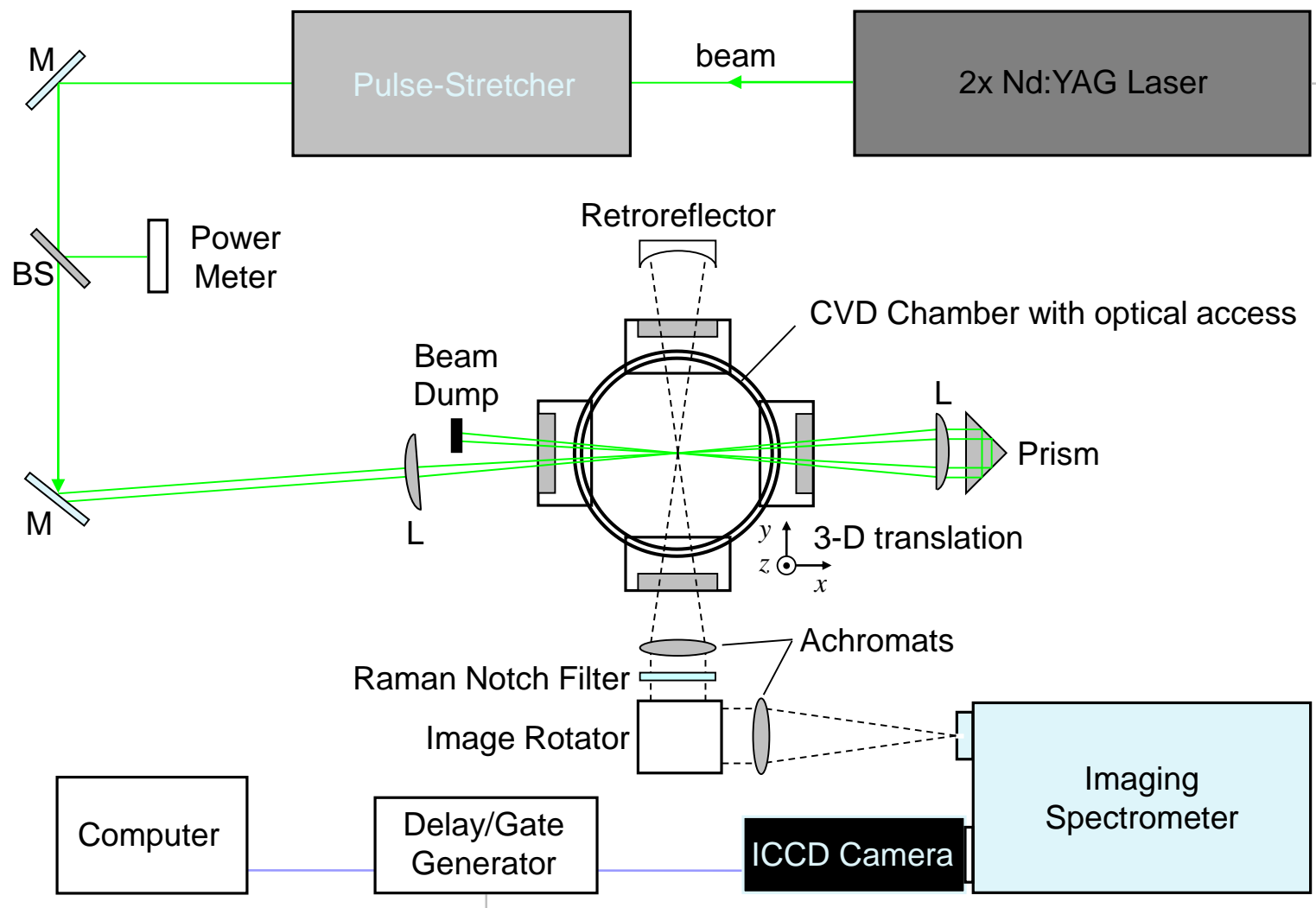
- Many approaches have been used to prepare nano-wires/rods, such as vapor-liquid-solid growth, solution-liquid-solid methods, template mediate growth, electron beam lithography, and scanning tunneling microscopy techniques
- However, these methods can be complex, involving pretreatment, catalysts, and vacuum systems, while still characterized by low single-nanowire growth rates and low total yield densities
- Consequently, studies on nanoscale materials and their applications are presently limited due to lack of easy processes for high- rate, yield, purity, and orientation synthesis of such materials
- The growth of metal-oxide nanowires over large areas remains especially challenging

Quasi 1-D Flame



Counterflow Diffusion Flame

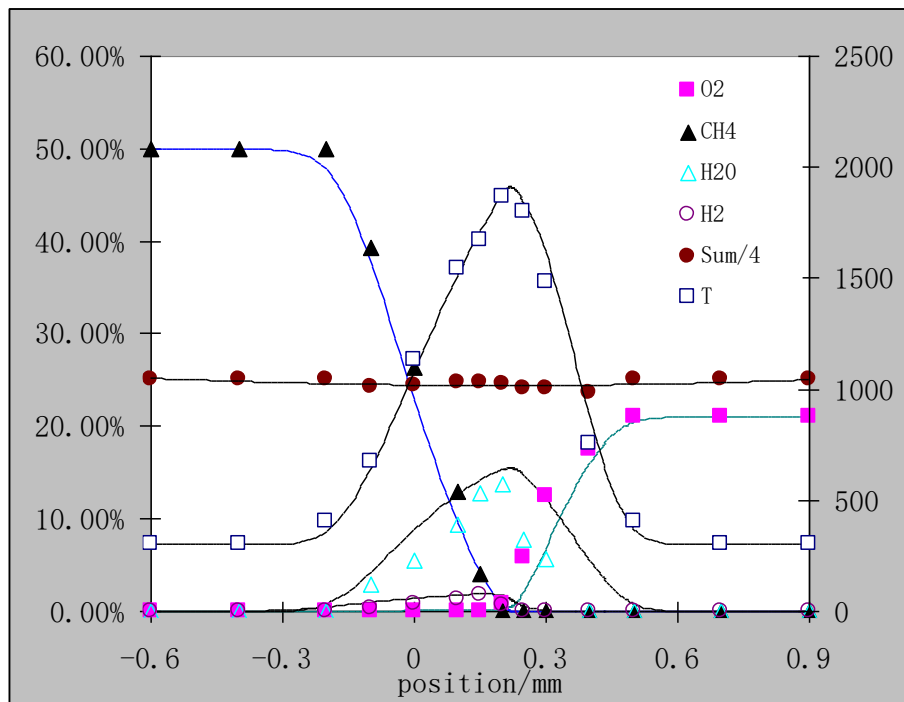
Spontaneous Raman Spectroscopy



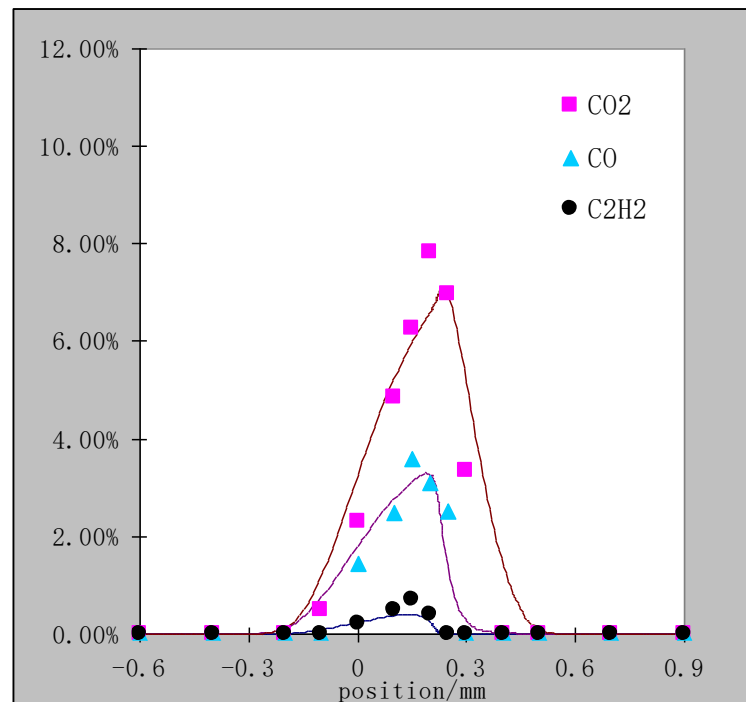
Gas-Phase Simulation

- Axi-symmetric counterflow diffusion flame code
- GRI-Mech 1.2 (32 species, 177 reactions)
- Transport properties computed with CHEMKIN subroutines
- Boundary conditions at burners specify plug flow inlet mass flux and temperature

Flame Structure Validation (Raman)

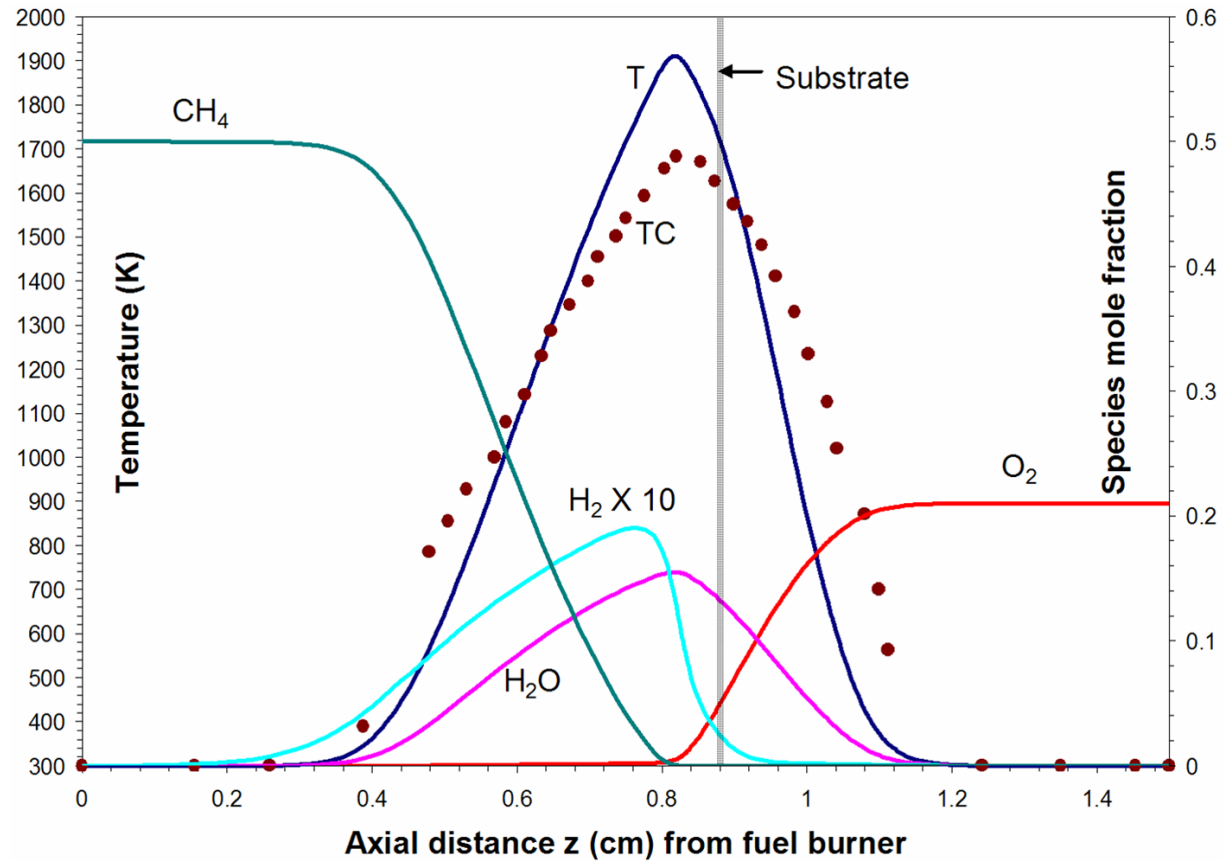
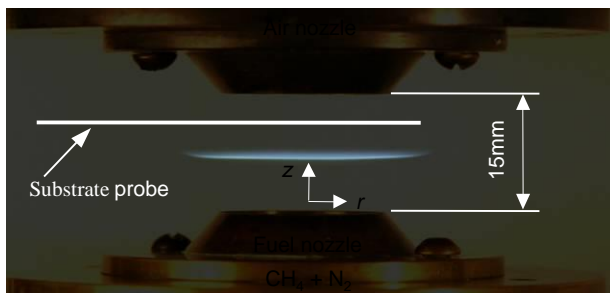


Temperature & major species

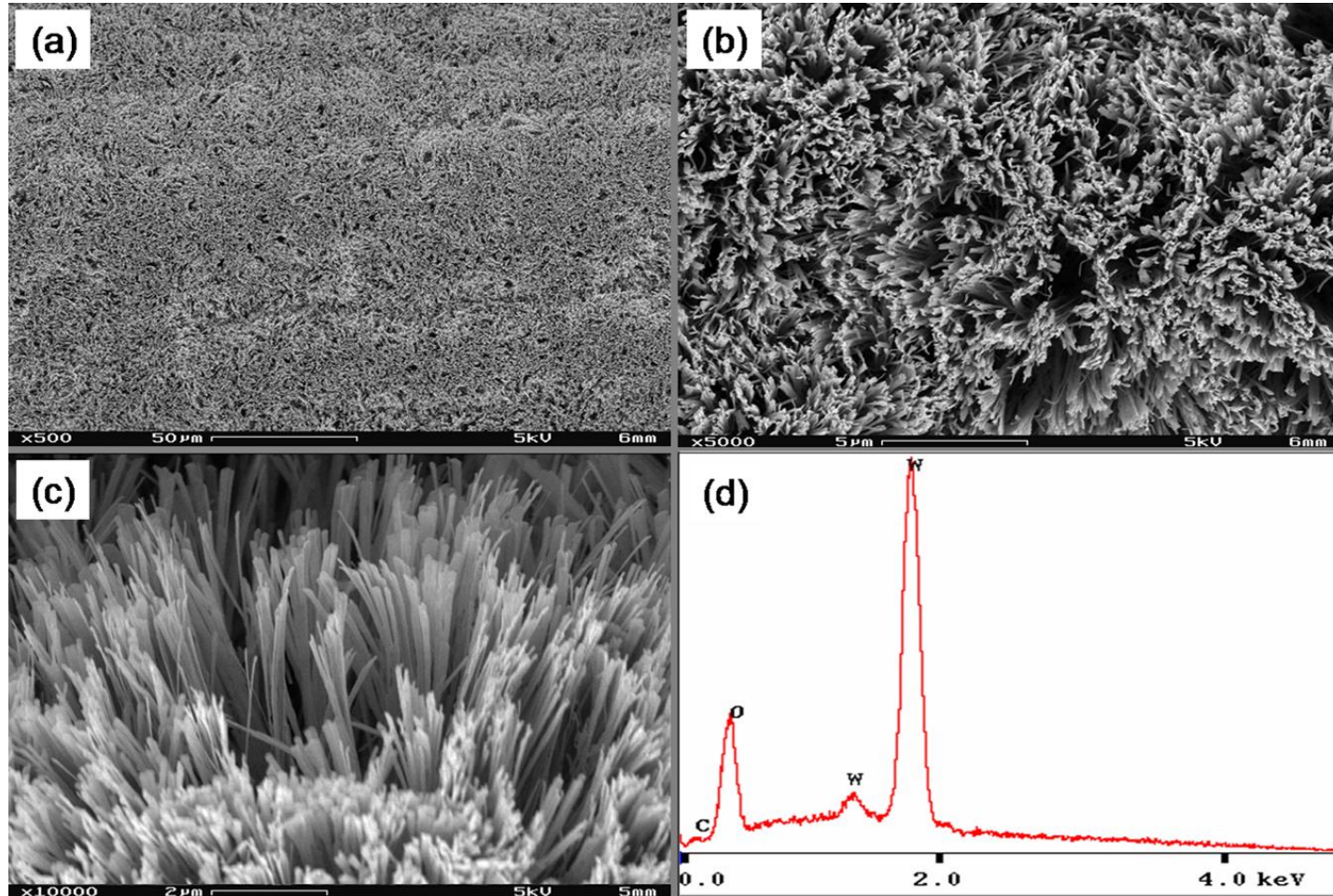


With correction from interference from C-containing radicals

Experiment and Flame Structure

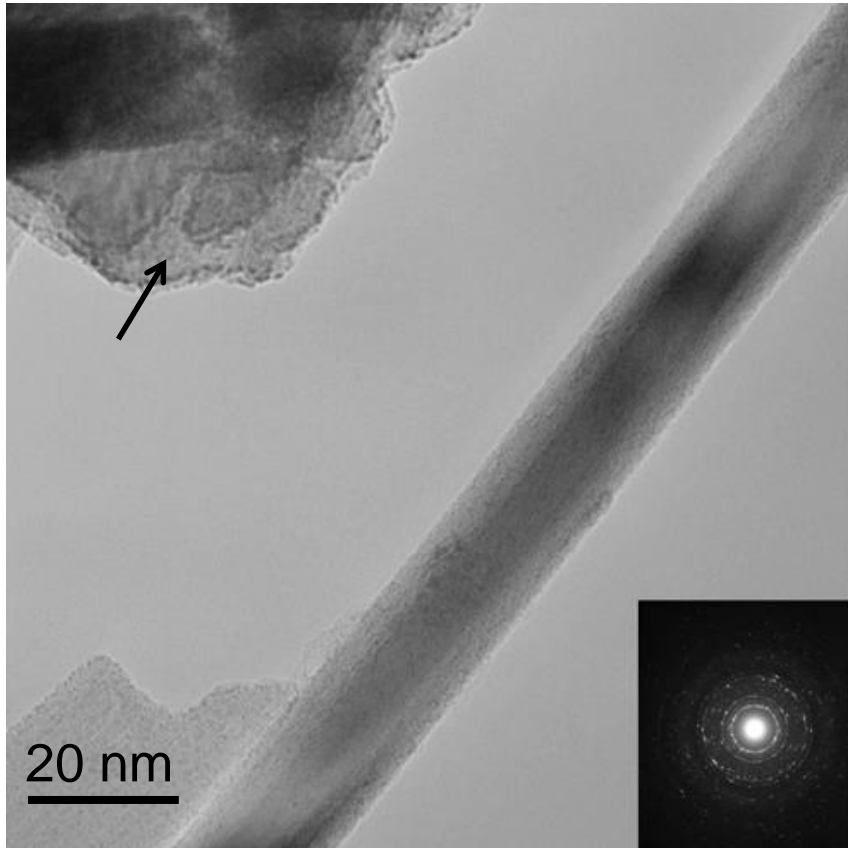


Aligned Tungsten-Oxide Nanowires



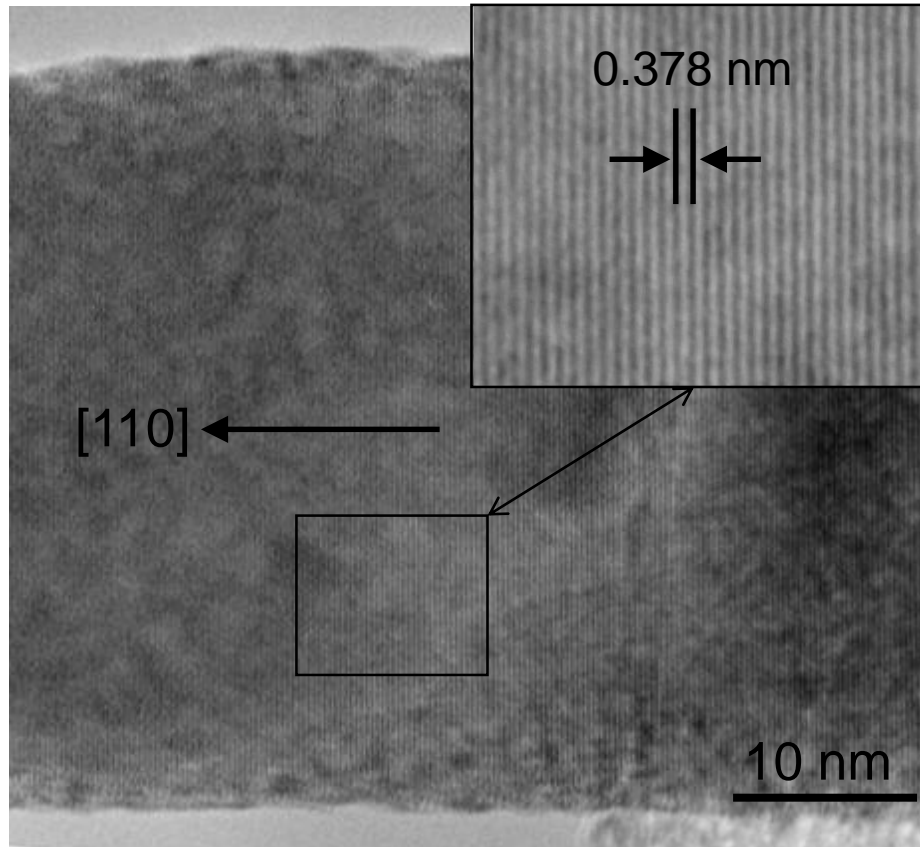
- Dense yield of nanomaterials grown directly on a tungsten substrate
- Diameters of 20-50nm, lengths > 10 μm , 10min sampling duration
- EDX \rightarrow tungsten oxide

TEM of Tungsten Oxide ($\text{WO}_{2.9}$)



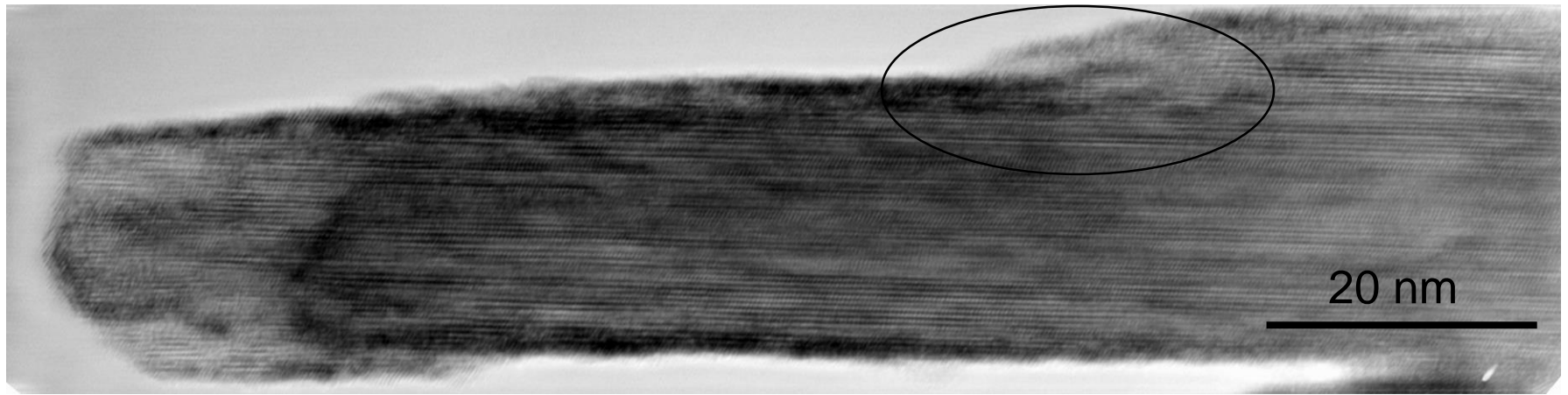
- Different crystal structures include: cubic and monoclinic WO_3 , tetragonal $\text{WO}_{2.9}$, and monoclinic $\text{W}_{18}\text{O}_{49}$
- Indexed SAED pattern with the first three highest intensities of 3.779\AA , 3.126\AA , and 2.67\AA match very well with the tetragonal phase of $\text{WO}_{2.9}$ with lattice constants of $a = 5.3\text{\AA}$, $b = 5.3\text{\AA}$, and $c = 3.83\text{\AA}$ (PDF card #18-1417)
- d -spacings correspond to $\{110\}$, $\{101\}$, and $\{200\}$, respectively

Crystallinity



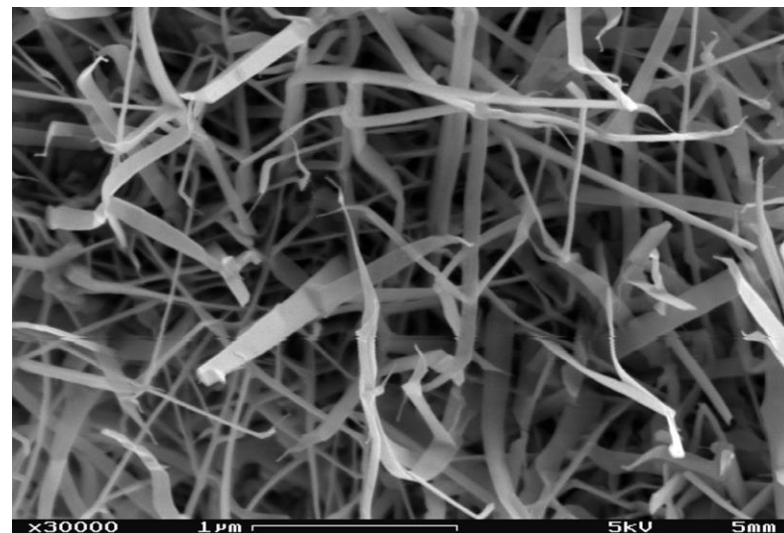
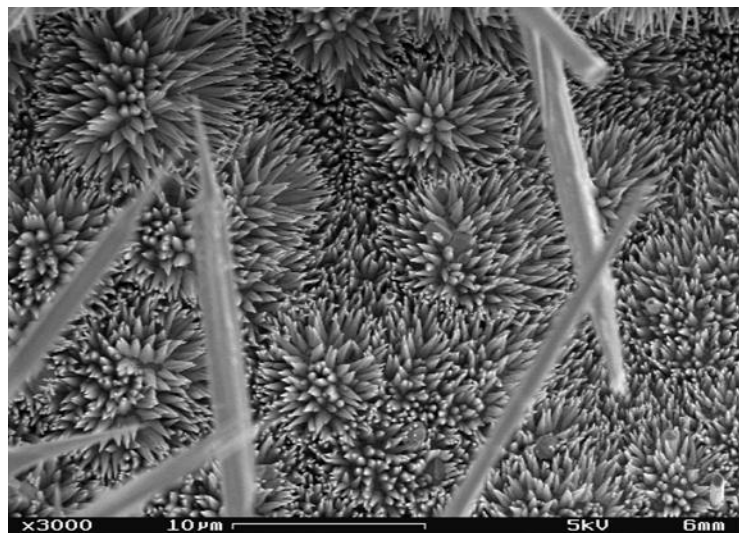
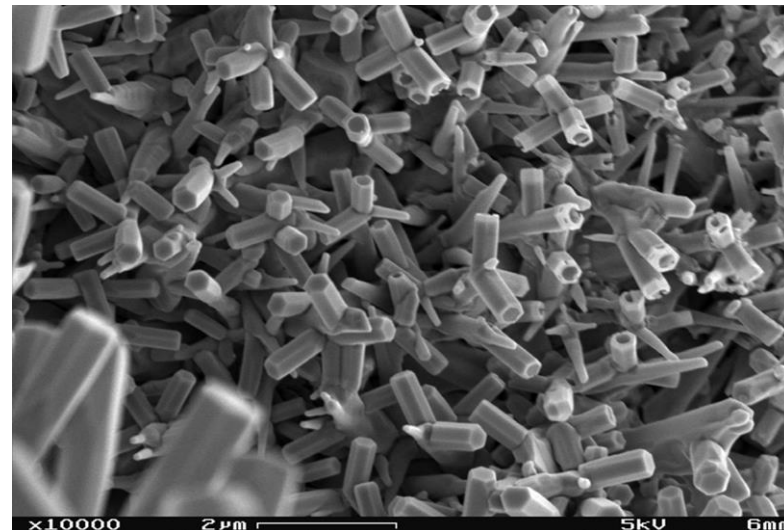
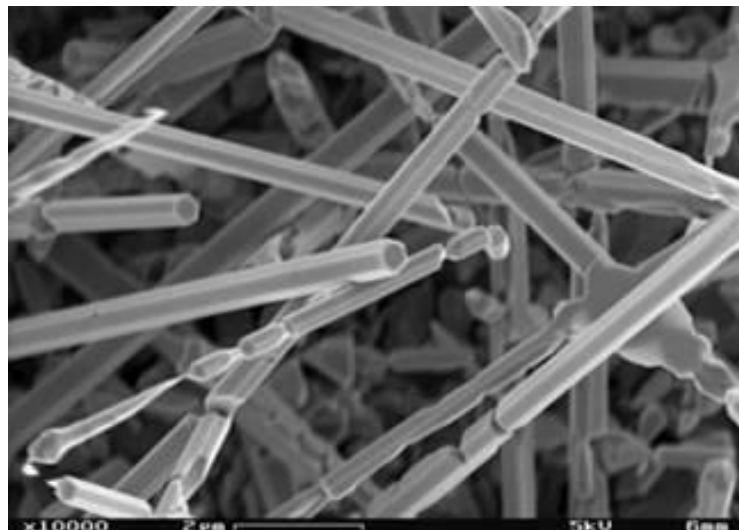
- Dislocation-free, single-crystalline
- 2-D Fourier transform pattern gives average spacing for lattice planes of 3.78\AA , which corresponds to the reflections from d -spacings of (110) planes of the tetragonal $\text{WO}_{2.9}$ phase
- Preferable growth along the [110] direction

Growth Mechanism

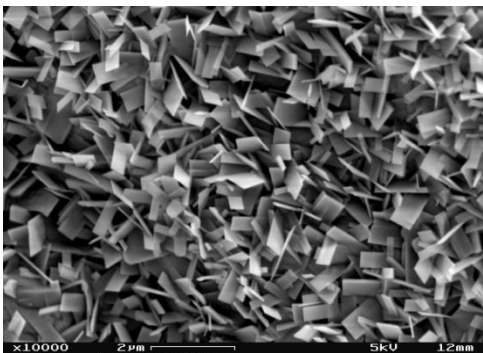
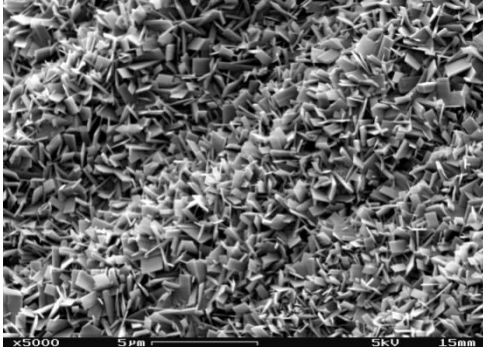


- Growth appears to be by vapor-solid (VS) mechanism
 - no metal nanoparticle at its tip (VLS)
 - thickening by a ledge-growth mechanism

Zinc Oxide

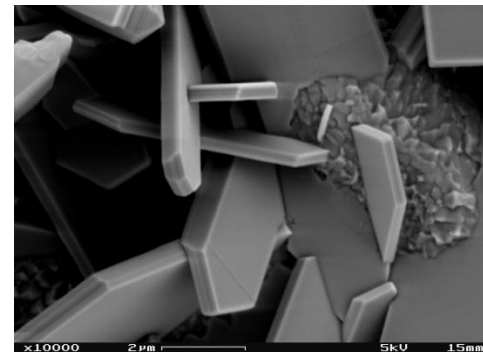
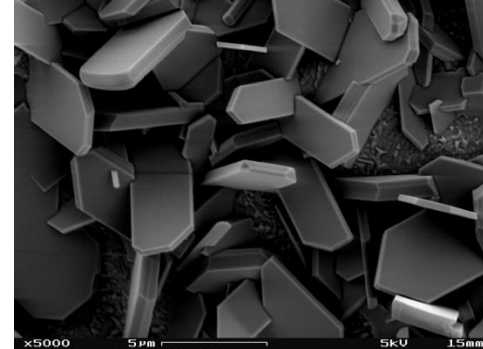


Molybdenum Oxide



Molybdenum oxide grown in the CH₄ flame on the air side (z=+.83cm) at low magnification (top) and high magnification (bottom)

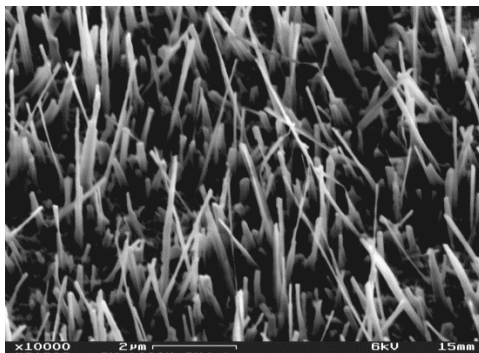
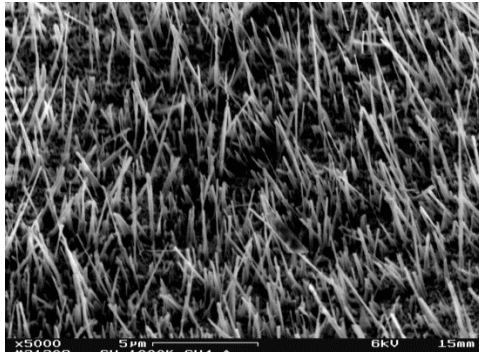
Air Side (2000K)



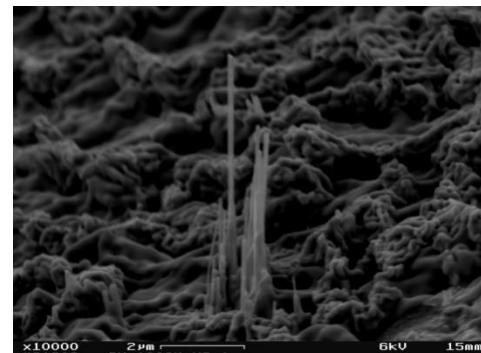
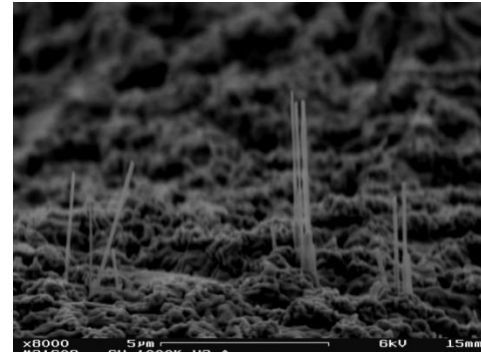
Molybdenum oxide grown in the H₂ flame on the fuel side at 5,000X (top) and 10,000X (bottom)

Fuel Side (2000K)

Copper Oxide

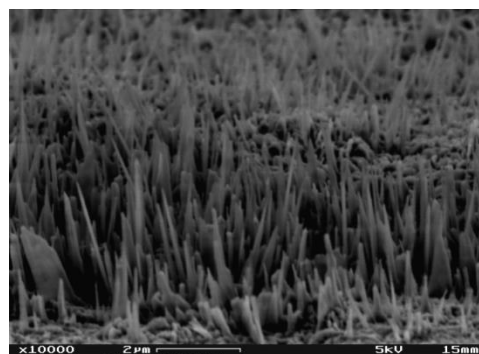
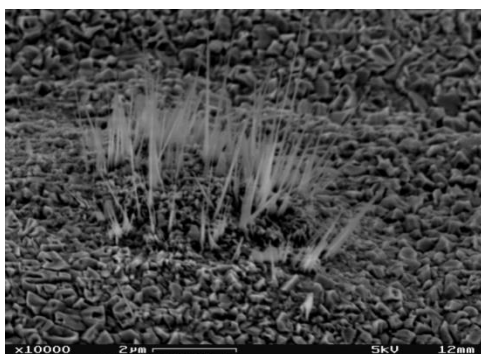
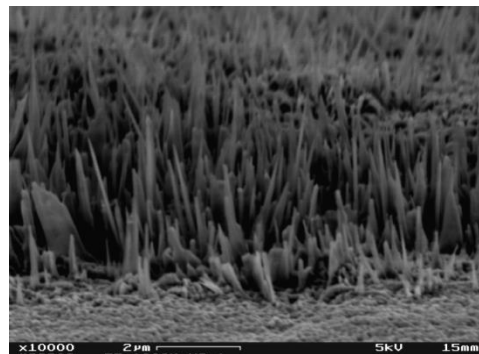
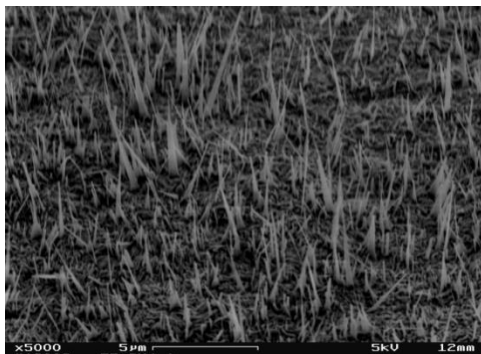


Low magnification copper oxide nanowires grown in a CH₄ flame (z=+0.97cm) (top)
Magnified FESEM image of nanowires grown in CH₄ (bottom)



Low magnification showing yield of copper oxide from H₂ flame (z=+0.97cm) (top)
Typical image of copper oxide grown in the H₂ flame (bottom)

Iron Oxide



Low magnification iron oxide nanowires grown in a CH₄ flame (top)
Magnified FESEM image of nanowires grown in CH₄ (bottom)

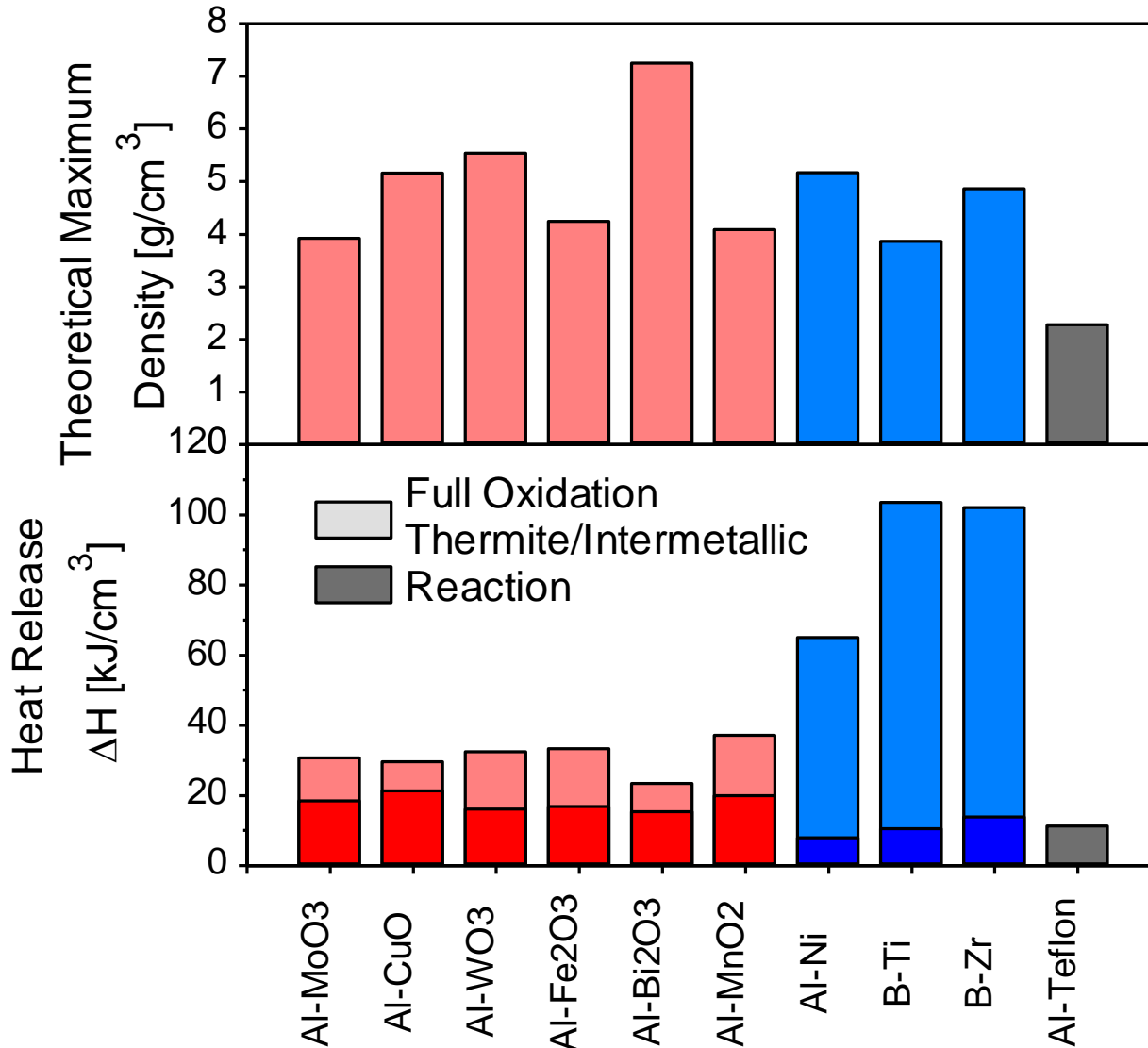
Low magnification showing dense yield of iron oxide from H₂ flame (top)
Typical image of iron oxide grown in the H₂ flame (bottom)

Air Side (1000K)

Energetics

- Nanoscale energetic materials have the potential for enhanced energy release and mechanical properties, versus their conventional counterparts
- Energetic nanomixtures and nanocomposites → e.g. Thermite reactions (Al/MoO₃, Al/CuO, Al/WO₃, Al/Fe₂O₃, Al/Bi₂O₃, and Al/MnO₂)
 - Based on intermolecular, rather than intramolecular, reactions, energetic nanocomposites require intimate mixing of the reactants on the nanometer length scale
 - The use of nanoscale structures enhance chemical kinetics due to their high surface area and short diffusion length
 - Given the proximity and uniformity of the fuel and oxidizer nanostructures, the final nanophase composite can be extremely dense in energy and capable of generating high power

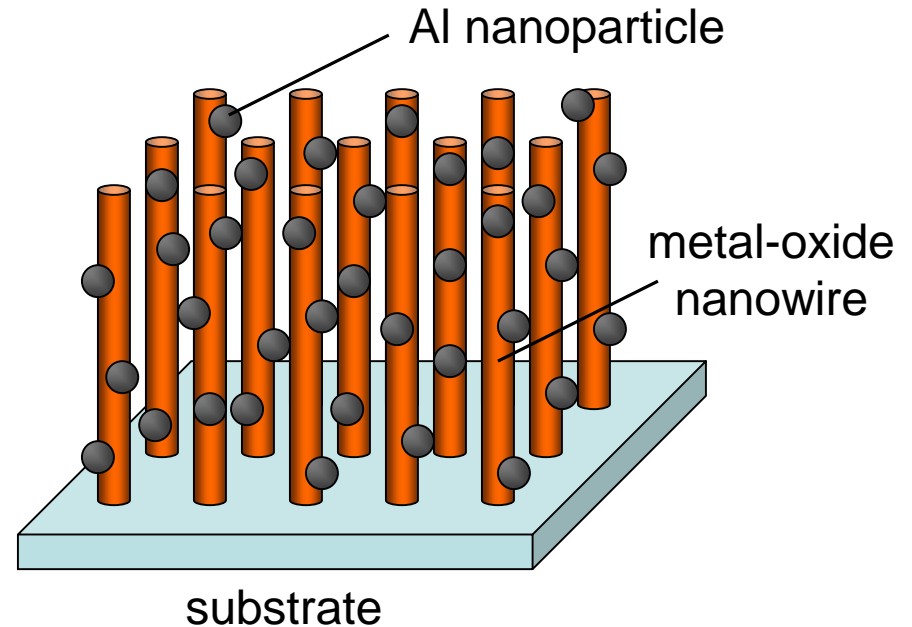
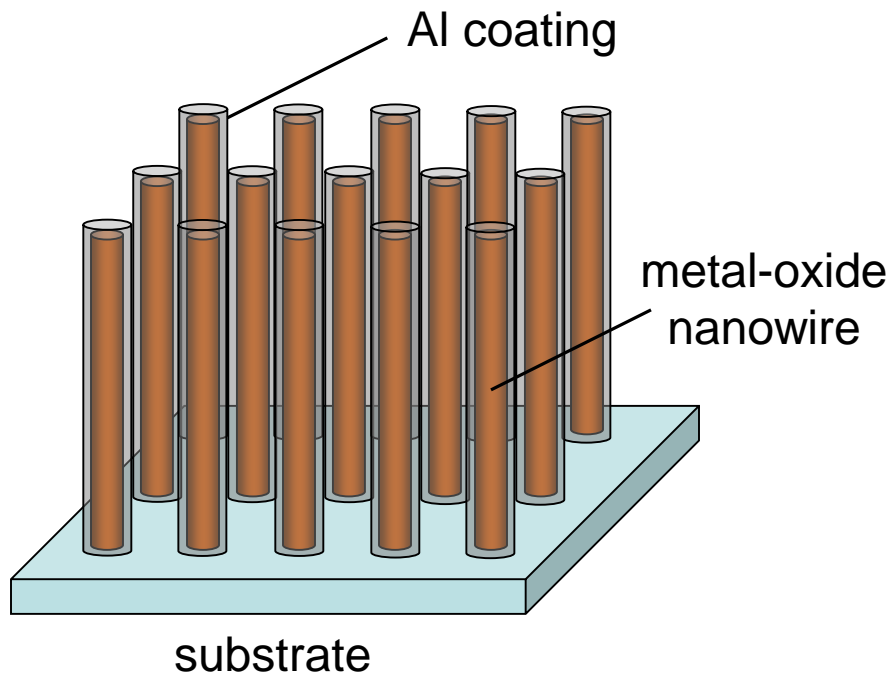
Densities and Reaction Enthalpies



- Wide range of material densities is readily available (Al-Teflon composite shown for comparison)
- Reaction enthalpies are very high
- Oxidation of the reaction products by ambient air adds significant combustion energy

Relevance -- Nanowires

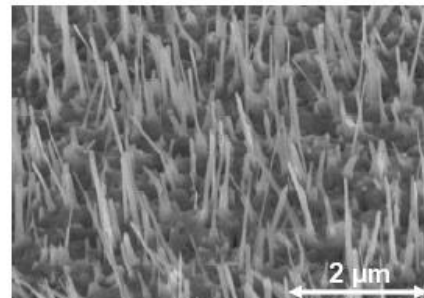
- Moreover, nanowires of MoO_3 , CuO , WO_3 , Fe_2O_3 , Bi_2O_3 , and MnO_2 can be exploited for tailored heat release in nano-energetic applications involving thermite reactions with nano-Al



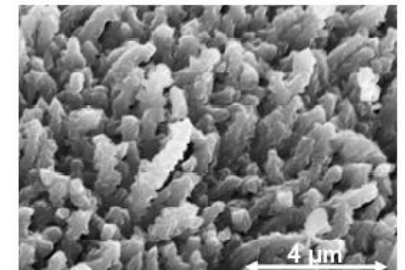
Nanoenergetic Materials for MEMS

- Zhang et al., *Applied Physics Letters*, 2007
 - Grew CuOx nanowires by thermal oxidation of electroplated Cu layer

r



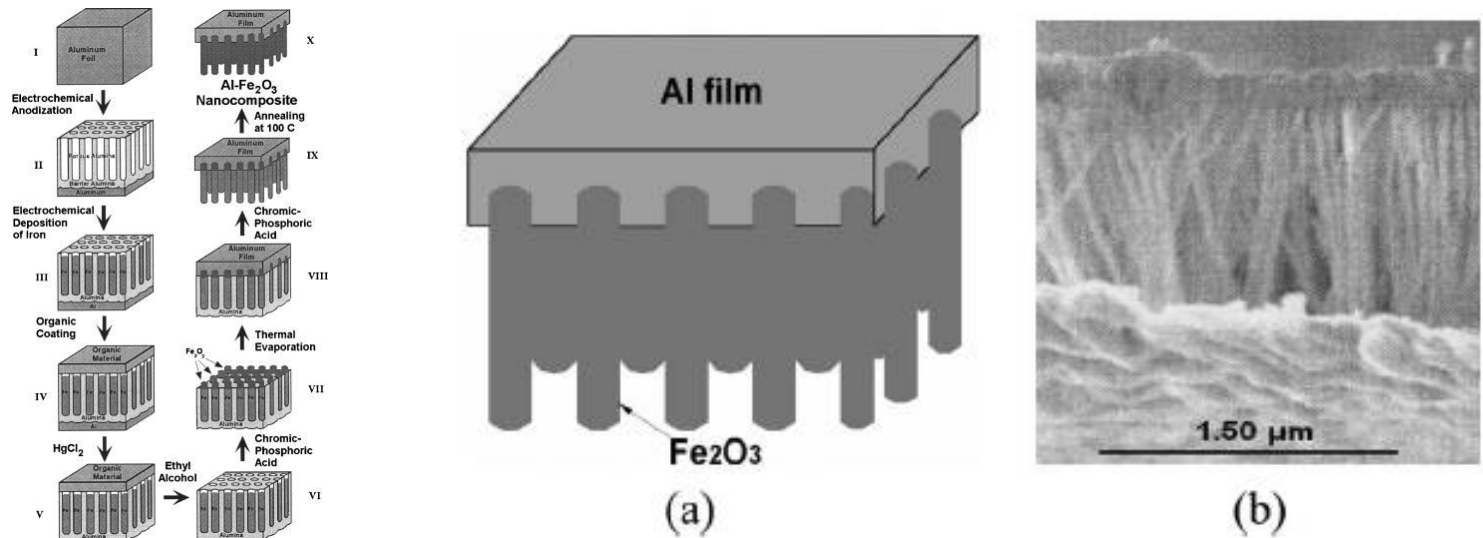
CuO nano-wires before aluminum deposition.



CuO nano-wires after aluminum deposition.

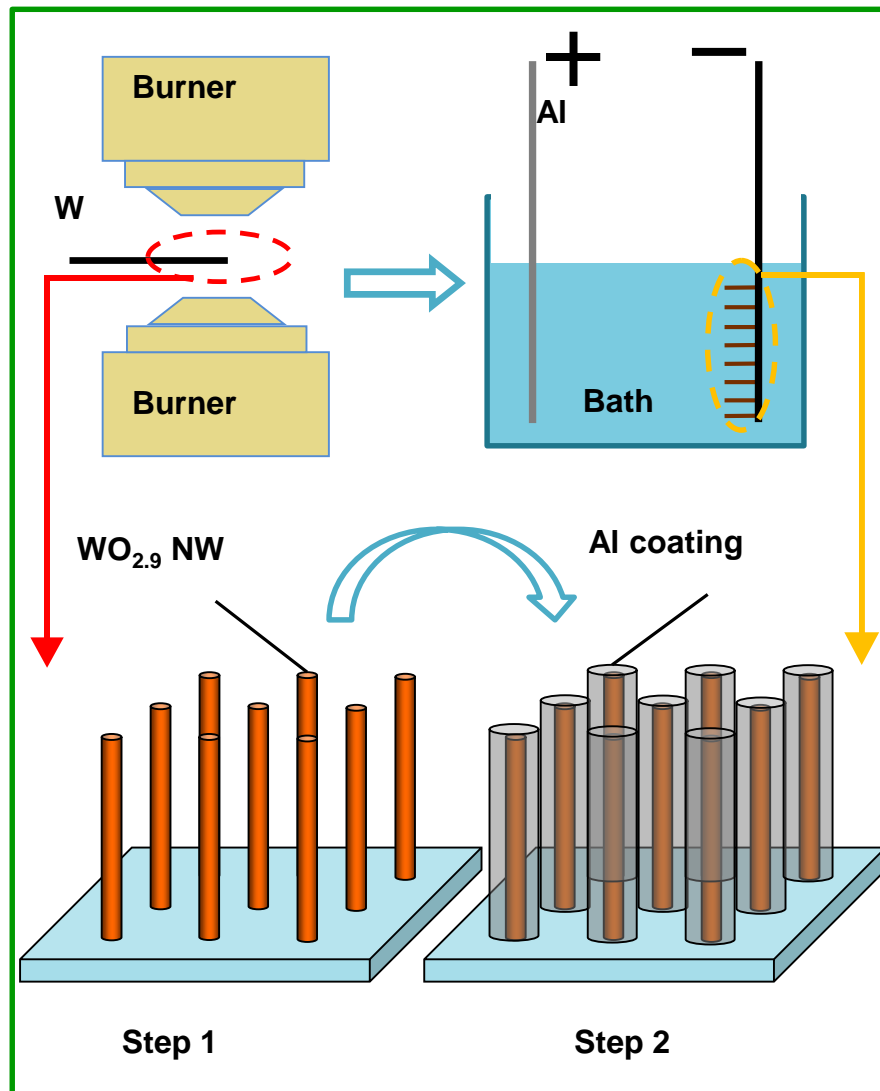
Nanoenergetic Materials for MEMS

- Menon et al., *Applied Physics Letters*, 2004
 - embedded an array of Fe_2O_3 nanowires inside a thin Al film



- (1) Electrochemical anodization of Al foil to form nanoporous alumina templates
- (2) Fe nanowire fabricated inside nanopores by electrochemical deposition
- (3) Etching of alumina walls to reveal Fe nanowires
- (4) Fe nanowires oxidized into Fe_2O_3 nanowires by annealing

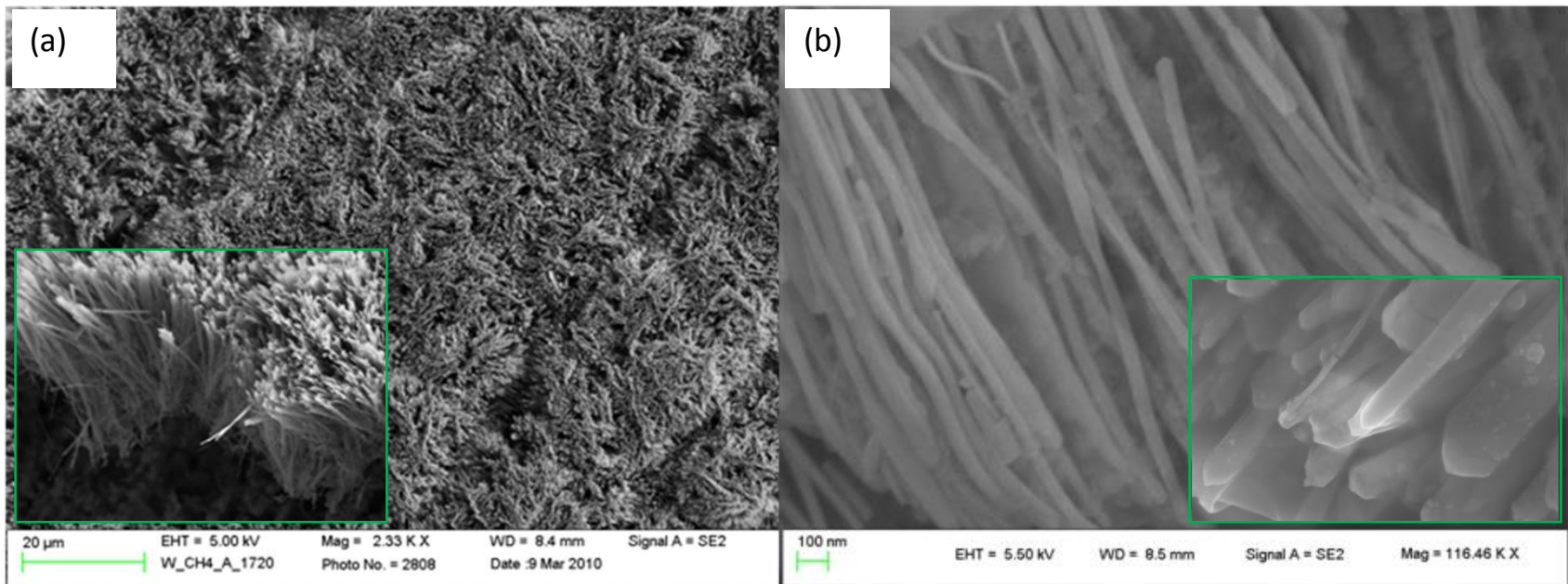
Experiment Set-up



Electrodeposition Procedure

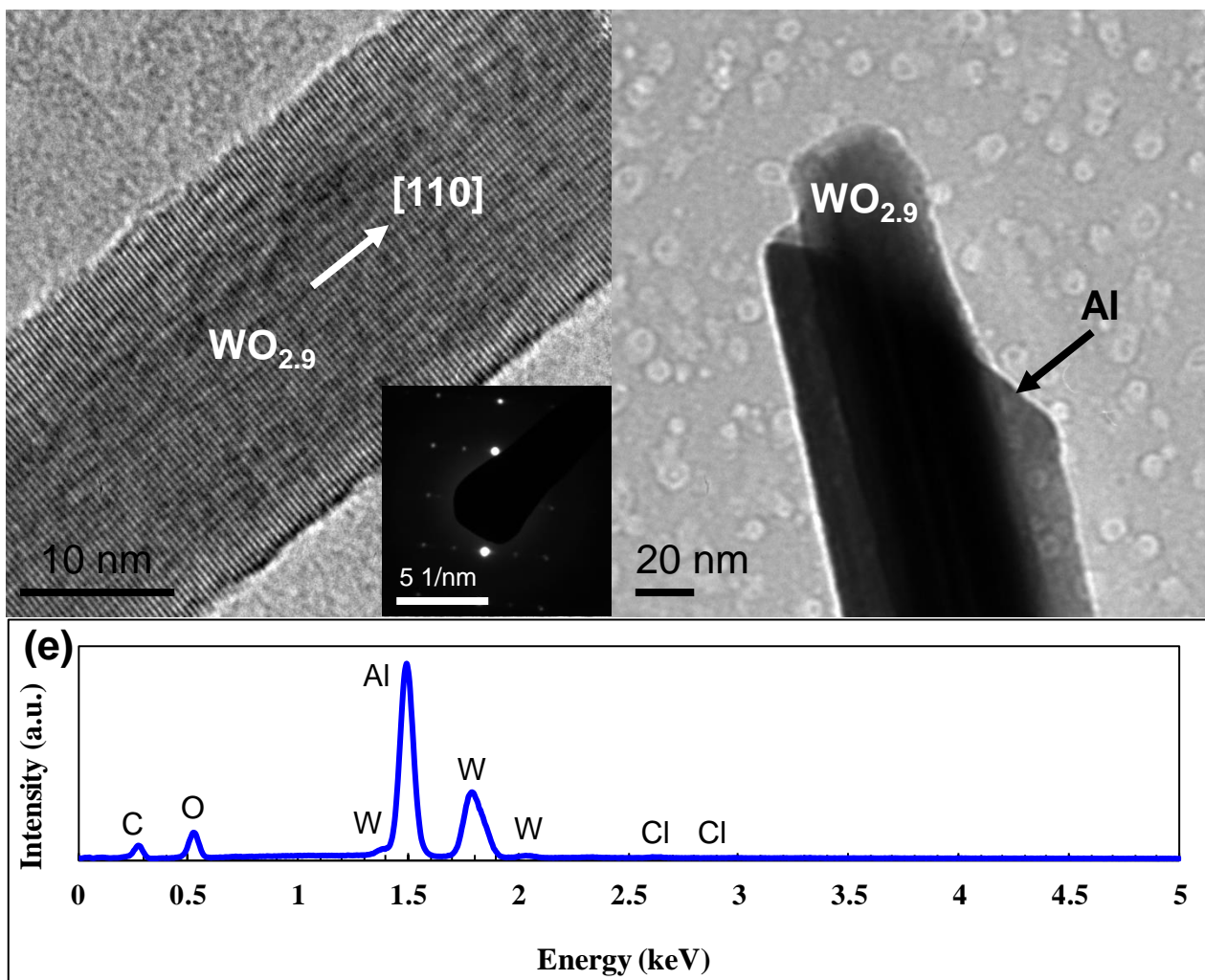
- Tungsten oxide nanowires array fabricated by flame synthesis method.
- Al layer with thickness of $\sim 16\text{nm}$ directly deposited on the surface of $\text{WO}_{2.9}$ nanowires by the ionic-liquid electrodeposition method under an inert atmosphere.
- A 1.5:1 molar ratio of aluminum chloride and 1-ethyl-3-methylimidazolium chloride ionic liquids were employed as the electrolyte at room temperature.
- The working electrodes were a tungsten wire with $\text{WO}_{2.9}$ nanowires grown on its surface and an aluminum wire. A potential of -1.5 V DC was applied for 15 minutes to fabricate the desired coaxial $\text{WO}_{2.9}/\text{Al}$ nanowires.

Morphology

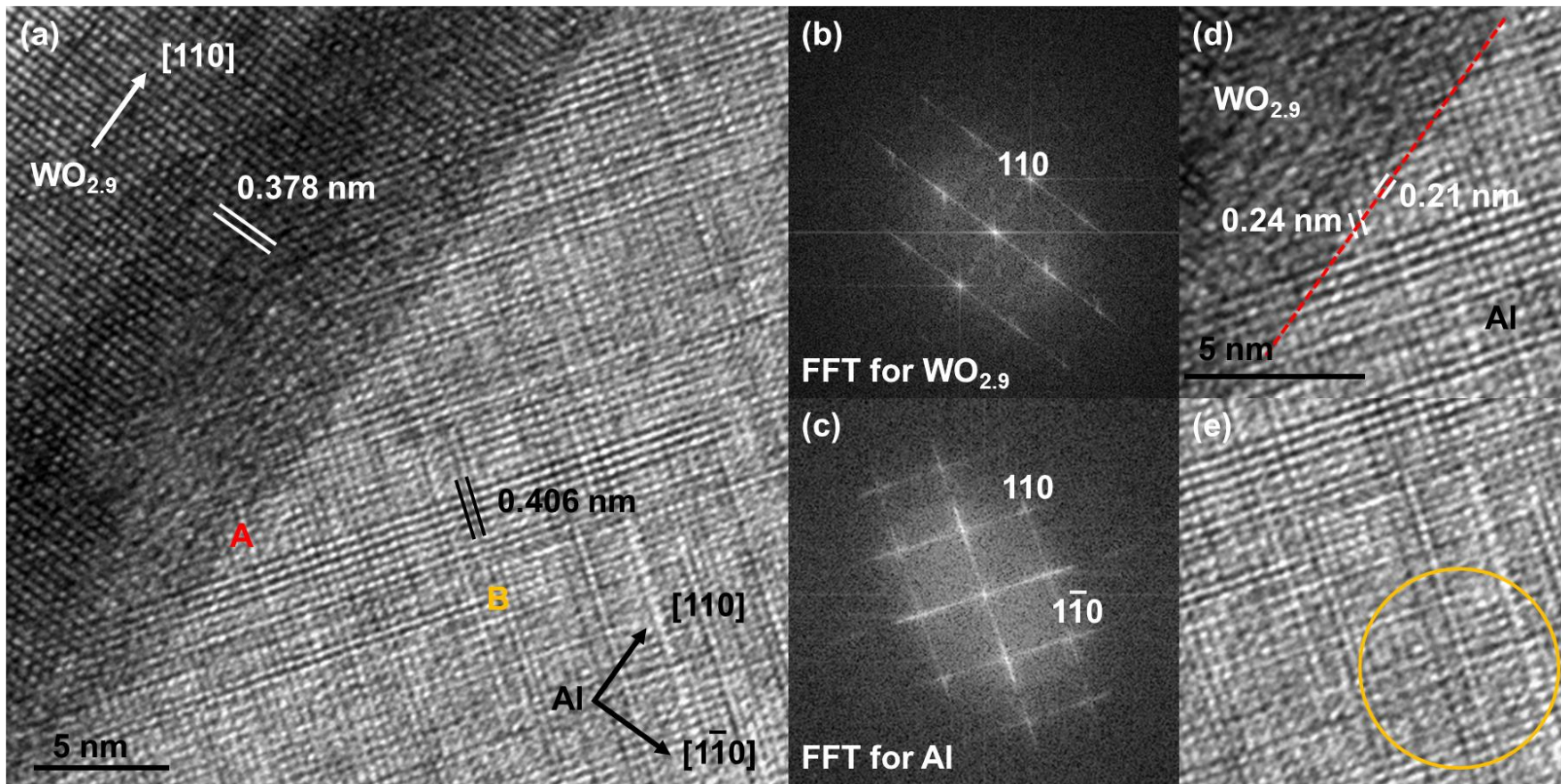


- (a) Low magnification FESEM image of as-synthesized tungsten oxide nanowires array by flame synthesis method and side-view image of the array showing well-aligned vertical growth (insert).
- (b) Low magnification FESEM image of as-grown $WO_{2.9}/Al$ coaxial nanowires after electrodeposition and high magnification FESEM image of the coaxial nanowires (insert).

Morphology and Elemental Composition

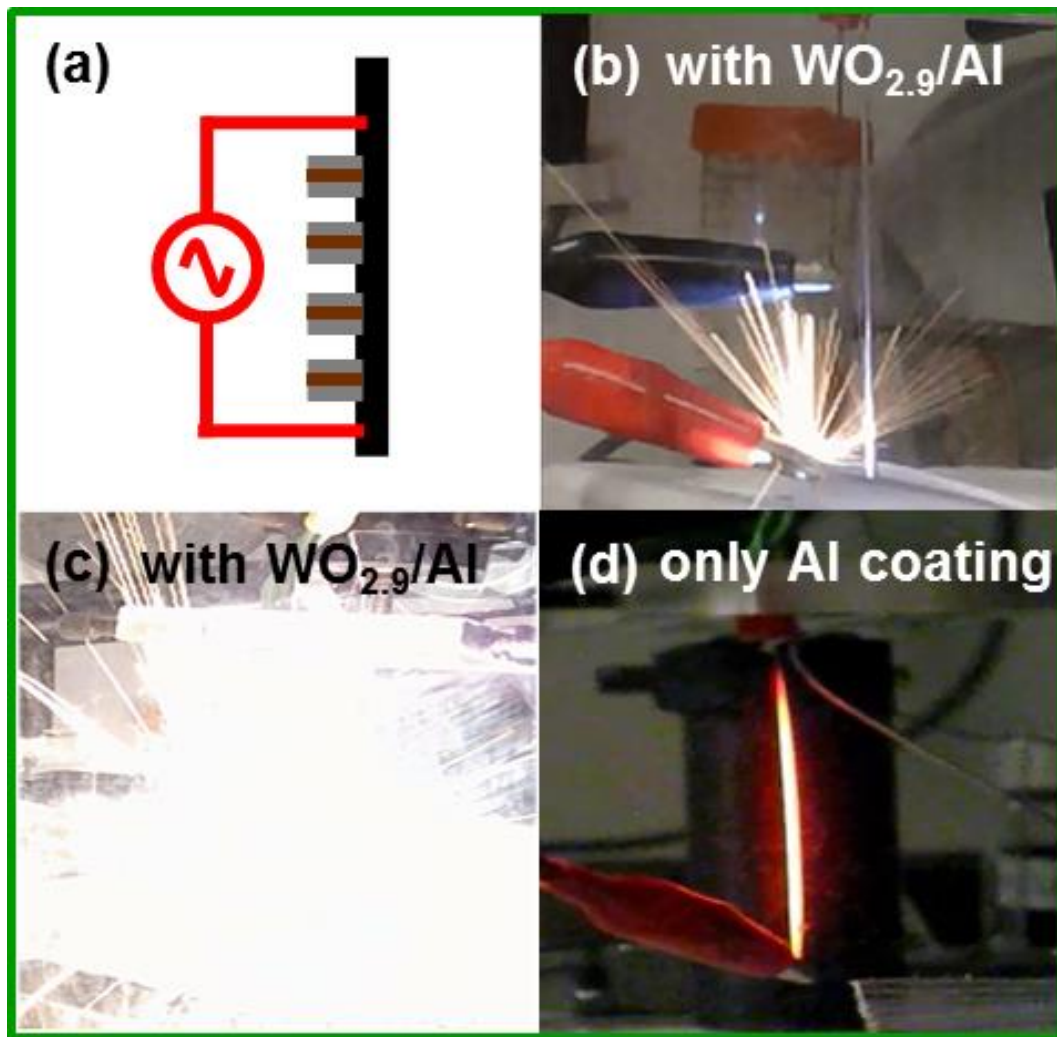


HRTEM Structure Characterization

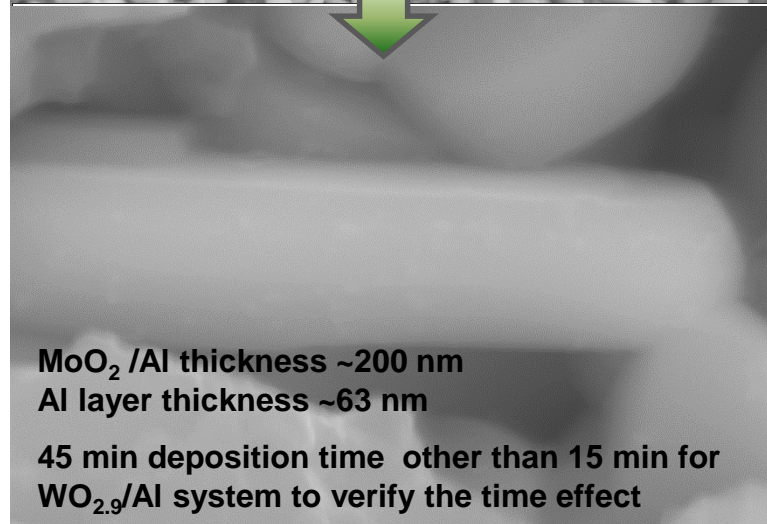
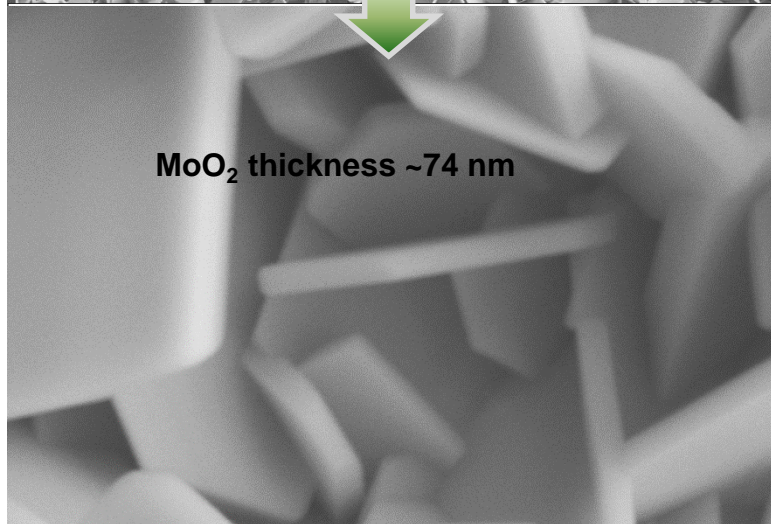
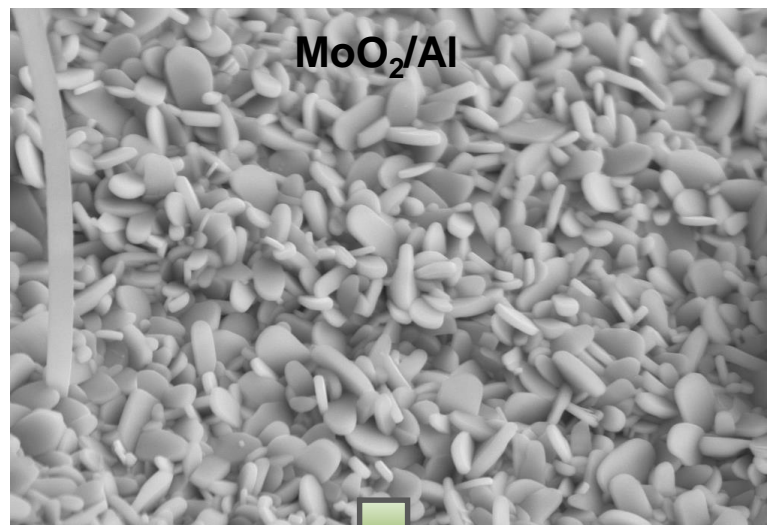


- Atomically abrupt interface
- Transition monolayer

Combustion Reaction



Al-Coated MoO₂ Nanoplates



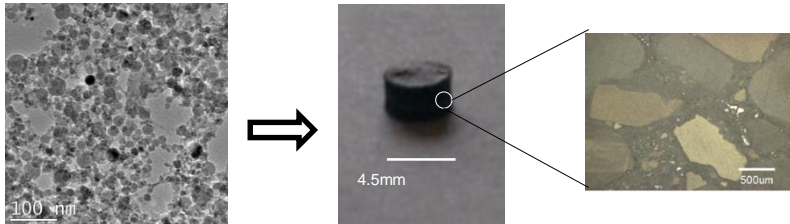
200 nm* EHT = 5.50 kV Mag = 140.24 K X WD = 6.5 mm Signal A = SE2

200 nm EHT = 15.00 kV WD = 8.5 mm Signal A = SE2 Mag = 112.84 K X

Nanoparticle Synthesis of Cubic Boron Nitride

Nanocrystalline Cubic Boron Nitride

Nanocrystalline Cubic Boron Nitride Monolith



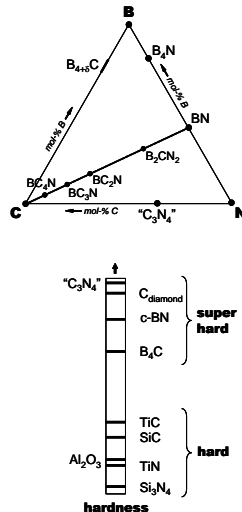
Synthesis of $< 20\text{nm}$ nanoparticles of metastable (high-pressure, extended solid phase) cubic boron nitride (c-BN)

95% c-BN 17nm grain bulk sample

Self nanocomposite of superhard (extended solid - cubic) and tough (equilibrium - hex) nanograined phases

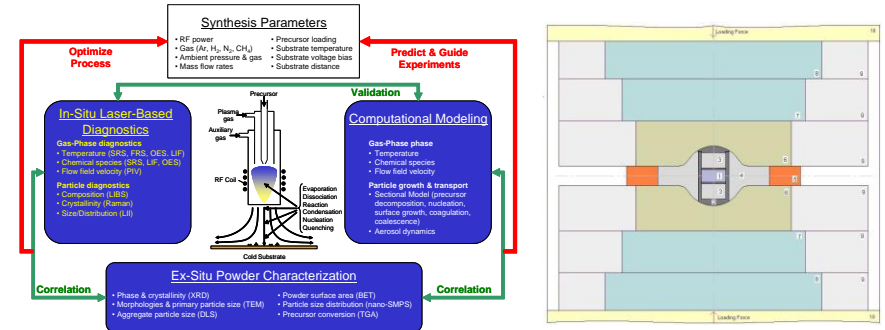
New Insights/Innovations:

- Synthesize and consolidate nanopowders of the c-BN to produce extended-solid nanomaterials with superior hardness, stiffness, bend strength, tensile strength, and fracture toughness.
- Reducing the grain size of single- or multi-phase materials to nanoscale dimensions yields significant improvements in mechanical properties (> 1.5 times).
- Ability to make large monoliths by working with end-user companies (e.g. DI, Megadiamond) that have up to 30,000 ton presses.



Scientific/Technical Approach Summary:

Program Approach:



- **Metastable Nanopowder synthesis:** plasma and flame synthesis, with in-situ laser-based diagnostics, computational modeling, and powder characterization
- **Consolidation:** high pressure and high temperature (e.g. 5GPa / 1000°C)

Pathway to Goal:

- Plasma synthesis and consolidation will be used to produce $\sim 1\text{-}2\text{cm}$ diameter ($\sim 0.5\text{-}1\text{cm}$) thick nanocrystalline c-BN samples.

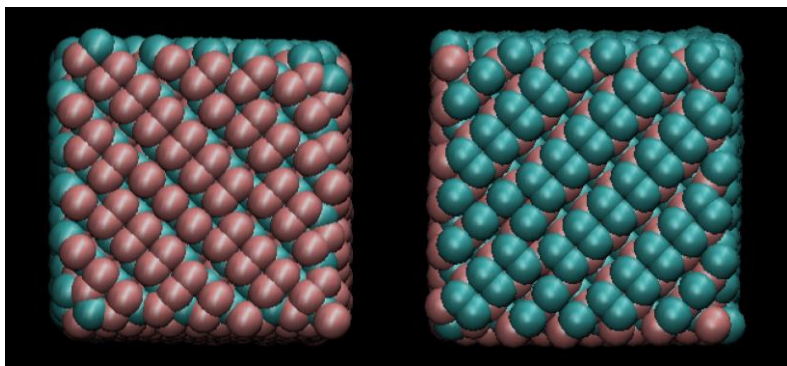
Potential Defense Application(s):

- Nano-ceramic composites provide superior hardness, stiffness, bend strength, tensile strength and fracture toughness.
- Robust materials of high strength and enhanced toughness are needed for many applications, including heavy and light (including transparent) armor, gun-barrels and liners, machine tools, lubrication-free bearings, and optoelectronic devices in harsh environments.

Dimer-stabilized {100} Facets

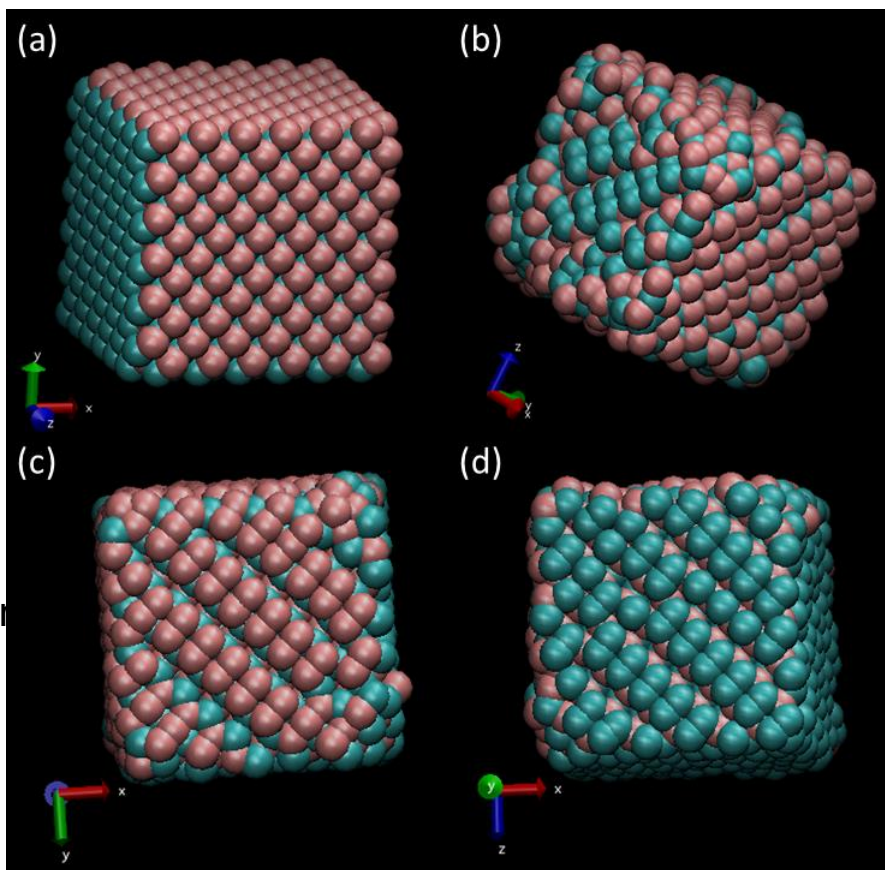
- ➔ Minimize ground state energy:
dangling bonds \rightarrow dimerization

<Relaxed structure at ground state>



Similar to silicon {100} surface reconstruction

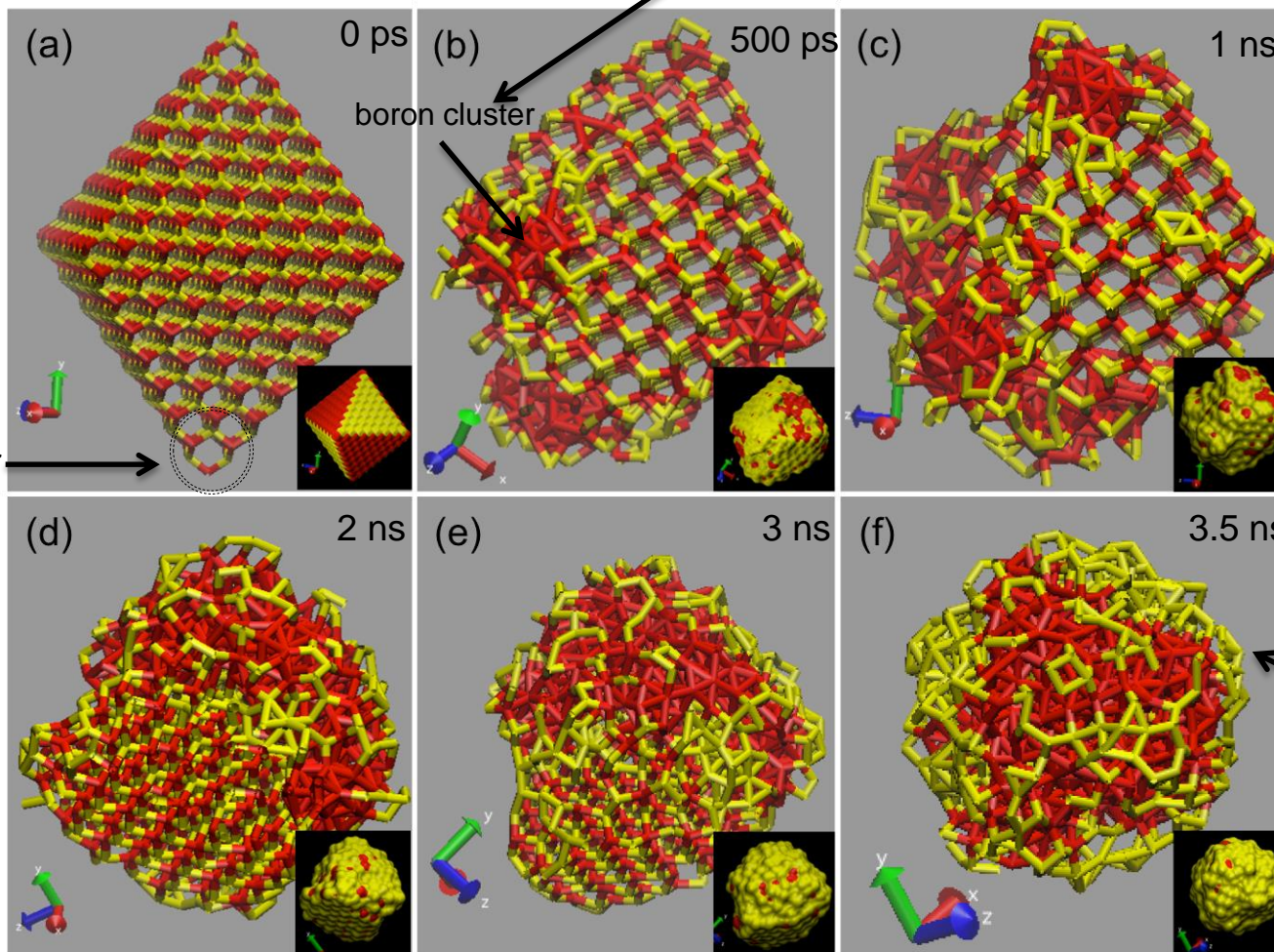
<Cube Nanoparticle: NVE 400K>



Phase Separation Driven Melting

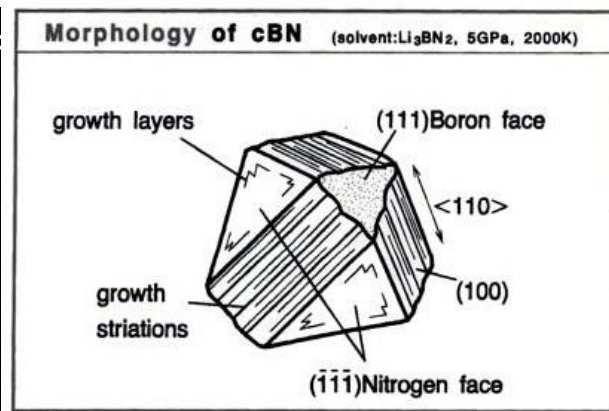
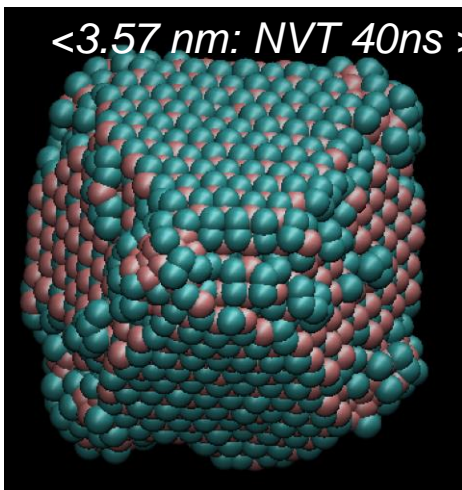
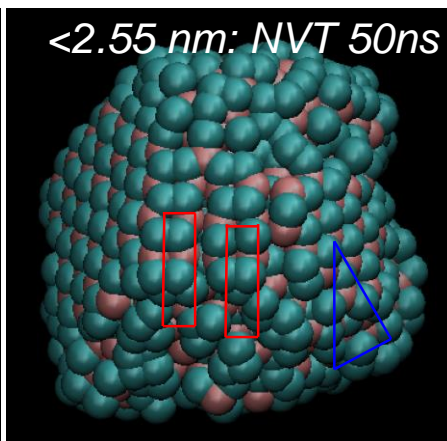
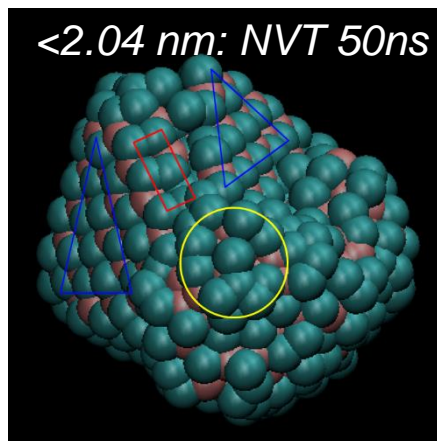
- NVT simulation: $T=3340\text{K}$

Corner-initiated melting



C-BN NPs: Mixture of {100} & {111} Facets

- Computational extensive NVT simulations: temperature is around



Mishima O, Era K. Science and technology of boron n
Electric Refractory Materials. 2000:495-556

Kagamida M, Kanda H, Akaishi M, Nukui A, Osawa T, Yamaoka S.
Crystal growth of cubic boron nitride using Li_3BN_2 solvent under high temperature and pressure. *J Cryst Growth*.

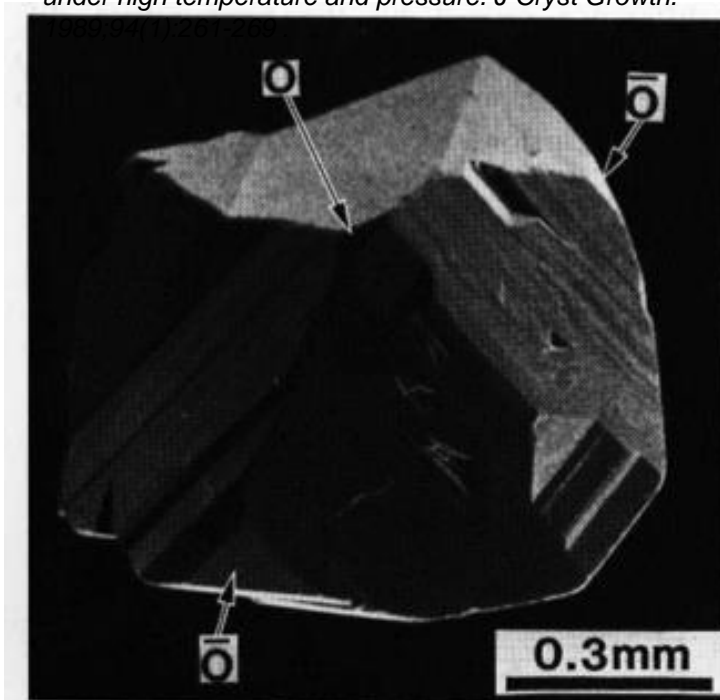
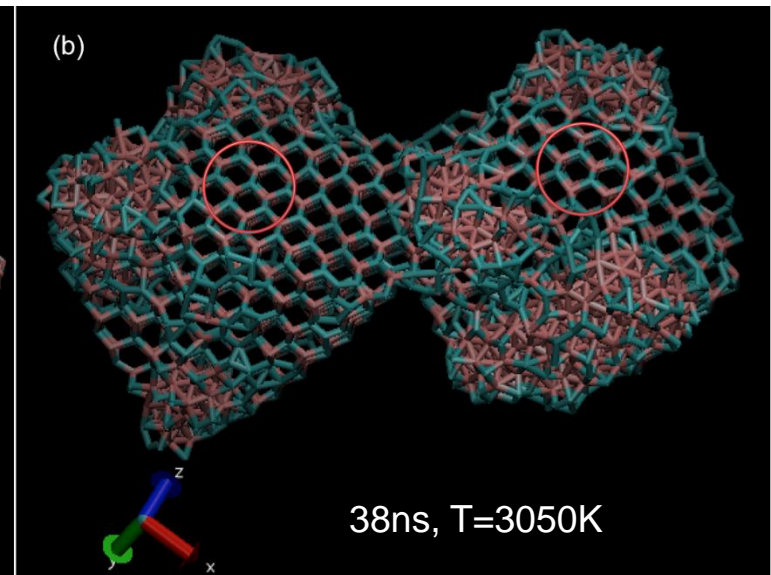
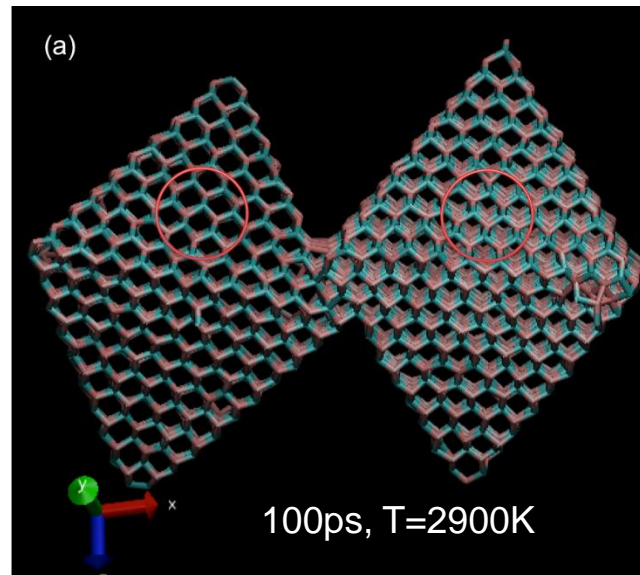
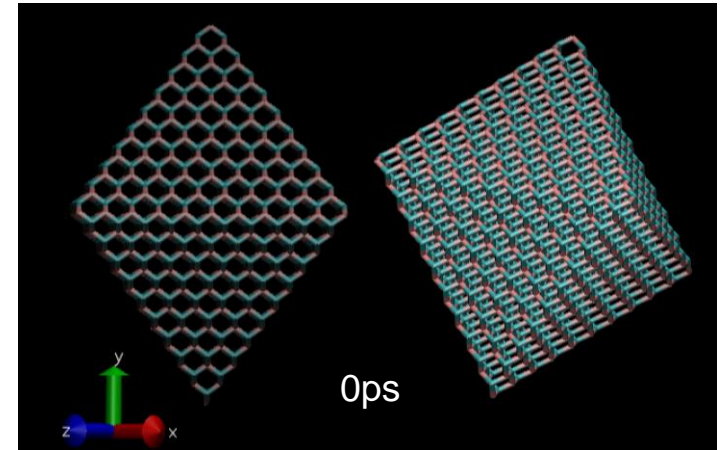


Fig. 6. Scanning electron micrograph of a crystal grown at 1770°C and $X - Y = 2 \text{ mm}$ for 17 h on a seed face of {111}, where o and \bar{o} are {111} and $\{\bar{1}\bar{1}\bar{1}\}$ faces.

Orientation Alignment and Grain Growth

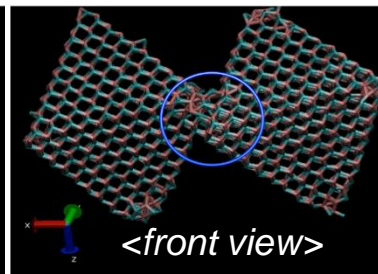
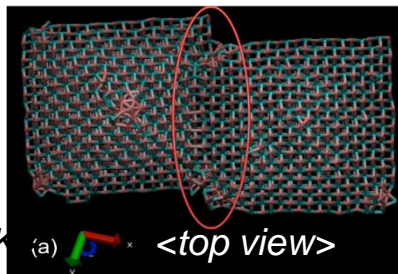
- 50-ns NVE simulation with initial $T=2815\text{K}$ (100K~200K below melting temperature)
- Two octahedron nanoparticles align gradually at temperature exceeds 2900K
- At 38ns, the temperature reaches 3050K (above melting temperature)



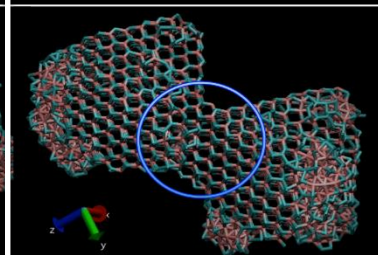
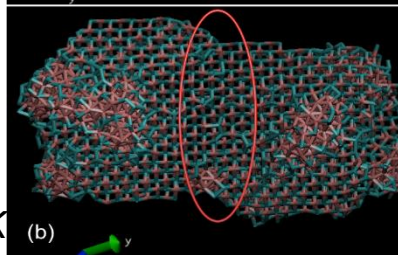
Rapid Grain Growth at High Temperature

Initial $T=3020\text{K}$
(~ melting temperature)

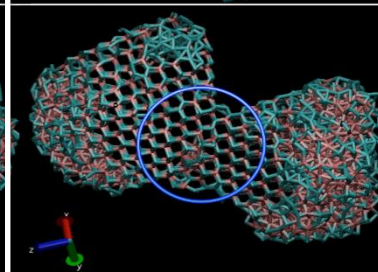
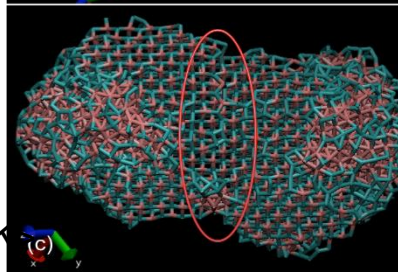
<100ps, $T=3050\text{K}$



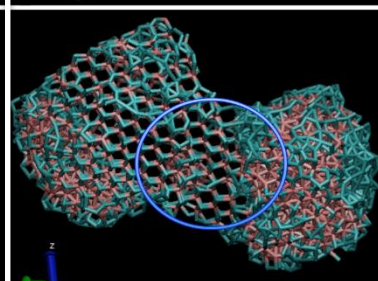
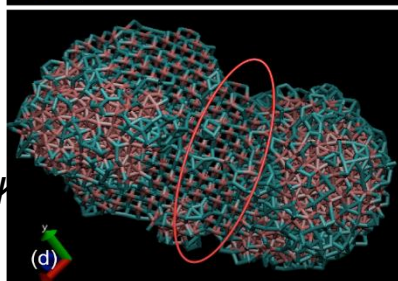
<8ns, $T=3125\text{K}$



<12ns, $T=3230\text{K}$

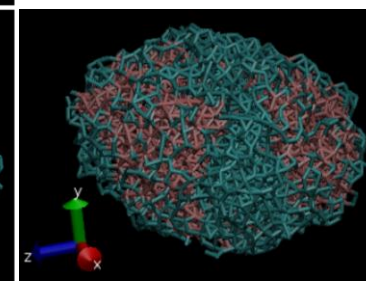


<15ns, $T=3320\text{K}$



Competition between
grain growth
&
phase separation

<16ns, $T=3540\text{K}$ >

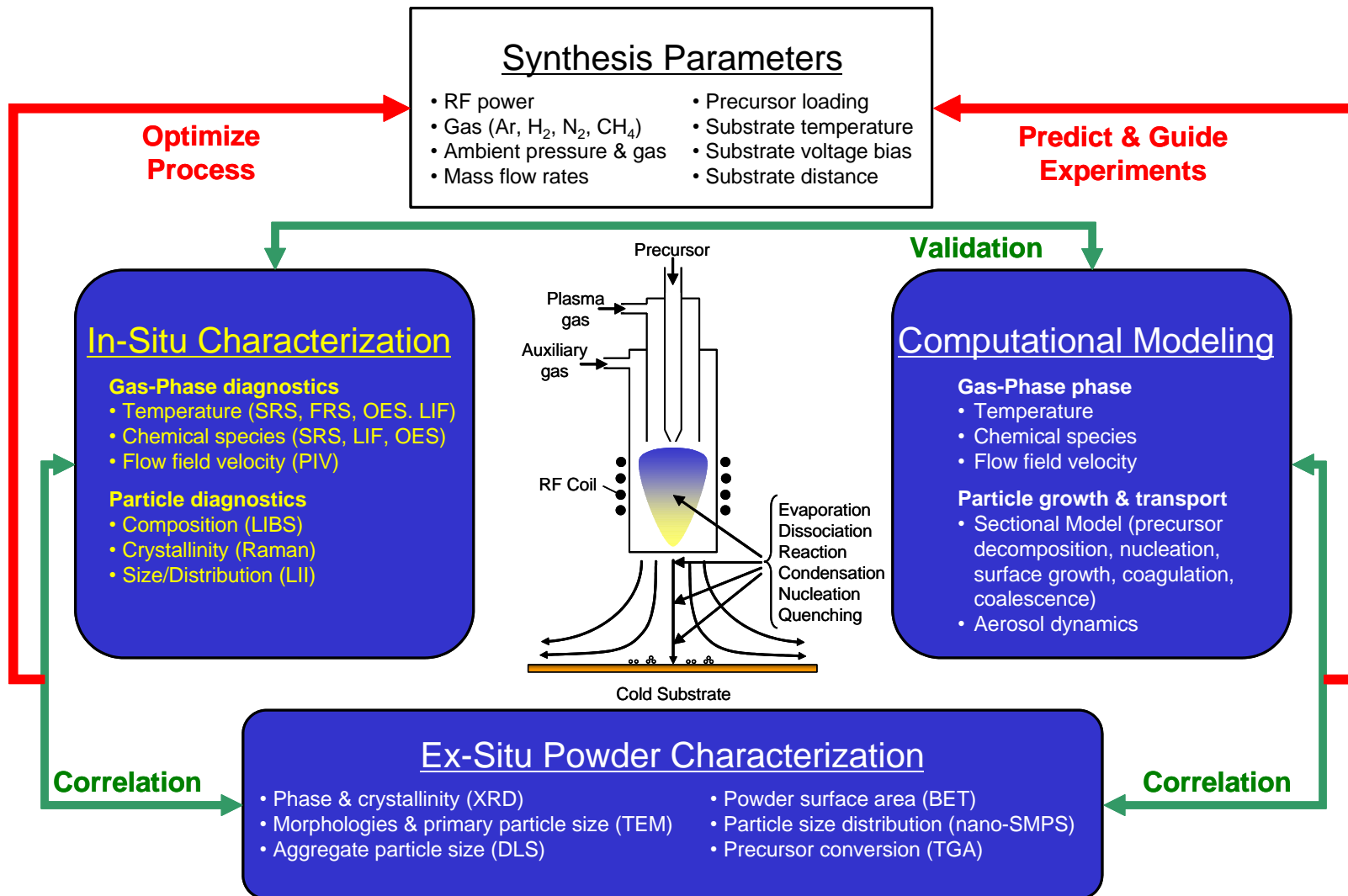


The image features a solid red background. In the top left corner, the word "RUTGERS" is written in a large, white, serif font. Below it, in a smaller, white, sans-serif font, are the words "THE STATE UNIVERSITY OF NEW JERSEY". A large, faint, circular seal of Rutgers University is visible in the background, centered behind the text. The seal contains the text "RUTGERS THE STATE UNIVERSITY" around its perimeter and a central emblem.

RUTGERS
THE STATE UNIVERSITY
OF NEW JERSEY

In-situ Laser-Based Diagnostics

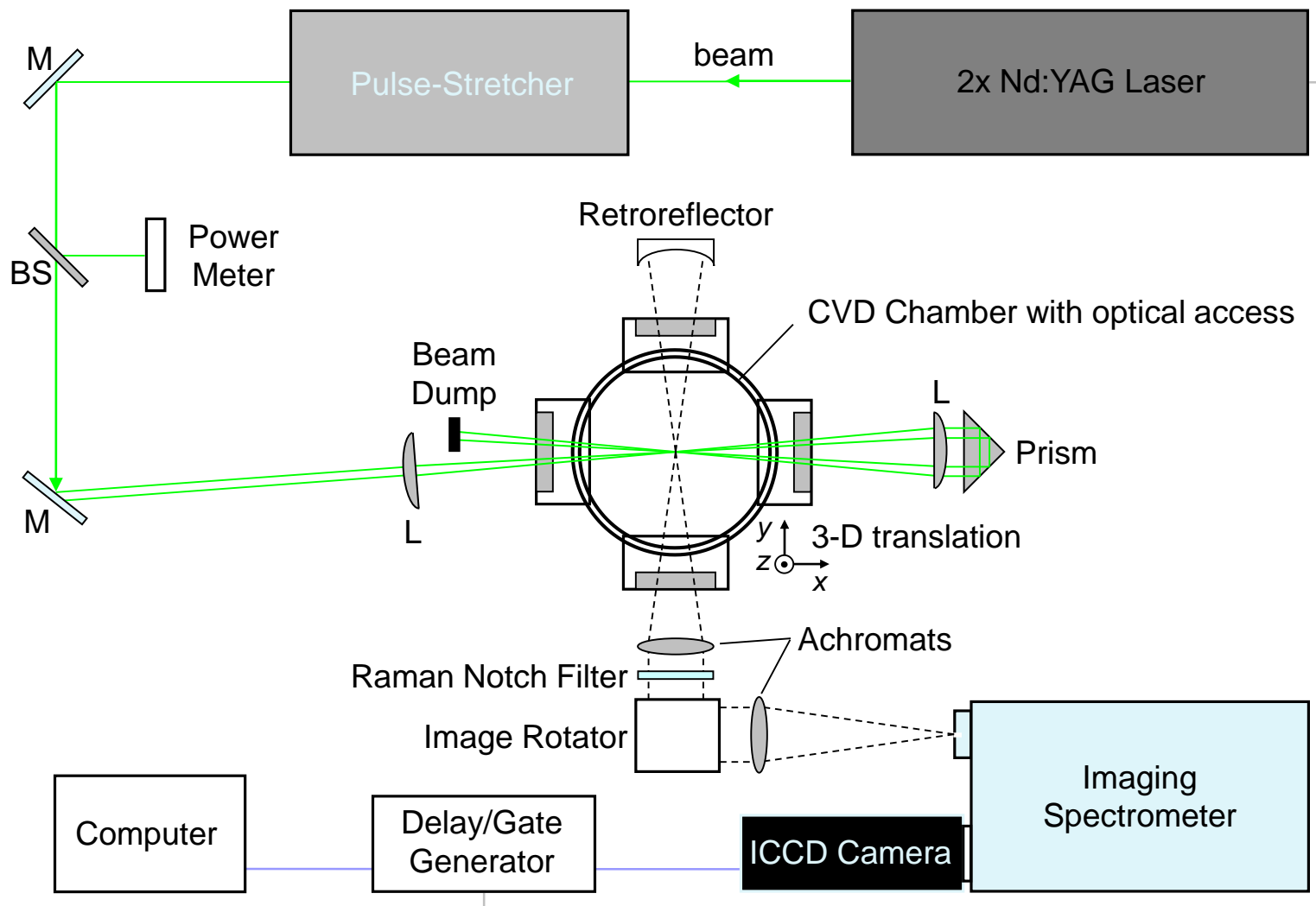
Research Paradigm



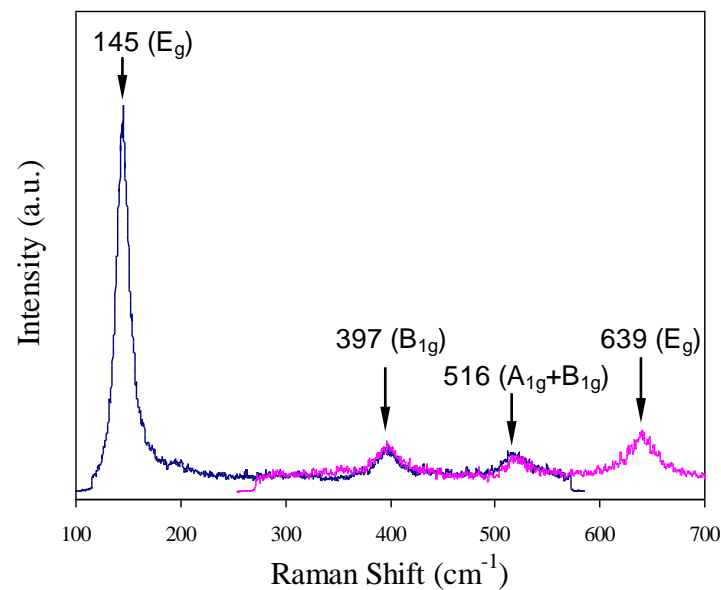
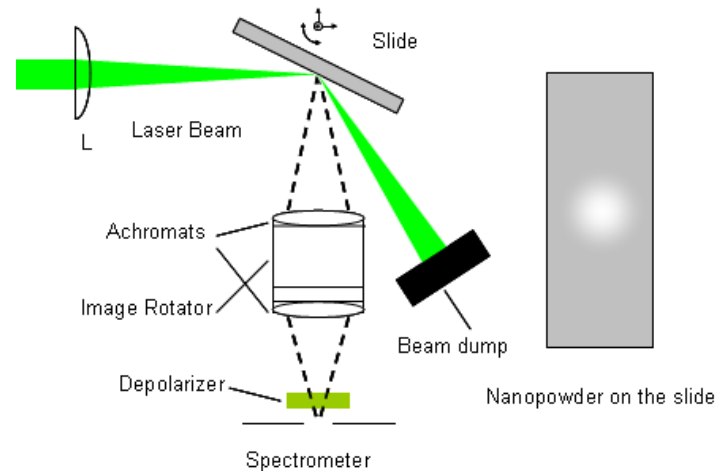
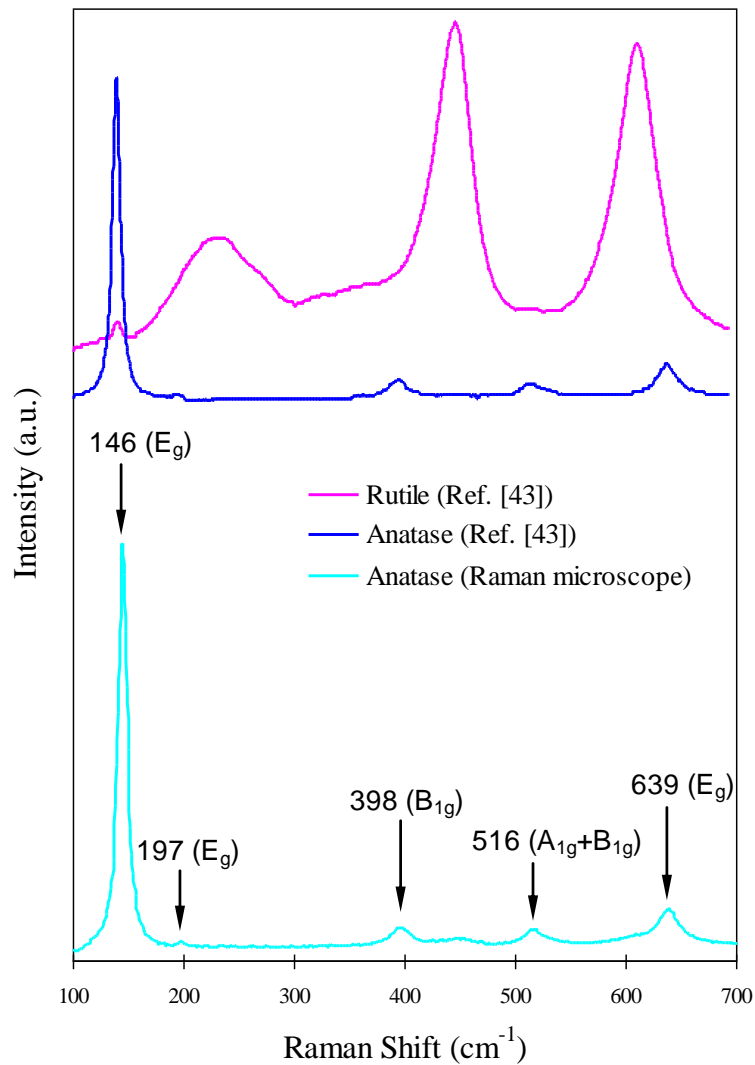
In-Situ Raman of Nano-Aerosol

- **Technique to characterize nanoparticles during gas-phase synthesis**
- **Validation and calibration with titania (and alumina) nanoparticles**
 - Powder on glass slides at RT with in-situ optics layout
 - Nanoparticle-seeded co-flow jet diffusion (phase evolution at high temperatures)
 - Application during flame synthesis of titania
 - Application during plasma synthesis of c-BN

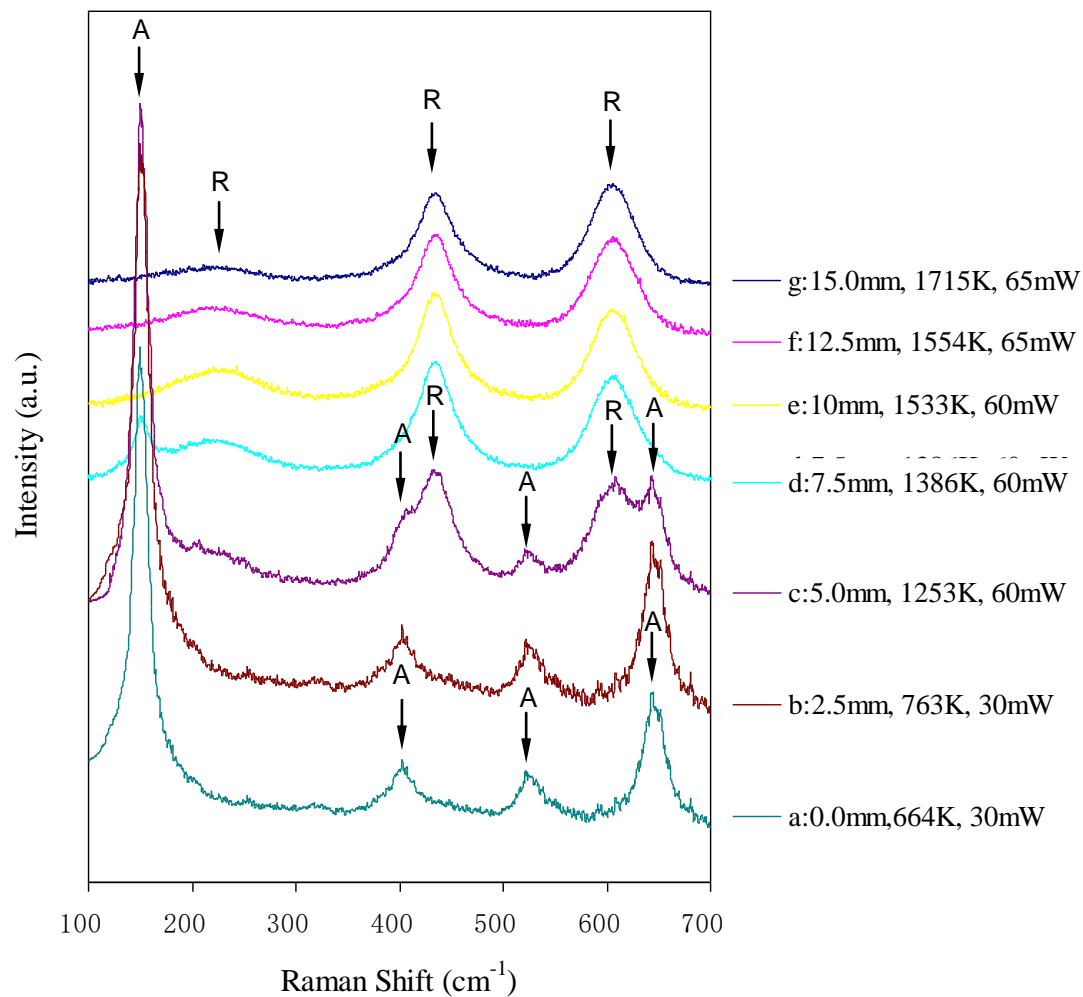
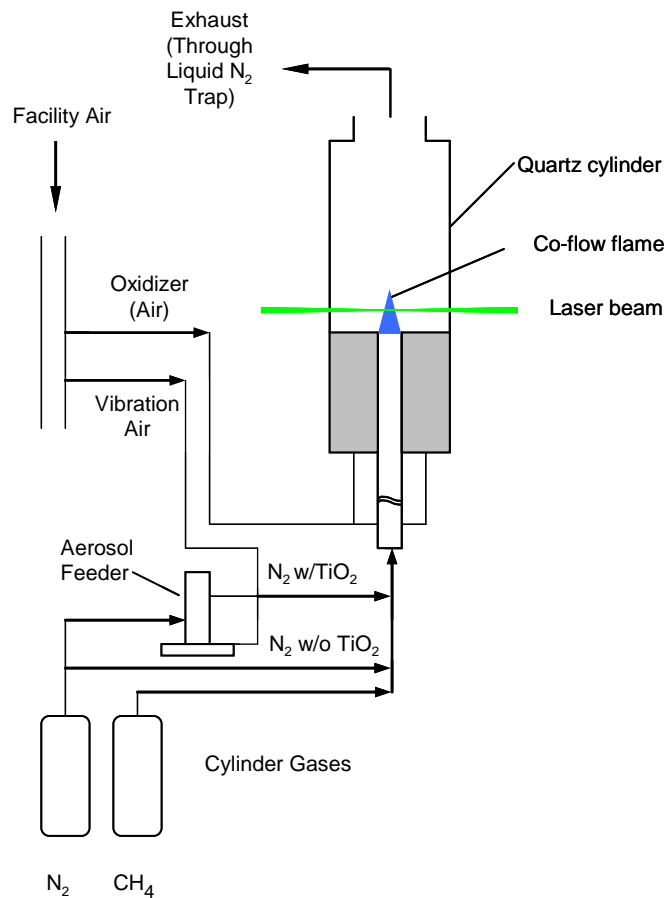
Spontaneous Raman



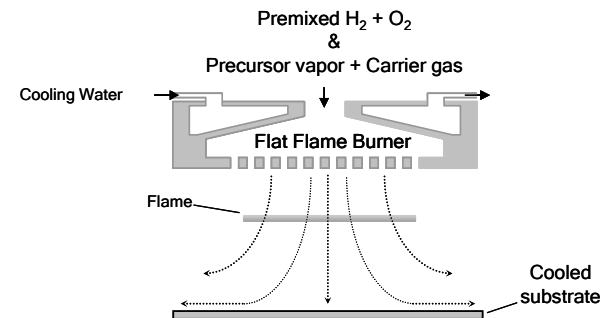
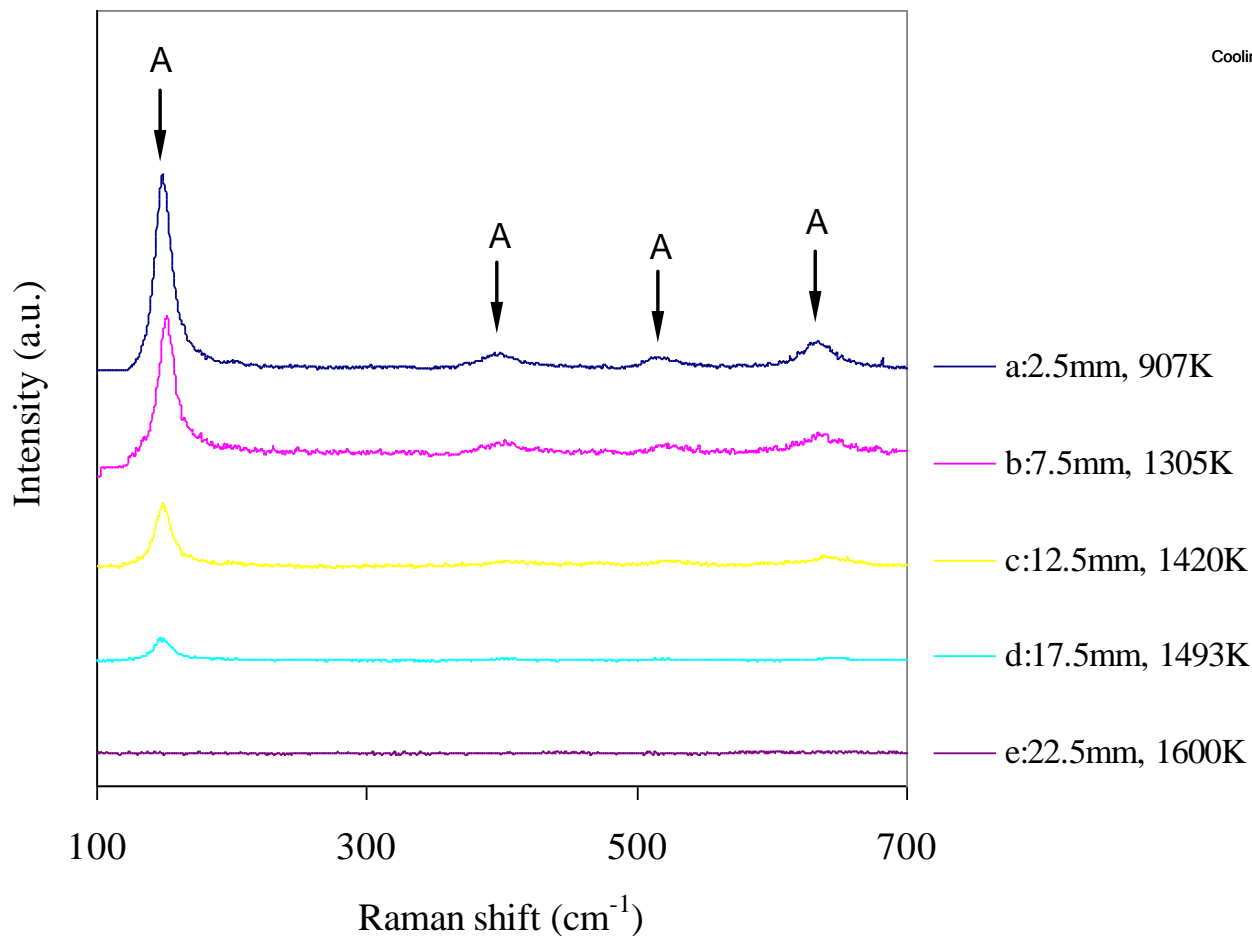
Powder Characterization



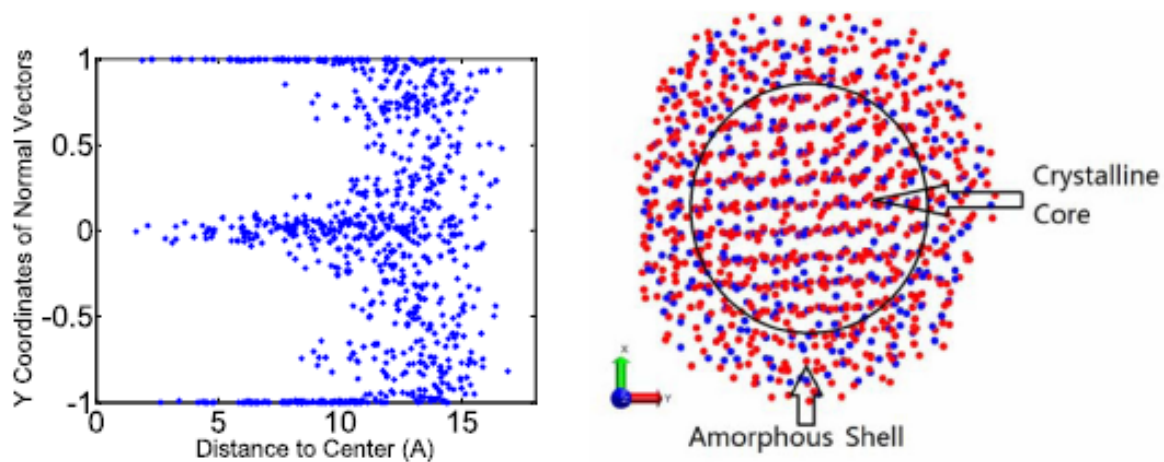
In-situ Calibration with Seeded Flame



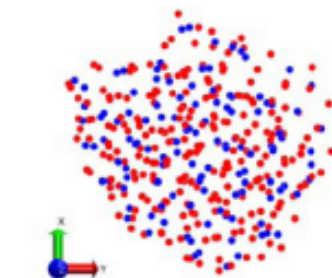
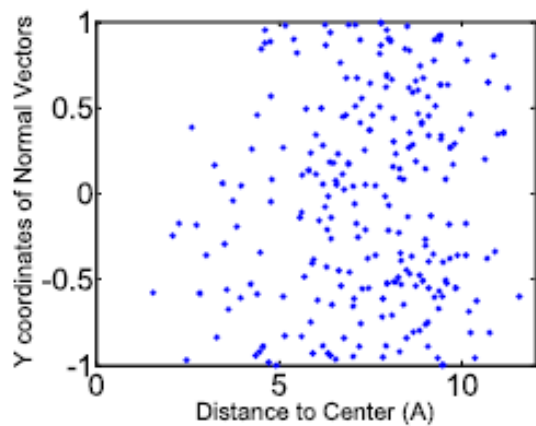
In-Situ Raman of Nanoparticles



MD of Nanoparticles



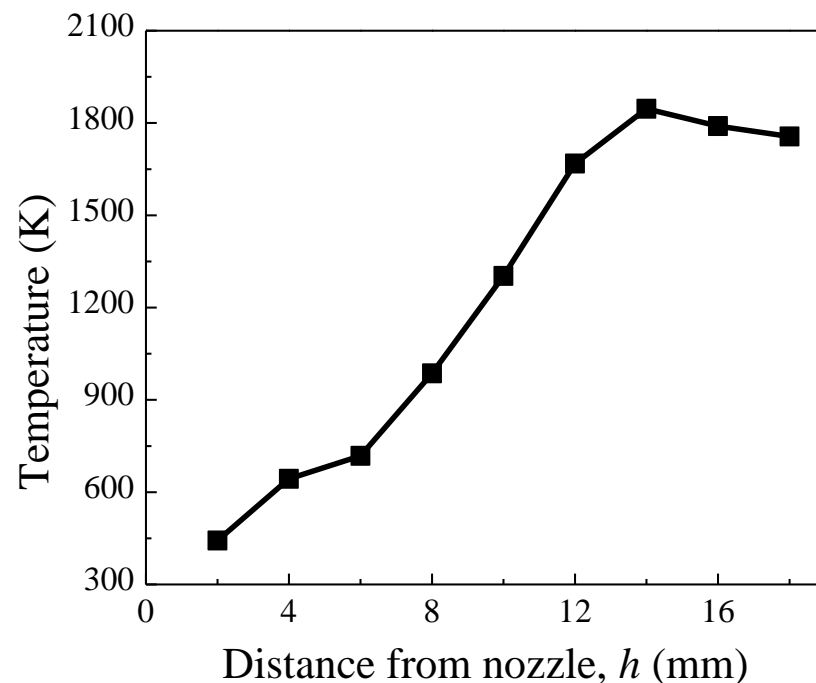
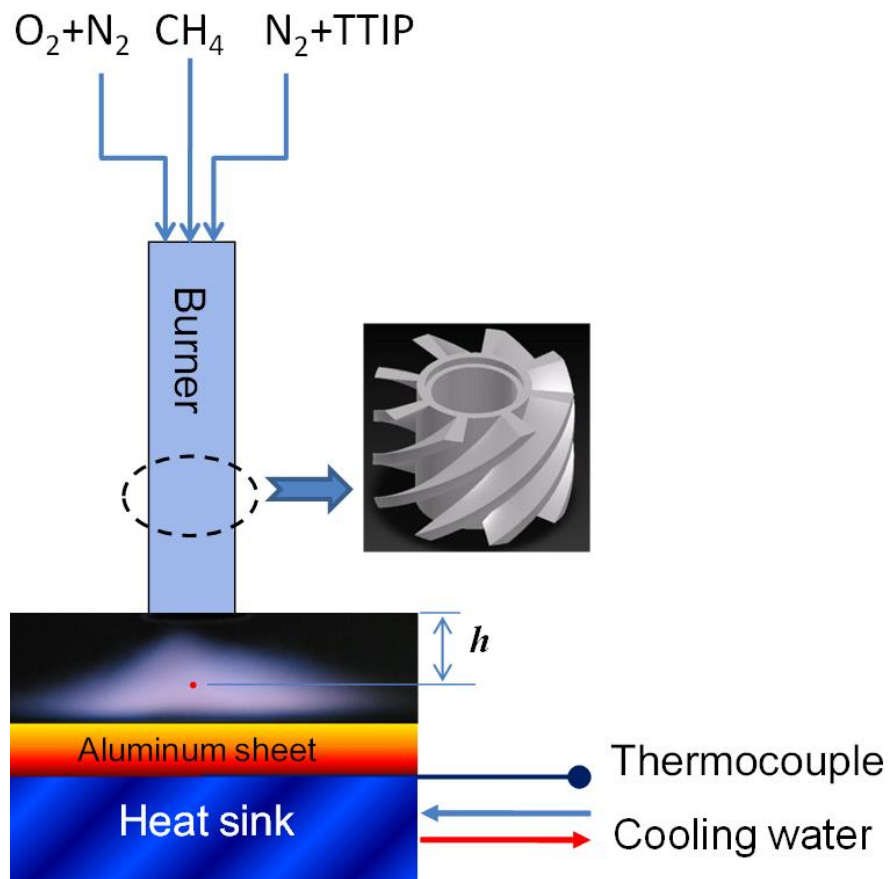
(a)



(b)

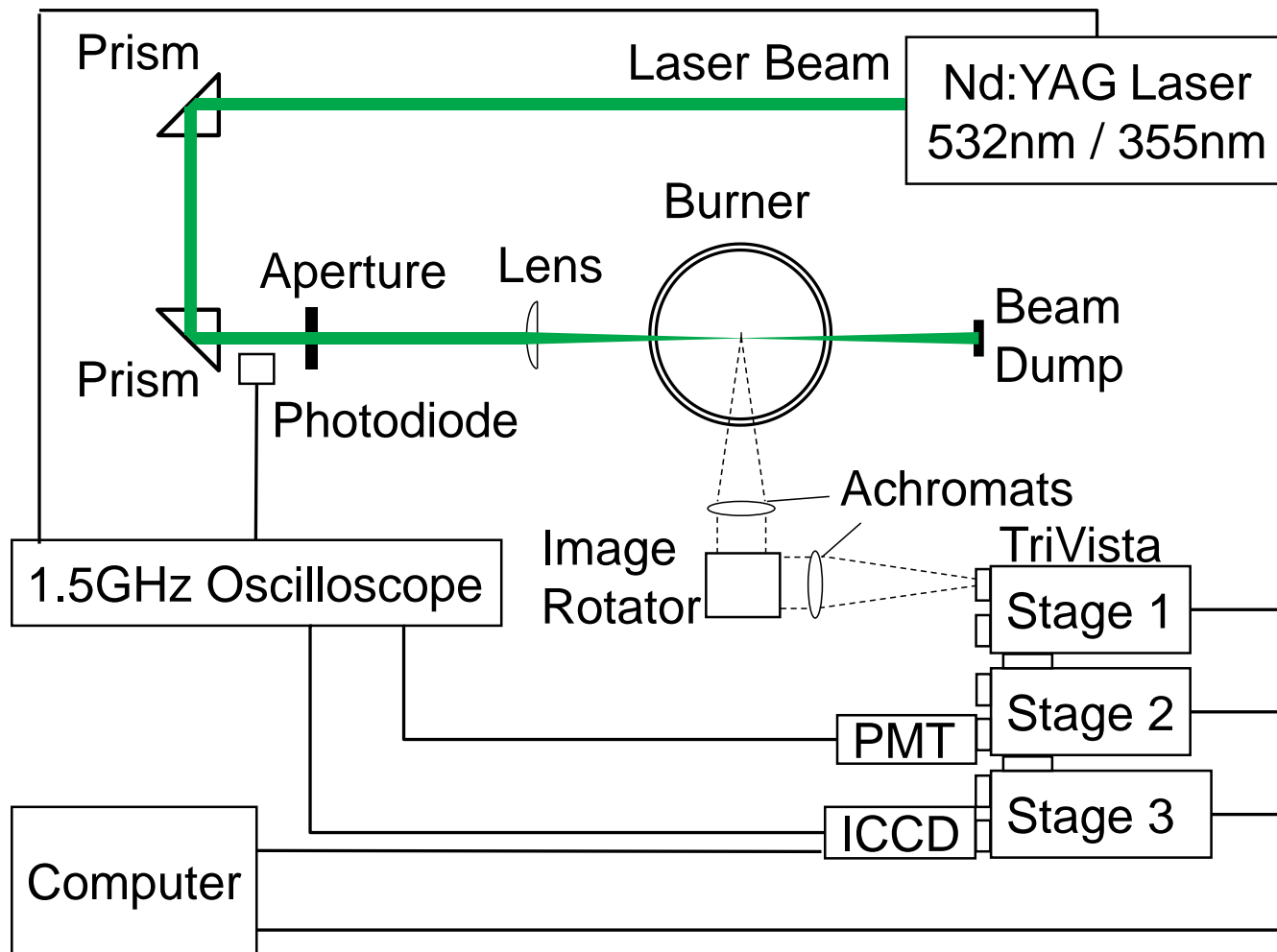
FIG. 2. Radial distribution of local lattice orientation, along with atomic structure of (a) 3 nm and (b) 2 nm nanoparticles at 573 K. The 3 nm particle shows a core-shell (crystalline-amorphous) structure, while the 2 nm particle has an overall amorphous structure.

Experimental setup



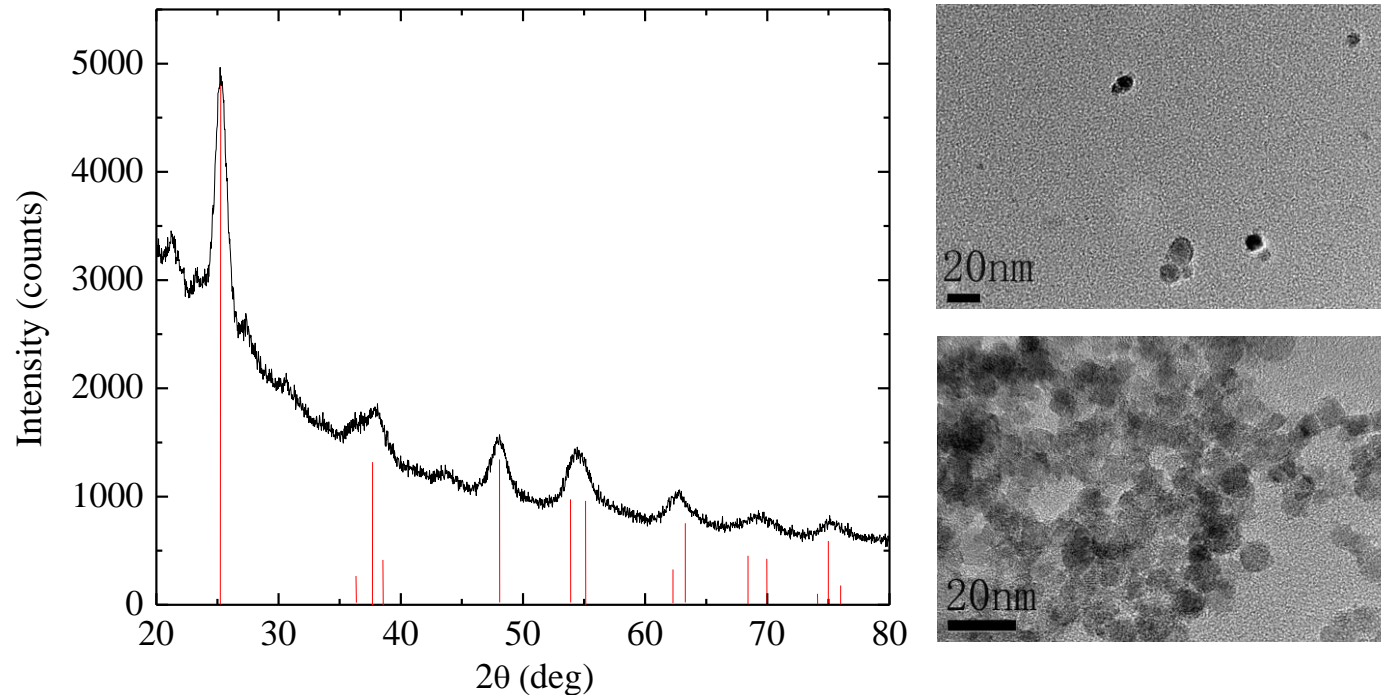
Schematic of the stagnation swirl flame setup for TiO_2 nanoparticle synthesis and the temperature along axis (measured by N_2 Raman)

Schematic of the laser diagnostic system



Sketch of the laser diagnostic system

Particle characterization

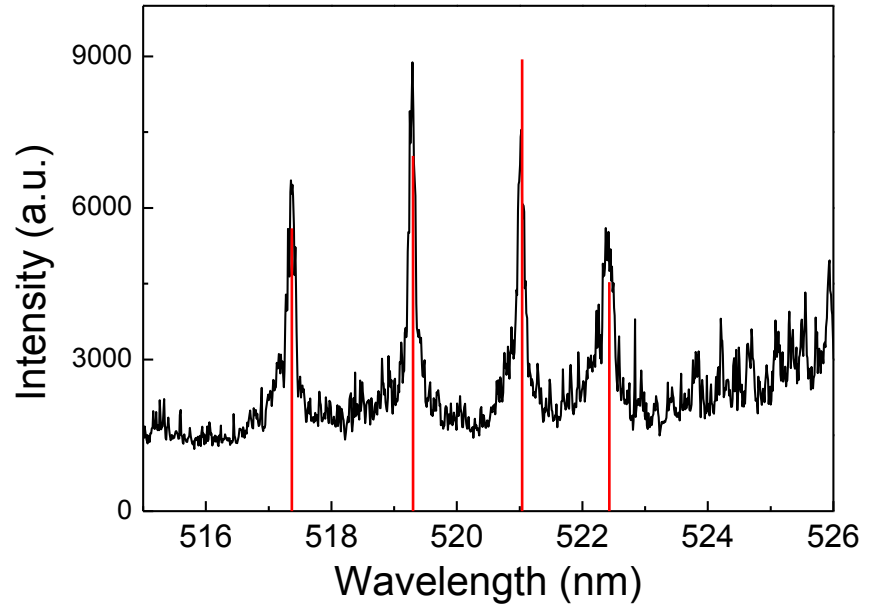
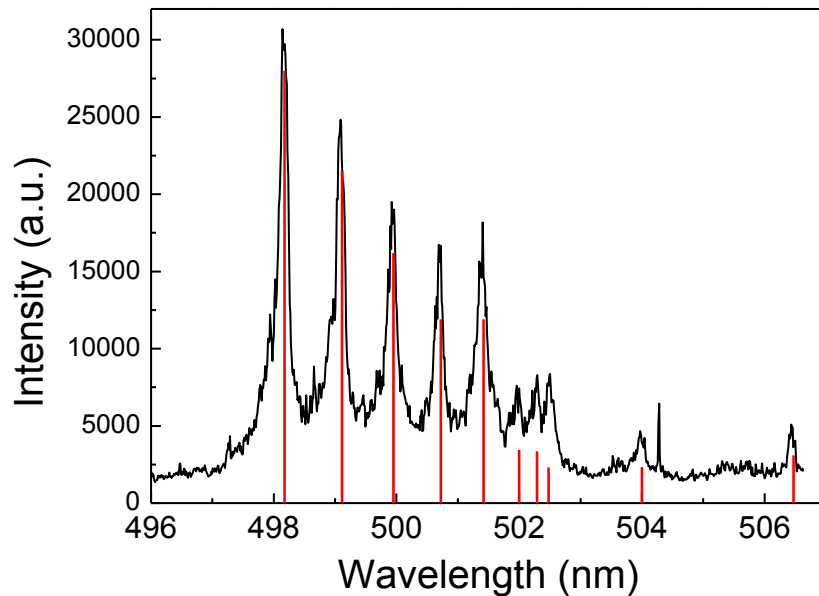


XRD and TEM of particles

XRD \rightarrow anatase (with database marked as red lines)

TEM \rightarrow particle size 6-8 nm (2mm above substrate and on substrate)

Typical LIBS signal from Ti atomic emission



Emission spectra acquired from a laser excitation of 532nm (35mJ/pulse, 28J/cm²), Ti atomic spectra from NIST database marked by red lines.

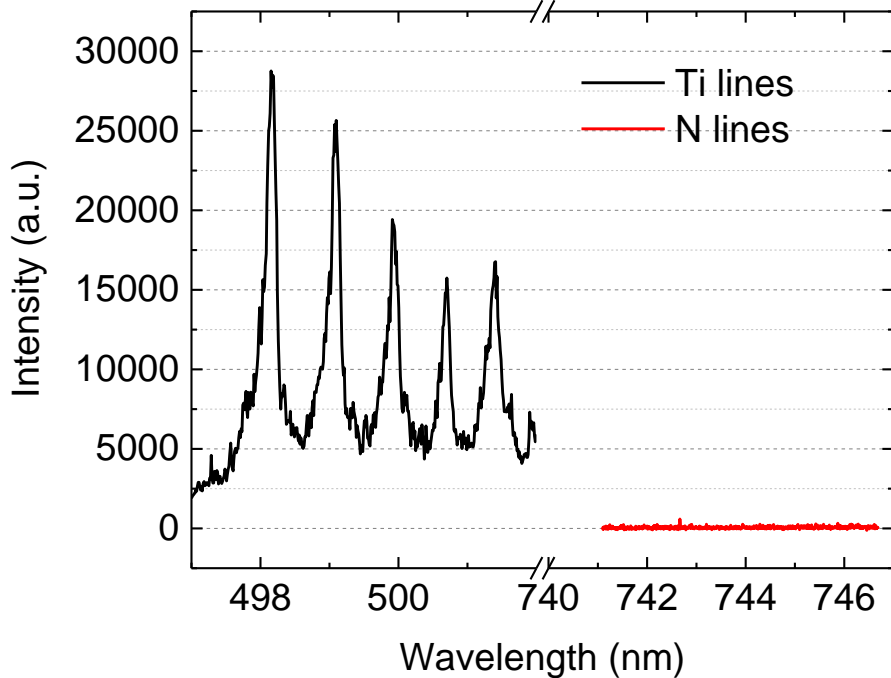
Low laser energy (28J/cm²), no visible plasma

Signal detected from particles on substrate → not excited by flame

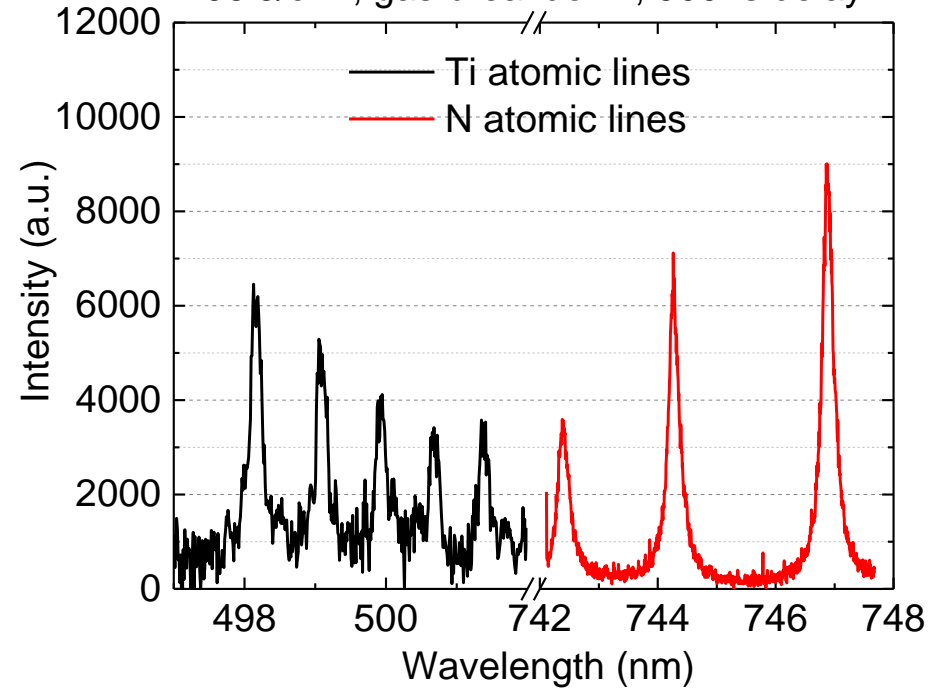
Al signal detected from Al₂O₃ particles → broad applicability

Existence of free electron \rightarrow plasma-proof

28J/cm², no gas breakdown, no delay



96 J/cm², gas breakdown, 900ns delay

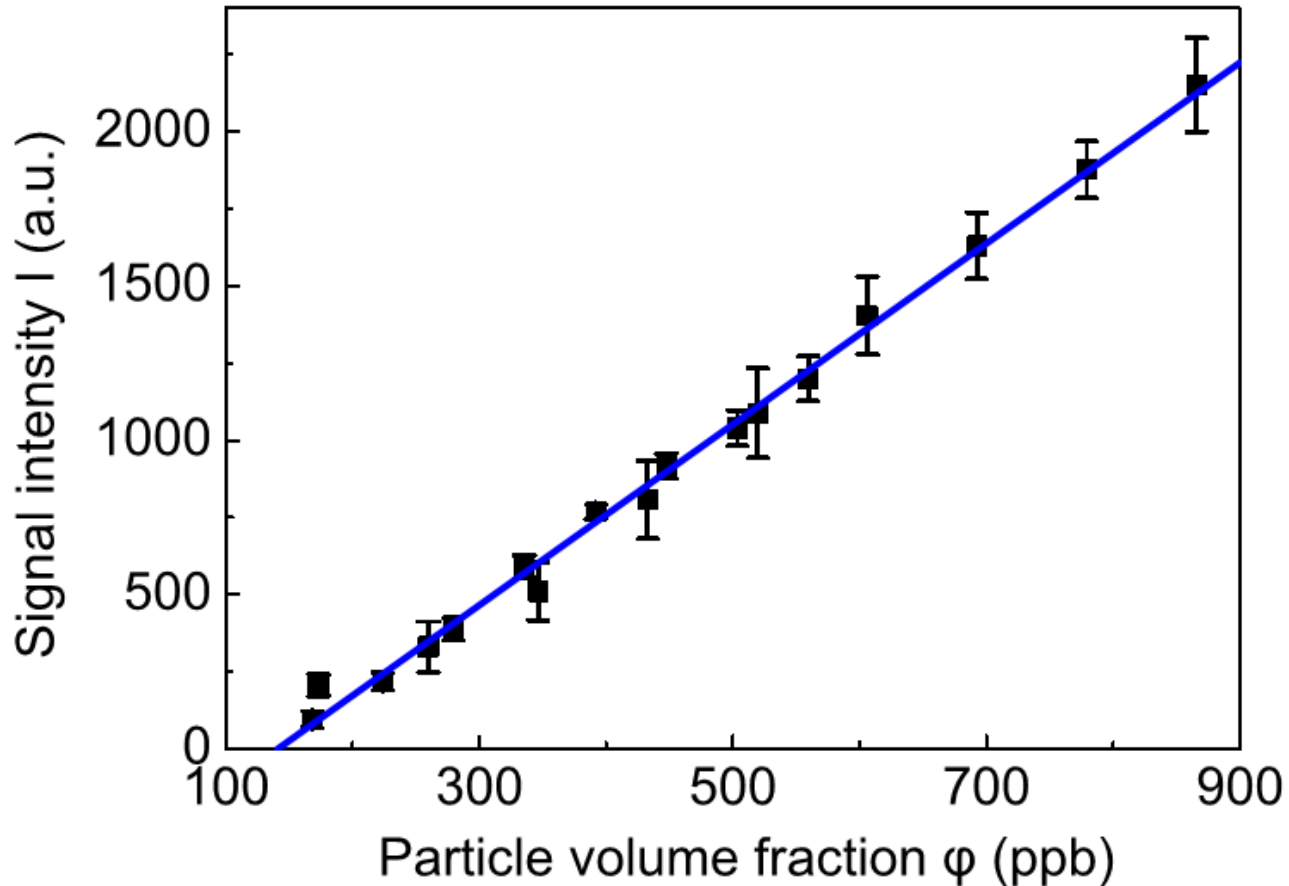


Peak fitting of Ti atomic emission with a laser fluence of 28J/cm²
 \rightarrow line broadening \rightarrow Stark broadening

Gas breakdown \rightarrow Calibration of Stark broadening parameter via comparing the broadening parameter of Ti and N \rightarrow Stark broadening parameter

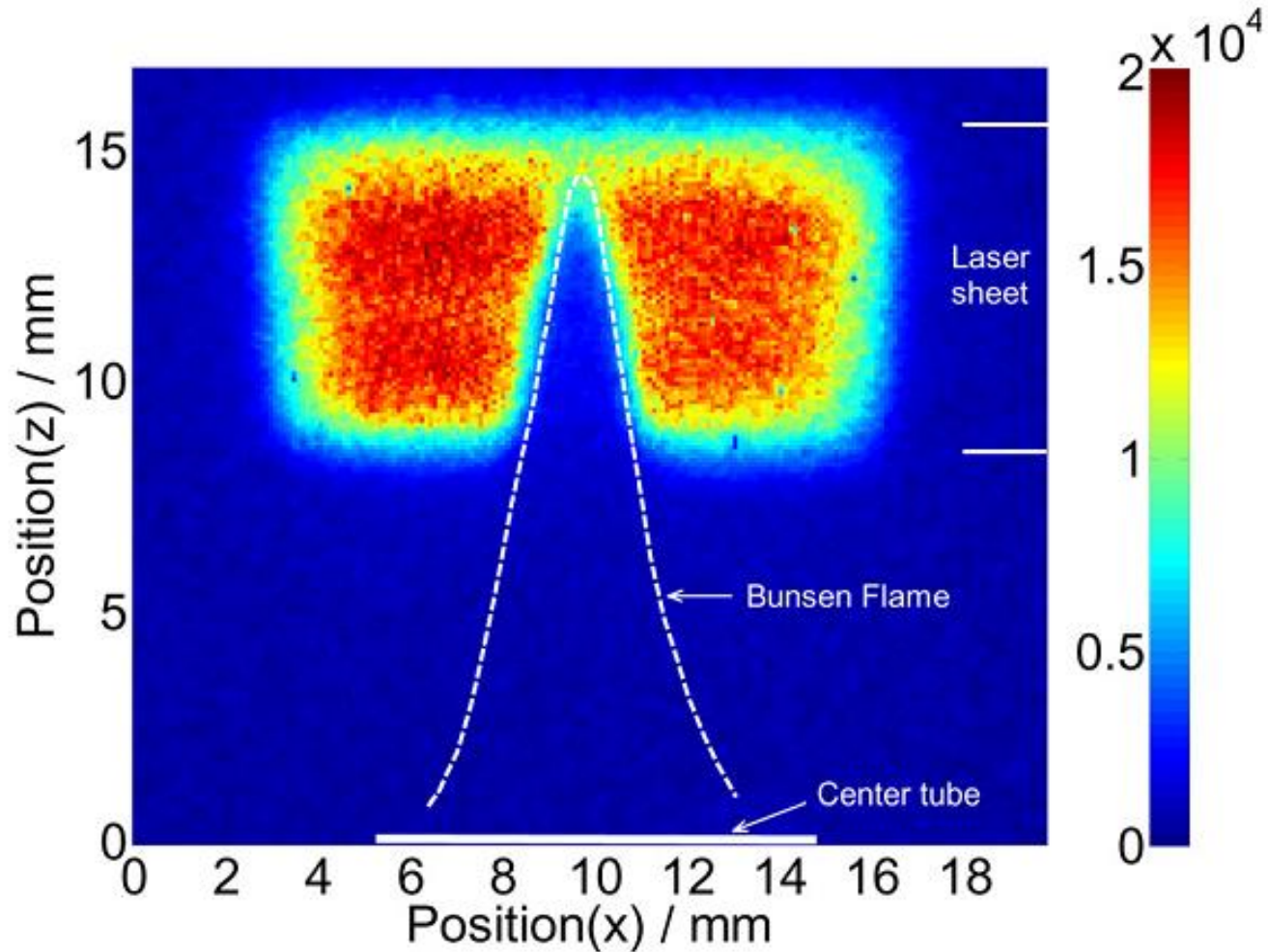
} Electron density
 3×10^{17}
 cm⁻³

LIBS for measurement of particle volume fraction



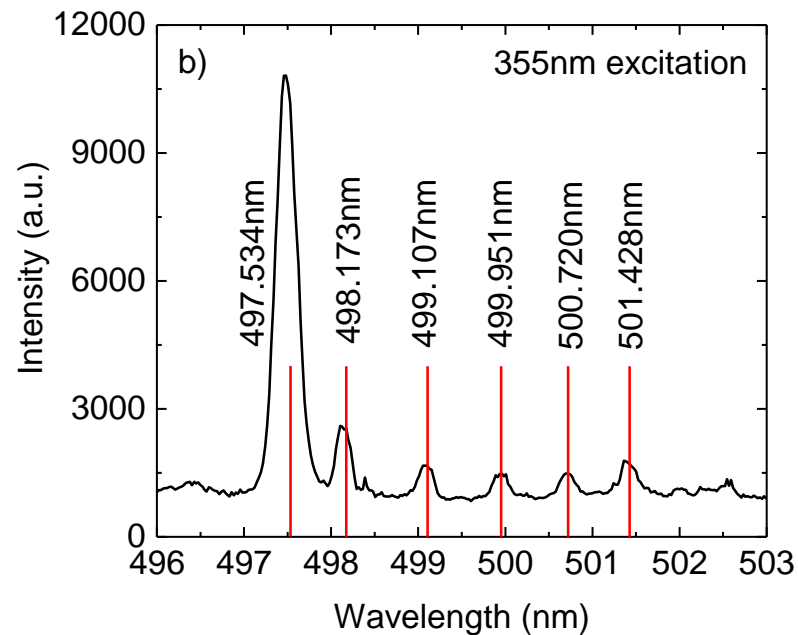
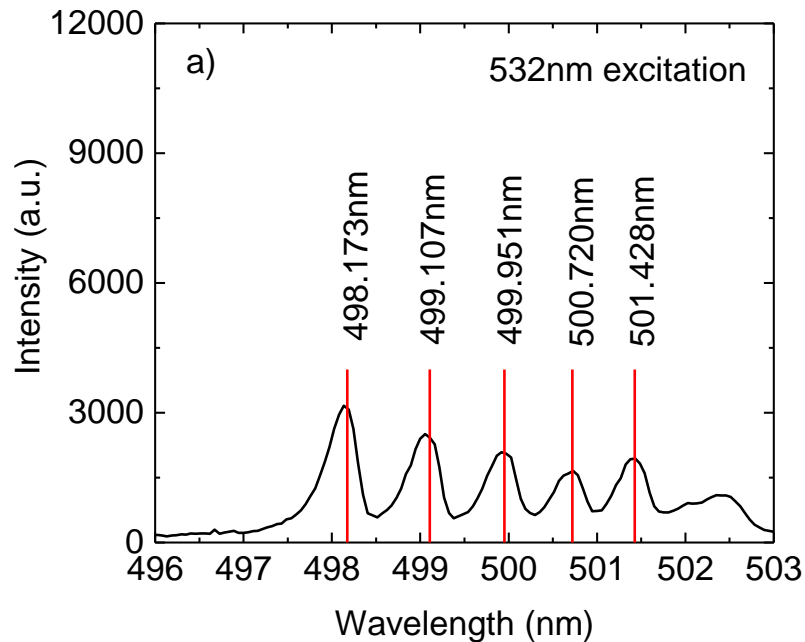
The increase of signal intensity versus particle volume fraction (controlled by the loading rate of precursor)

2D measurement



Two-dimensional distribution of particle-phase Ti imaged with a 500 nm band pass filter (FWHM 10 nm), laser fluence $24\text{J}/\text{cm}^2$

Low-intensity LIBS with subsequent resonant excitation



Comparison of the emission spectra from a) 532nm and b) 355nm laser excitation

New emission line at 497.534nm

Much stronger than other emissions – better detection threshold

Confirmed by Ti particles only (in Ar atmosphere)

Discussion

- 355 nm laser line is actually 354.70nm.
 - Resonant excitation
- Combine phase selective LIBS and resonant enhancement
 - Phase-selectivity (particles only)
 - Select lines or atoms to excite
 - Enhance the emission signal

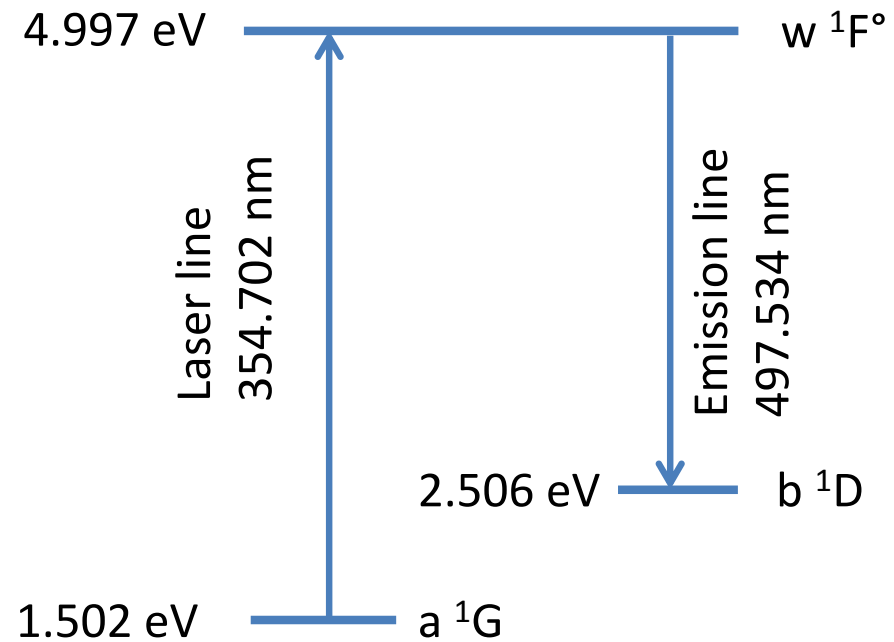
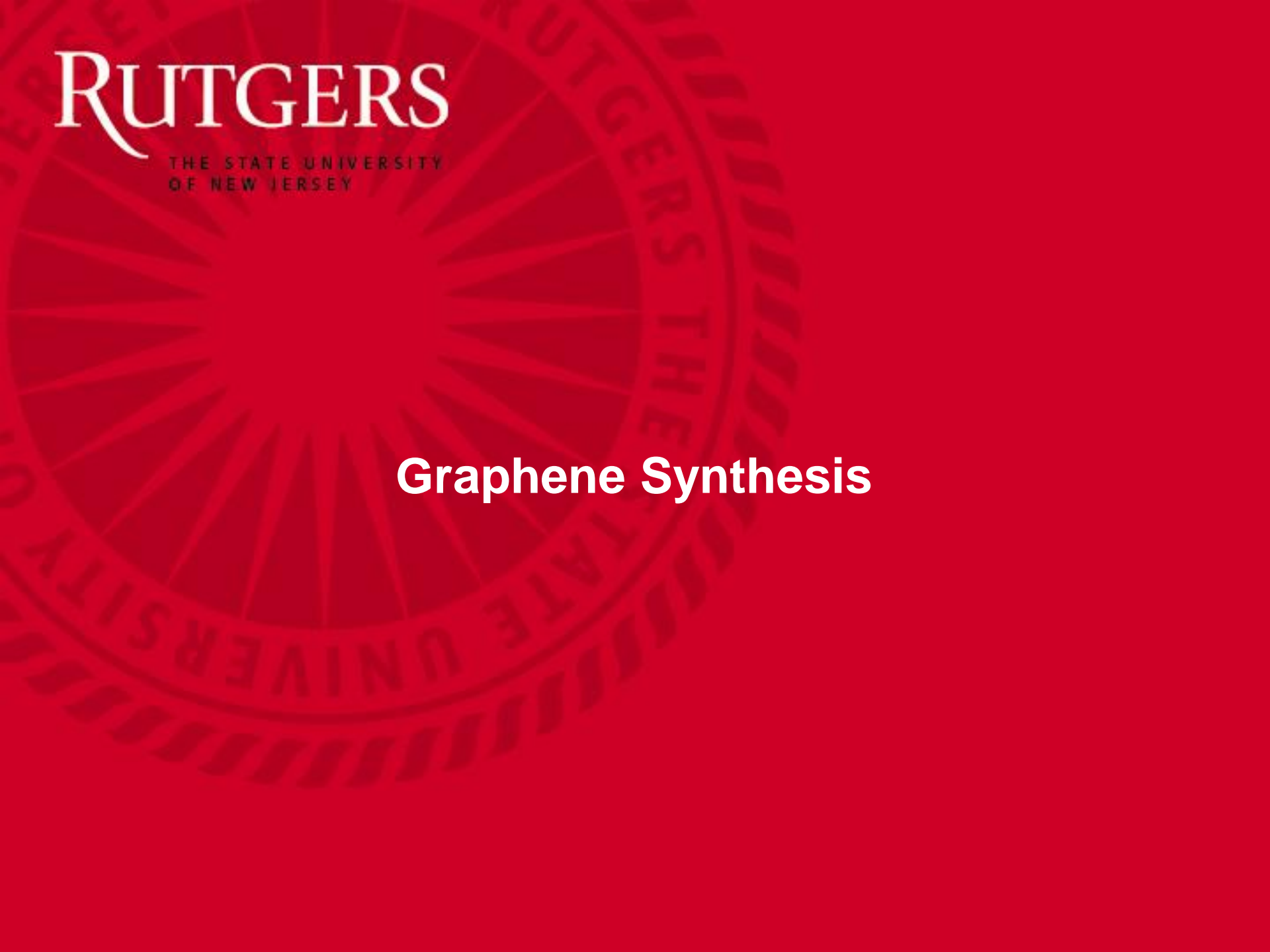


Diagram for resonant excitation of the titanium neutral atoms

The image features a solid red background. In the top left corner, the word "RUTGERS" is written in a large, white, serif font. Below it, in a smaller, white, sans-serif font, are the words "THE STATE UNIVERSITY OF NEW JERSEY". A large, faint, circular seal of Rutgers University is visible in the background, centered behind the text. The seal contains the text "RUTGERS THE STATE UNIVERSITY" around its perimeter and a central emblem.

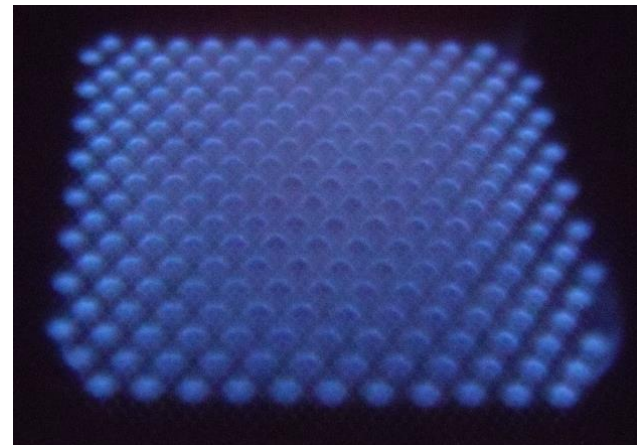
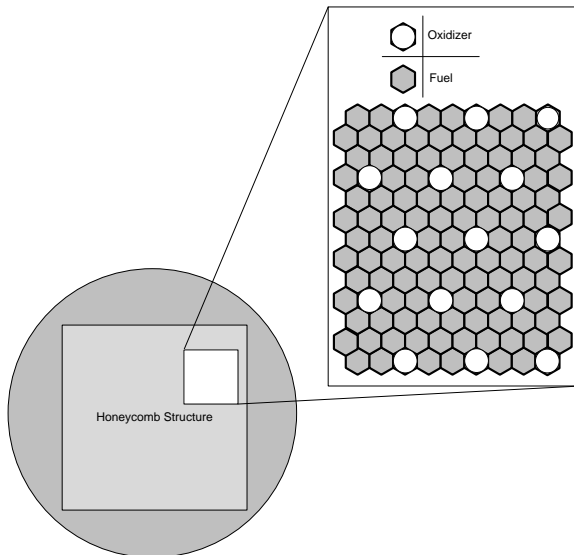
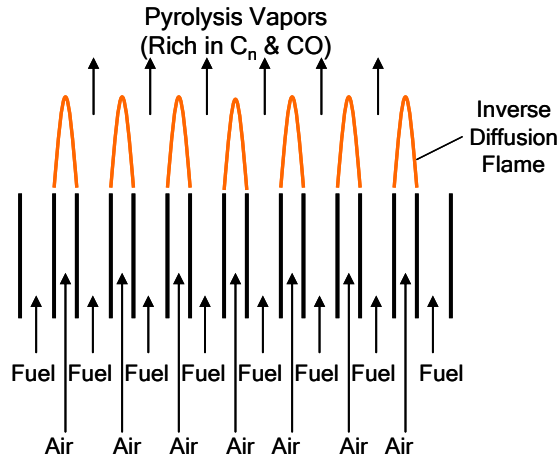
RUTGERS
THE STATE UNIVERSITY
OF NEW JERSEY

Graphene Synthesis

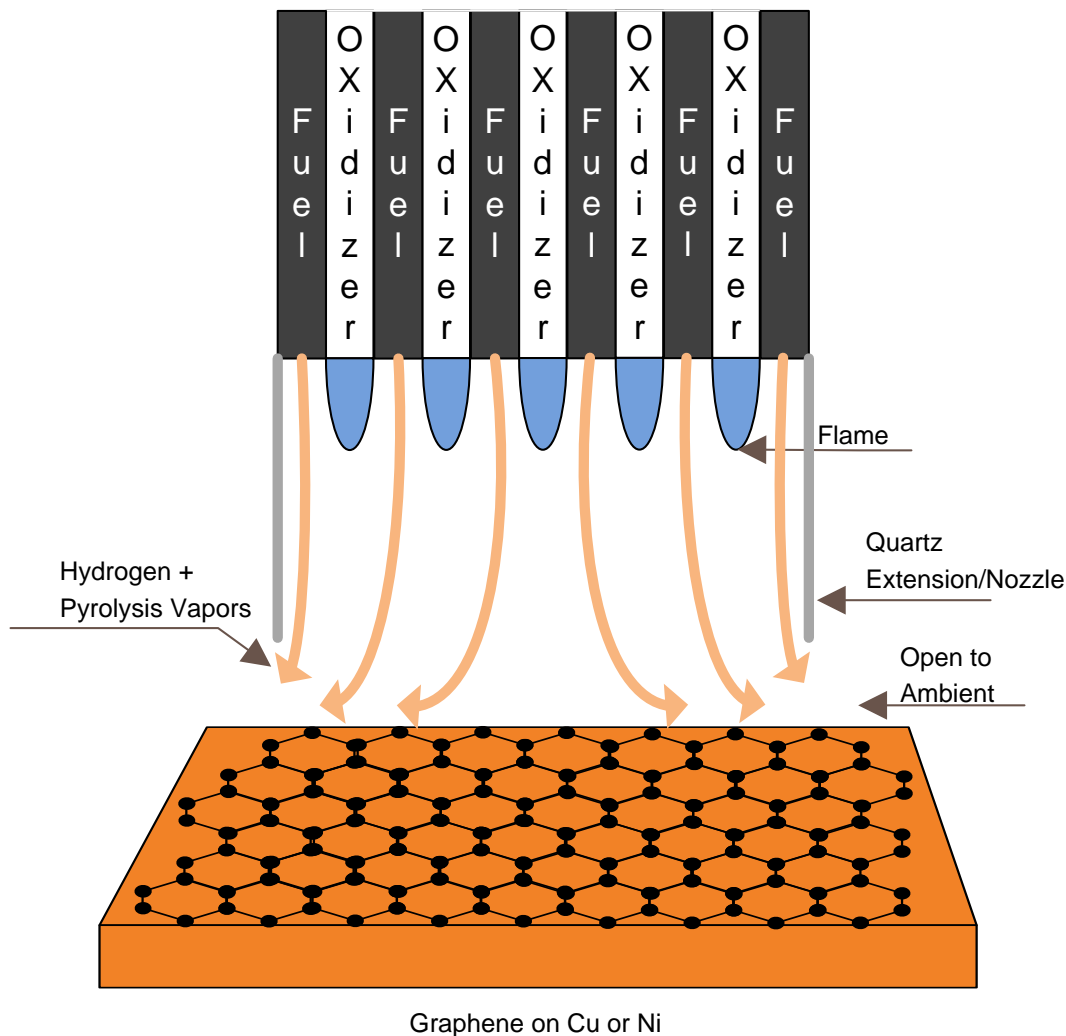
Motivation

- Common methods for *graphene/CNT/diamond* synthesis include arc discharge, laser ablation, and chemical vapor deposition (CVD)
- But, *large-scale* applications require synthetic methods that are continuous, energy efficient, and do not require expensive starting materials
- *Flame synthesis* is scalable and offers potential for high volume production at reduced cost
- Flames readily provide *temperatures and carbon species* needed for graphene/CNT/diamond growth

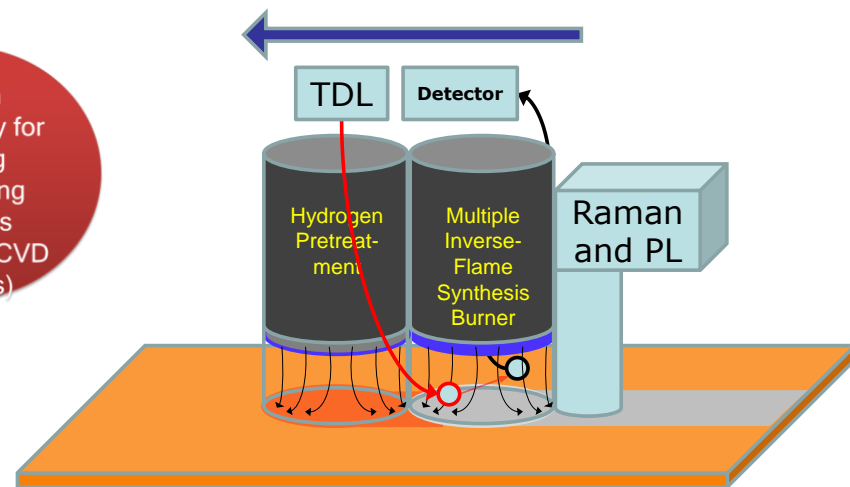
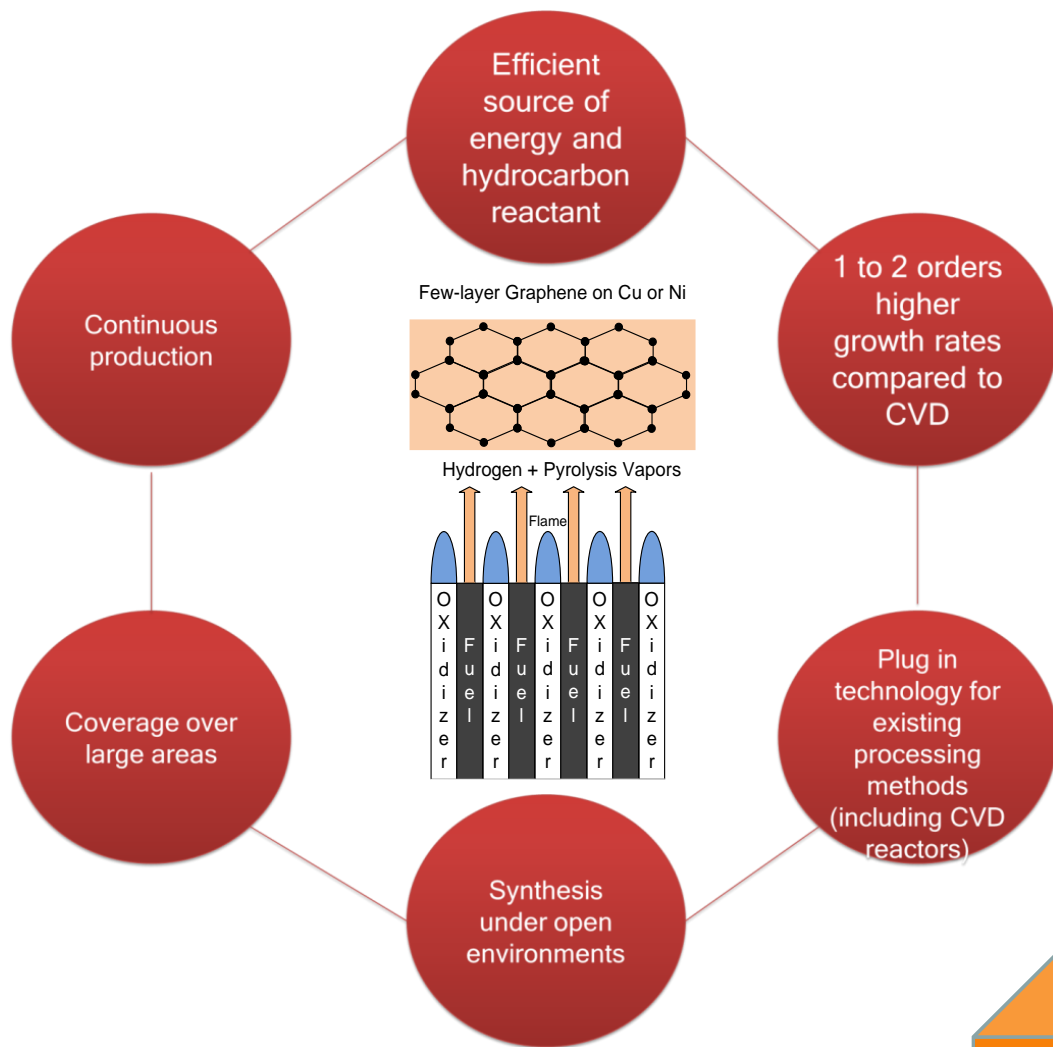
Details of Multiple IDF Burner



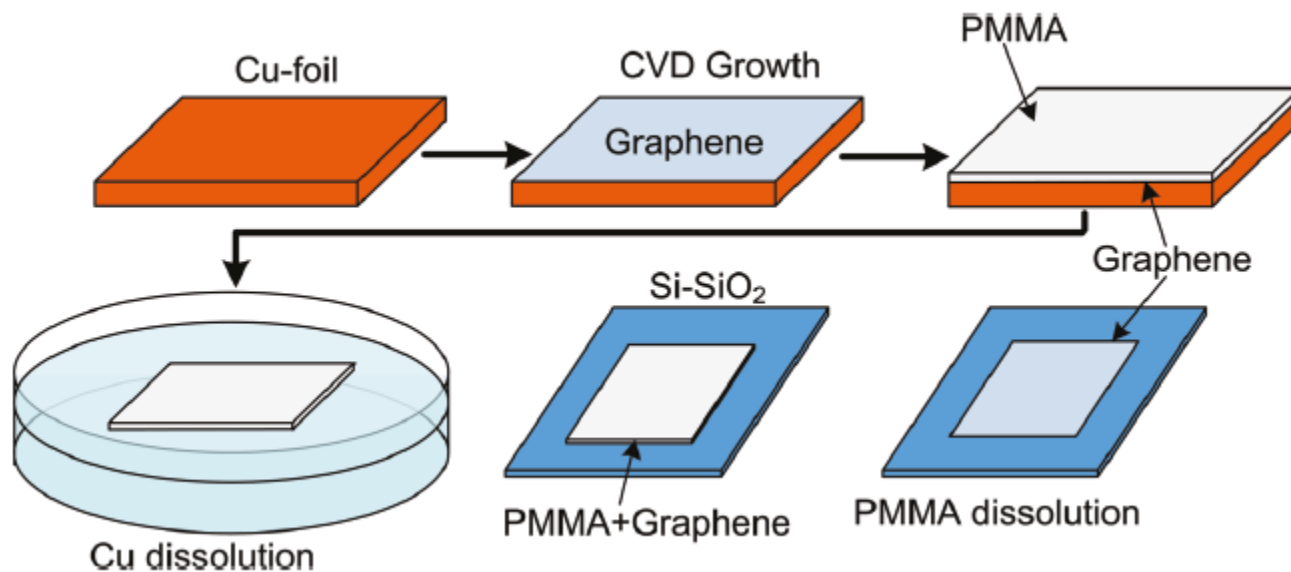
Flame Synthesis of Graphene on Substrates



Flame Synthesis

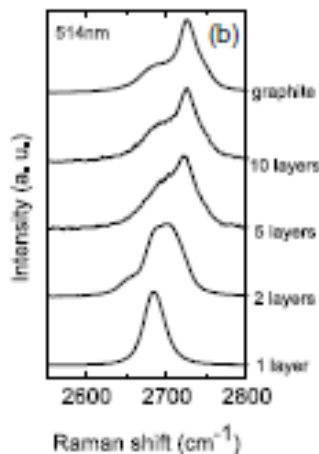
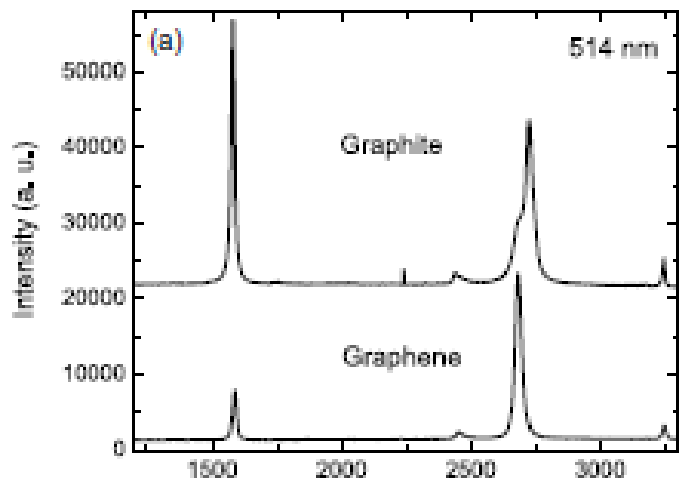


Graphene Transfer

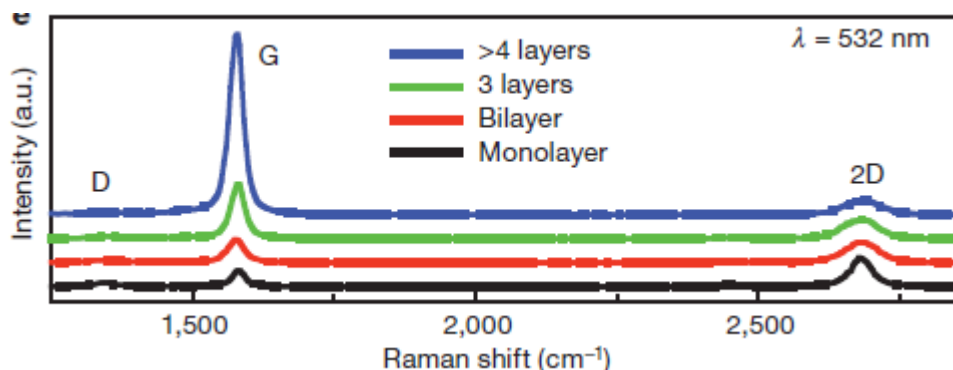


Srivastava A et. al. Chemistry of Materials 2010.

Raman Spectrum of Graphene



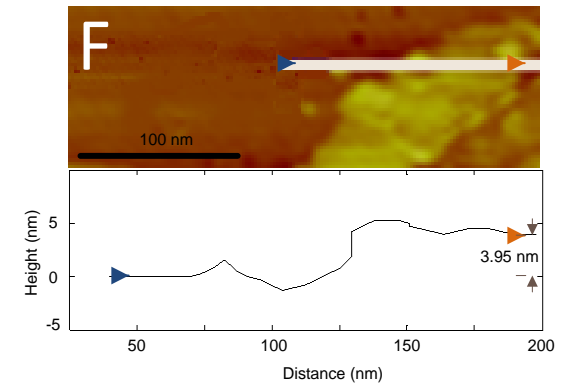
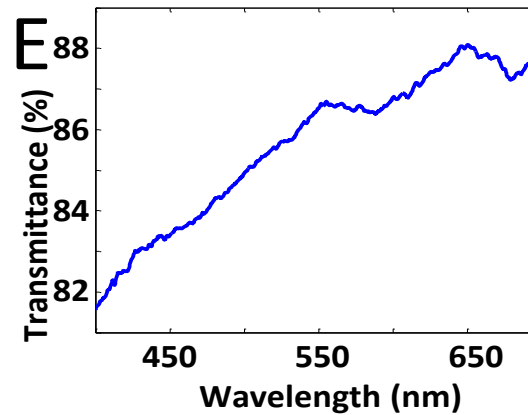
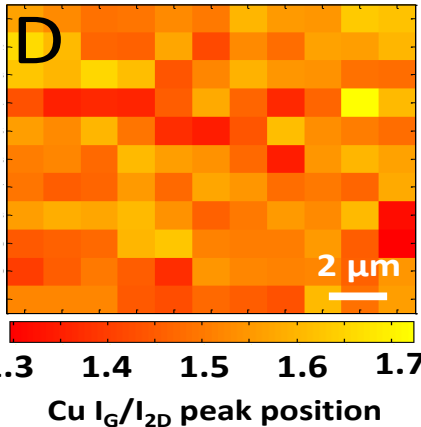
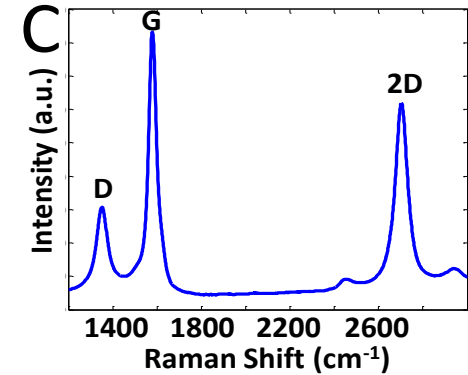
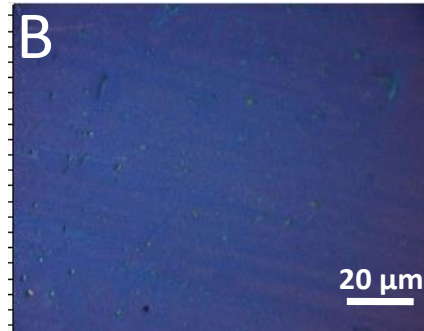
Ferrari, a; et al. *Physical Review Letters* **2006**, 97, 1-4.



Kim, K. S. et. al. *Nature* **2009**, 457, 706-10.

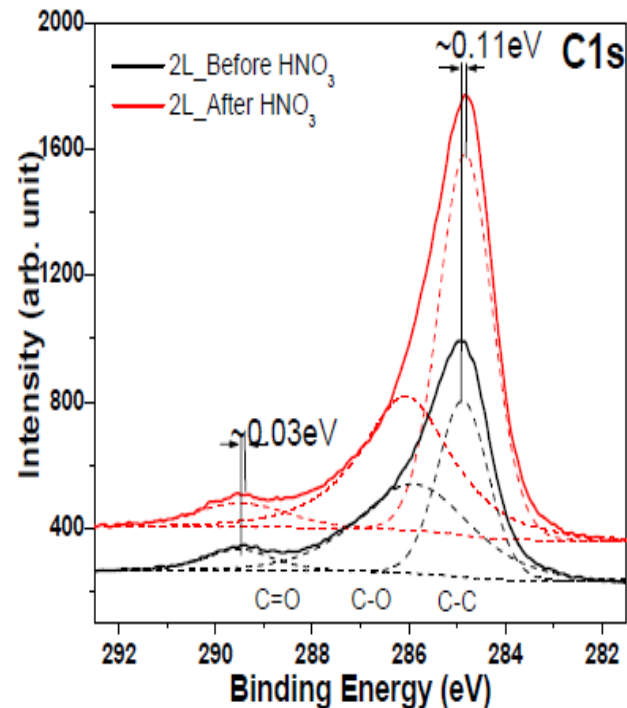
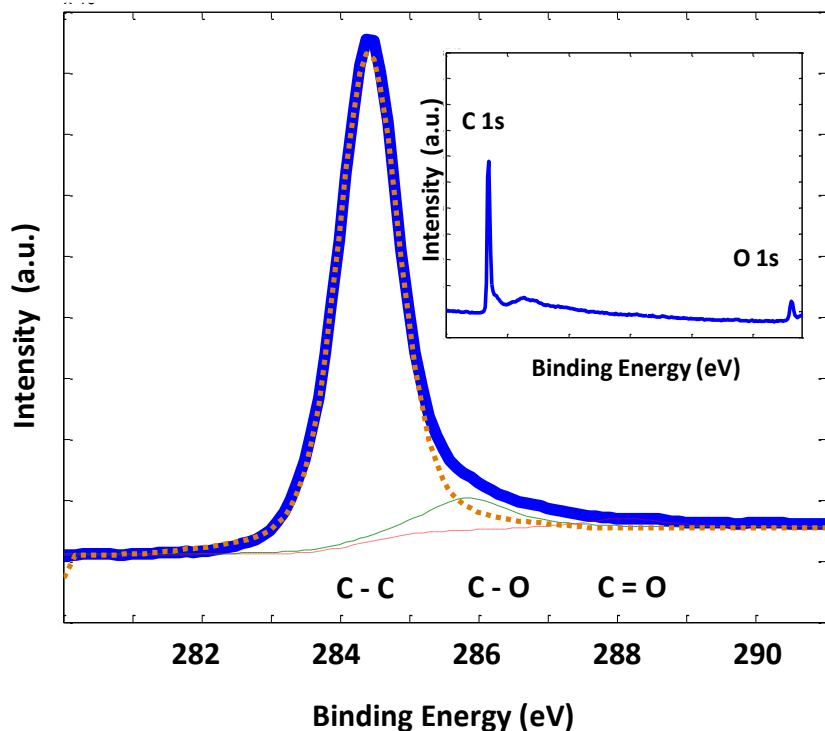
- D peak at 1351 cm^{-1} , which is due to the first-order zone boundary phonons and is used to determine the disorder present in the graphene
- G peak at 1580 cm^{-1} , which is related to the bond stretching of sp^2 bonded carbon atoms
- 2D peak at 2700 cm^{-1} , which is caused by the second-order zone boundary phonons
- Ratio between the intensities of the G peak (I_G) and the 2D peak (I_{2D}) provides an estimate of the number of layers
 - For mono and bi-layer graphene, this ratio is <1
 - If $>$ two layers are present, ratios ranging from 1.3 to 2.4 have been reported for FLG

Graphene Growth on Cu (950°C)



- I_G/I_{2D} peak provides an estimate of the number of layers
- FWHM of our 2D peak is 75 cm^{-1} , consistent with FLG grown at atmospheric pressure
- Transmittance (2.3% per layer) of our FLG films at 550 nm is 86%, correlating to 6 layers
- AFM: 4nm thickness \rightarrow 4-8 monolayers of graphene

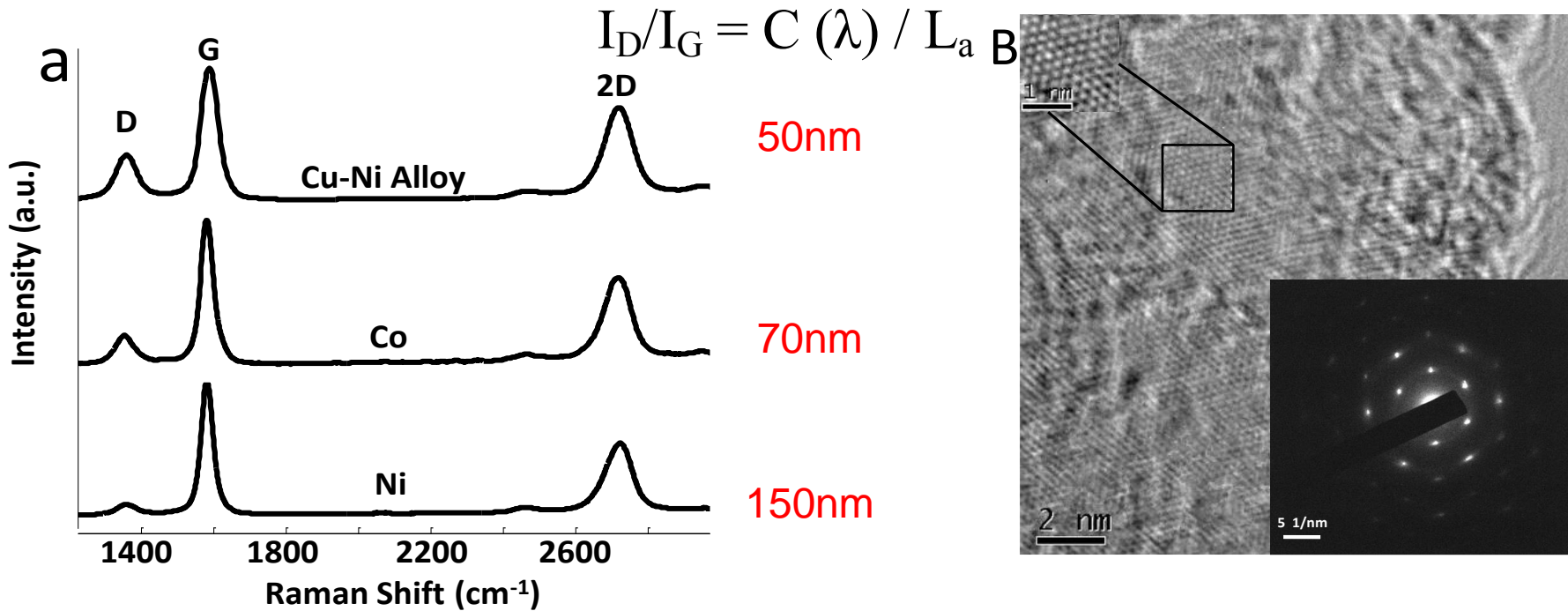
Graphene Growth on Cu – XPS



Bae, S.; et. al. *Nature Nanotechnology* 2010, 5, 1-5.

- H₂O product → at high temperatures can result in oxygen doping of graphene
- However, with abundant H₂ present in the post-flame species, and at relatively “low” growth temperatures (950C), such oxidation reactions are minimized
- XPS of the C 1s peak (main peak at 284.4 eV) indicates that most of the atoms are in the sp² C state
- Less than 10% of oxygen incorporation (e.g. CO) → less than that for CVD-grown

Graphene Growth on Ni, Co, Cu-Ni (850°C)



- I_D/I_G is used as a metric for the disorder present in the graphene, which develops from domain boundaries, wrinkles, edges, impurities, and other factors
- A lower D peak, compared to that for Cu (~45nm), is observed for all three substrates
- The relatively higher D peak for the Cu–Ni alloy is likely due to the presence of Cu, and to the increased role of a surface growth mechanism

Experimental setup

Open atmosphere

Top view

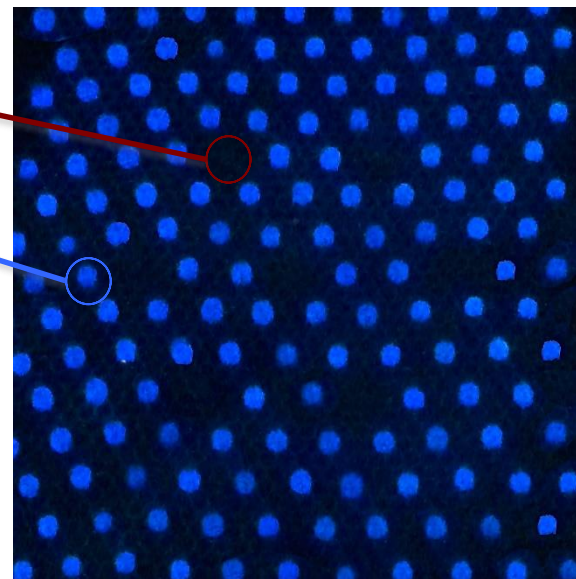
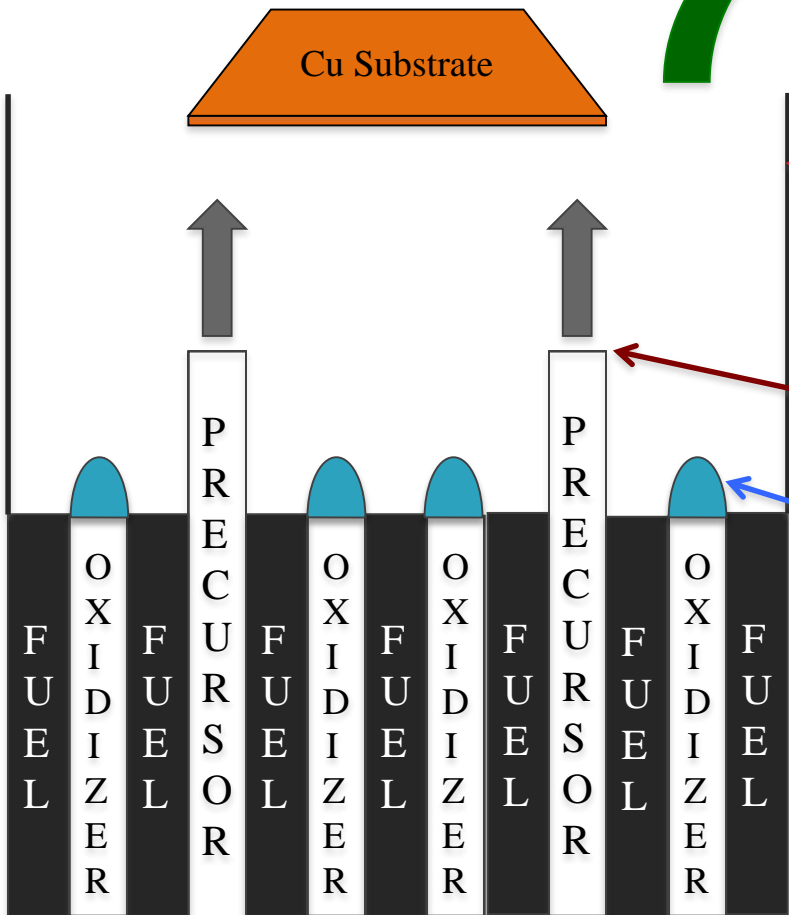
Cu Substrate

Quartz enclosure

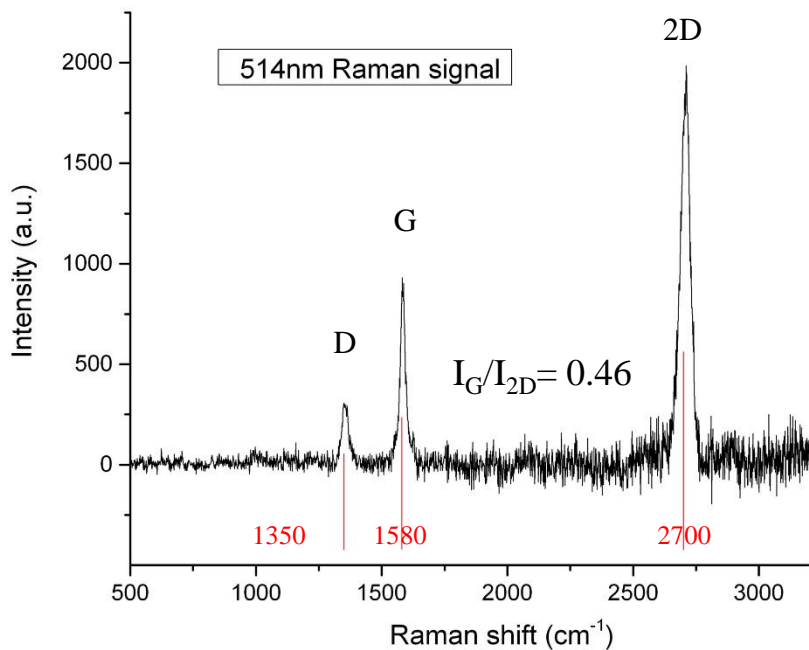
Pyrolysis Vapors

Hydrogen flame

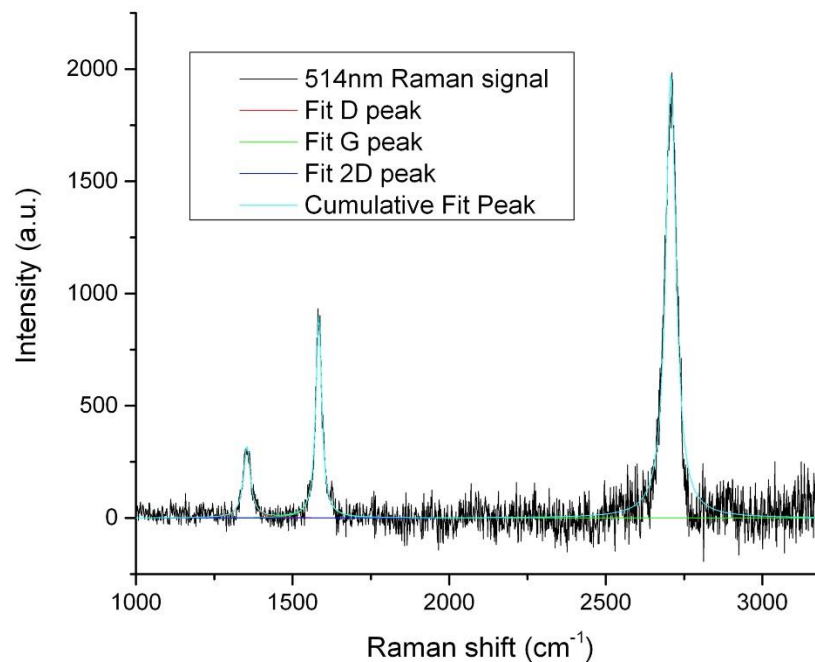
Photograph of multiple inverse-diffusional-flame



Characterization of Monolayer graphene films



$$I_G/I_{2D} = 0.5$$



2D peak up-shifted 7 cm^{-1} and its FWHM = 39 cm^{-1}

The slight up-shift of 2D peak is caused by a small percentage of Bilayer films.



Characterization and Continuous Automation of an Environmentally Green Primer

Tasks for Paste-Like Material

- Rheology
 - Designed device for rheology measurement
 - Study on placebo materials Device for filled weight study
 - Designed device to fill cups and study weight variability
 - » First generation device (non energetics) was machined and studied
 - » Energetics filling device was machined and transferred
 - » Dosating study on placebo materials completed
- Modeling
 - Implemented modeling method using DEM

Task for Slurry Materials

- Rheology
 - Implemented technique for rheology measurement
 - Started study on placebo materials
- Device for filled weight study
 - Designed device to fill cups and study weight variability
 - » Device was transferred
 - » Study on placebo materials
- Modeling
 - Implemented modeling method using CFD software

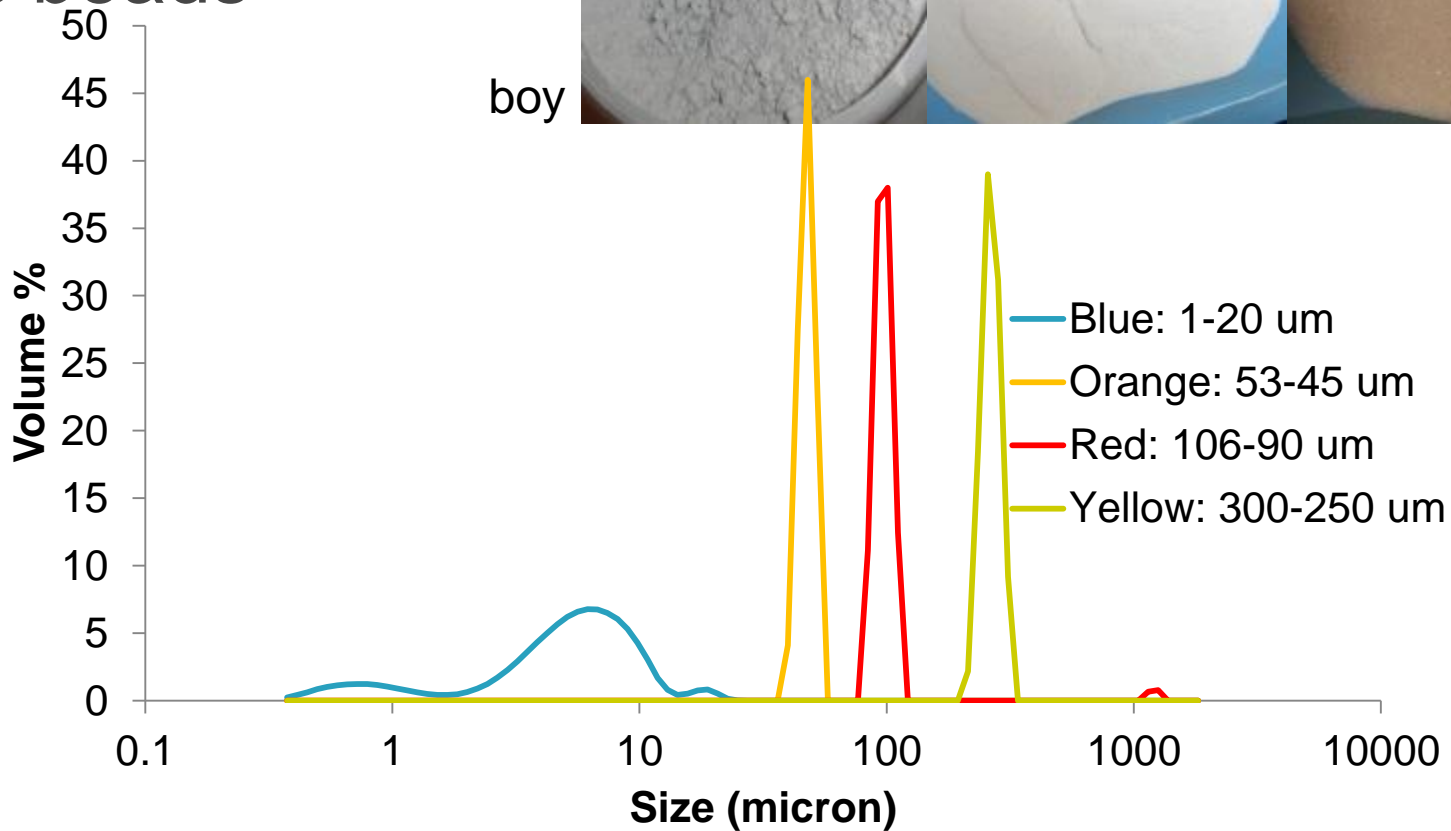
Characterization of Pastes/Wet Powders

- *GOAL: To find a placebo material that behaves similarly to energetic material by matching packing behavior*
- Placebo characterization was performed on a small scale (20-100mg) and a larger scale (4-20g)
- Small scale compressibility experiments were performed at Rutgers and at Picatinny using sister devices (ARES and RDA-III)
- A novel small scale attachment was designed by Rutgers and machined to perform compressibility tests on the ARES and RDA-III
- Compressibility testing of live material was performed on the Picatinny RDA-III

Characterization of Pastes/Wet Powders

- Larger scale placebo characterization was performed at Rutgers using a Freeman FT4 Powder Rheometer
- Compressibility results obtained by the ARES and RDA-III were compared to FT4 results to validate the novel cup and piston design
- Using the FT4, several characterization methods were implemented to test the flow and packing properties of placebo material: Compressibility, Permeability, Flow Energy, Shear

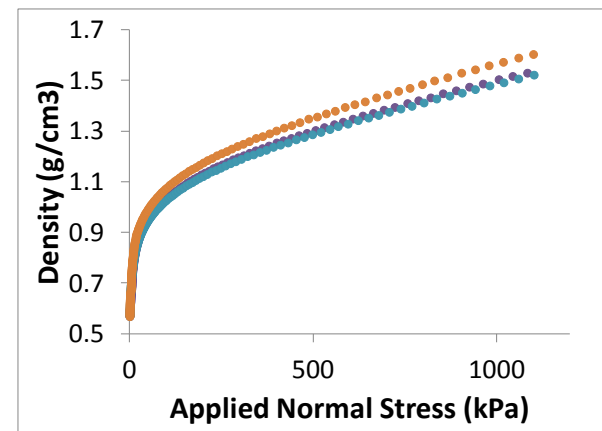
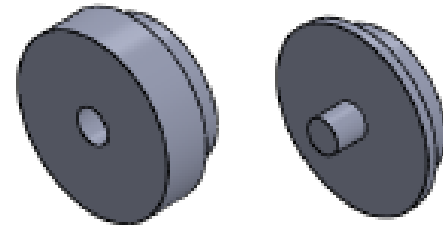
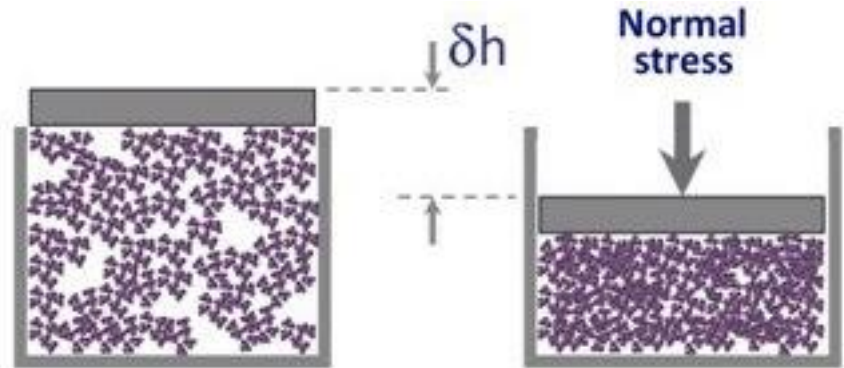
Placebo Glass beads



	Blue: 1-20 μm	Orange: 53-45 μm	Red: 106-90 μm	Yellow: 300-250 μm
d_{10} (μm)	1	45	91	244
d_{50} (μm)	6	50	102	276
d_{90} (μm)	11	55	114	309

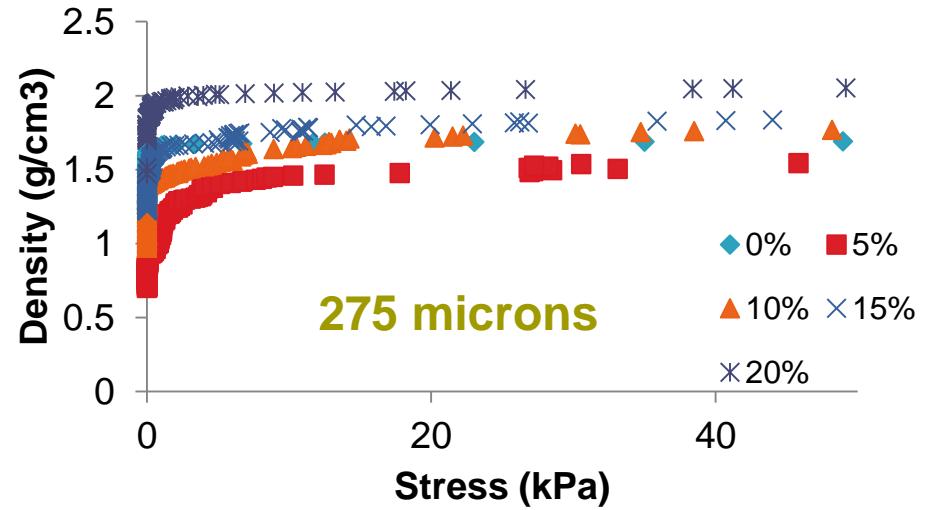
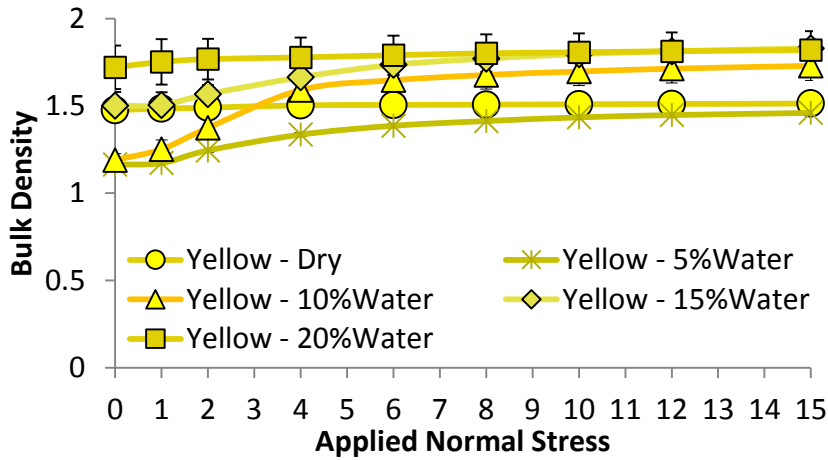
Compressibility

- Measures cohesion by relating it to the amount of entrapped air
- Technique shows general correlation to particle size and therefore cohesion, but some exceptions exist
- Commercial equipment use vessels ranging from 10 to 85mL
- We have developed a test that uses ~30mg of material
 - Cup size is 5mm in diameter and 1.5 – 5mm in depth
- Procedure:
 - Sample is loaded into vessel
 - Piston is lowered at a constant rate of 0.005mm/s
 - The vertical position of and the force exerted on the piston is recorded in time
 - The density of the powder bed as a function of applied normal stress is calculated

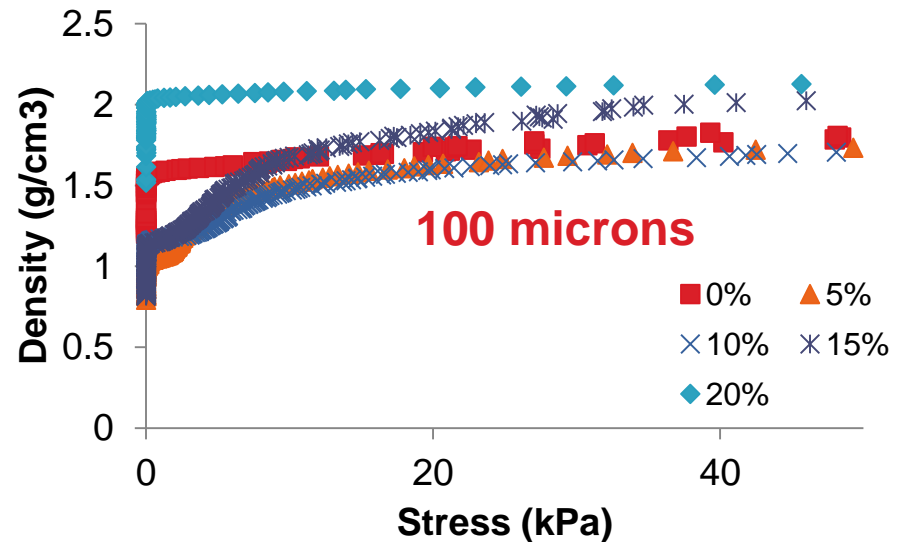
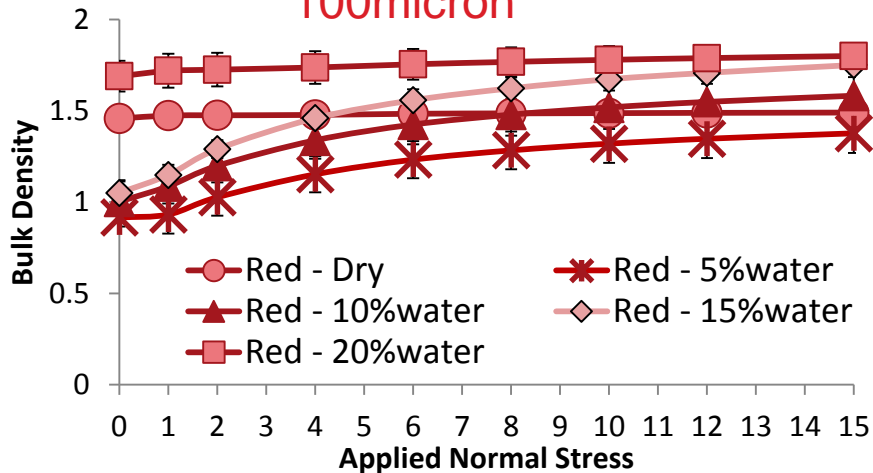


Compressibility: FT4 vs Small Scale Cup and Piston

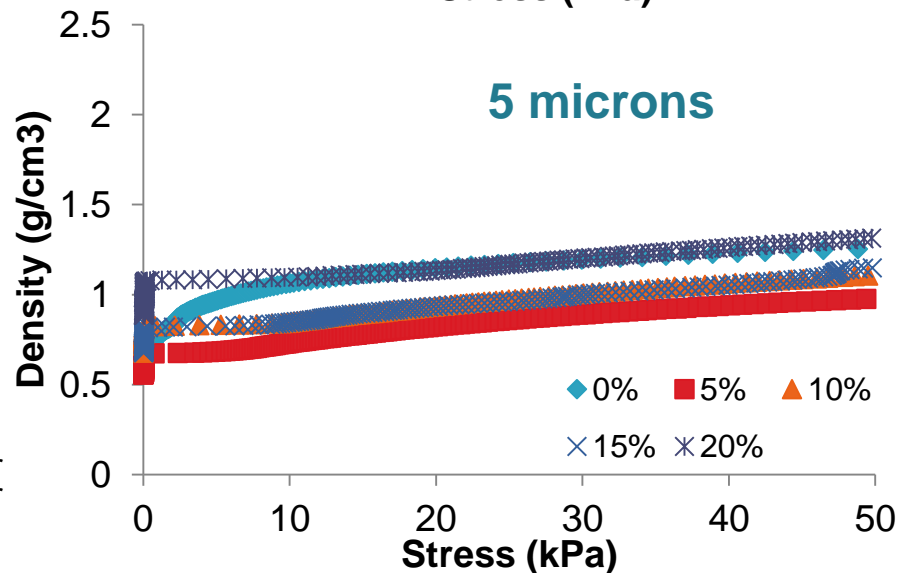
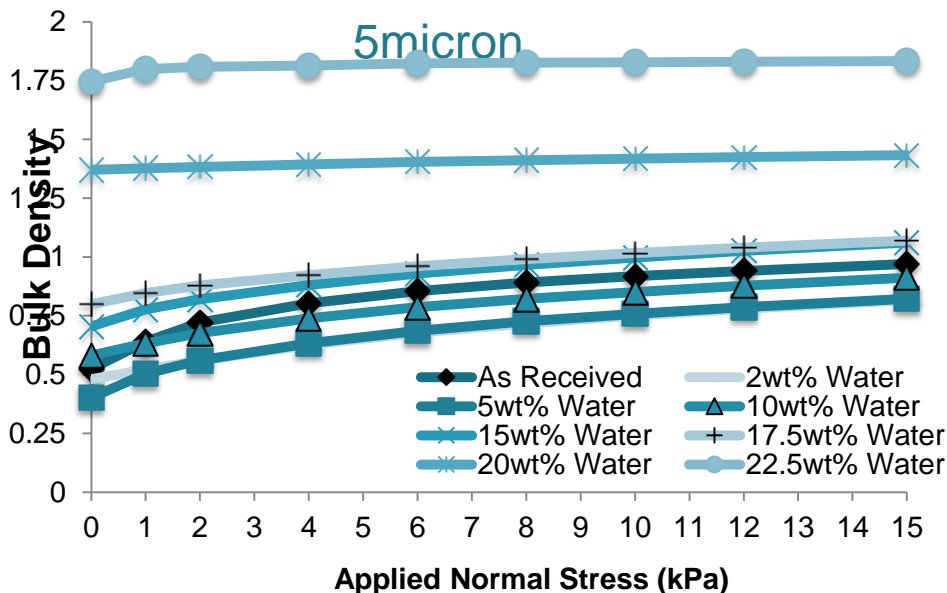
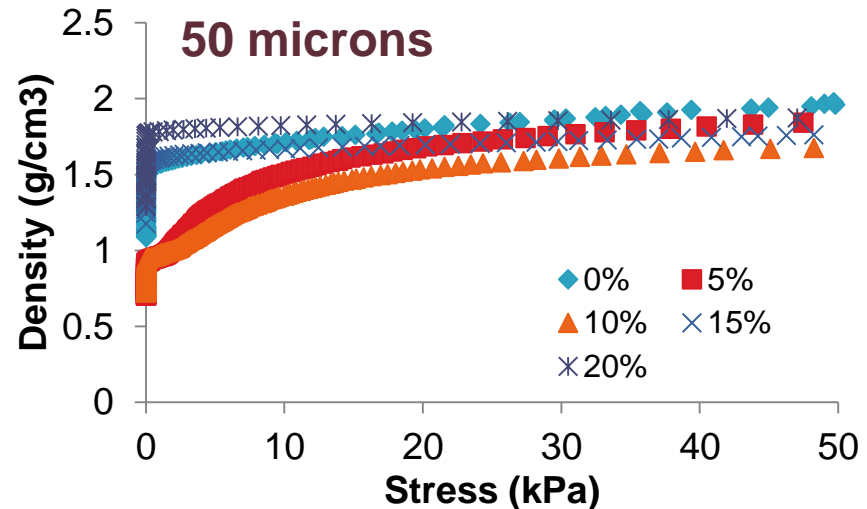
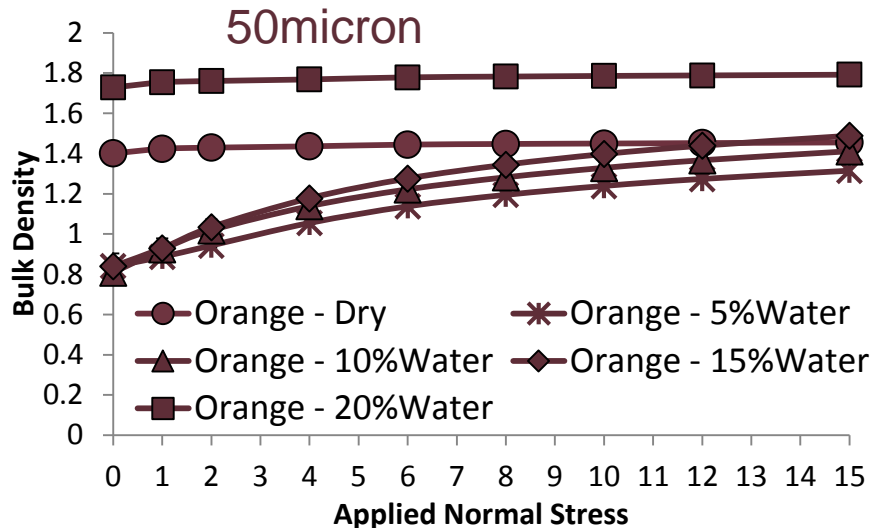
275micron



100micron

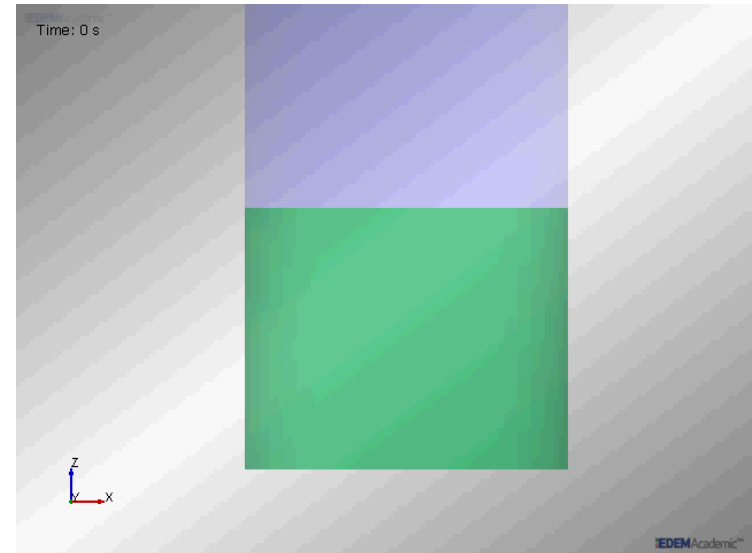
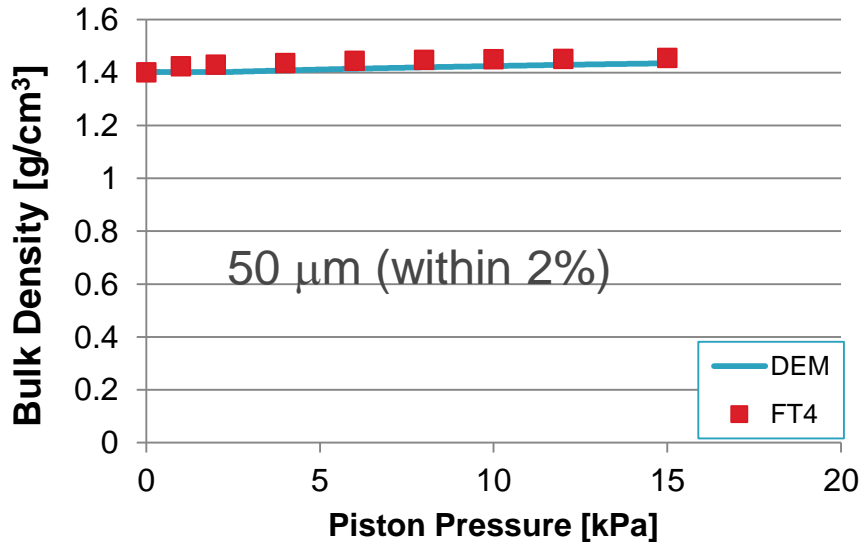
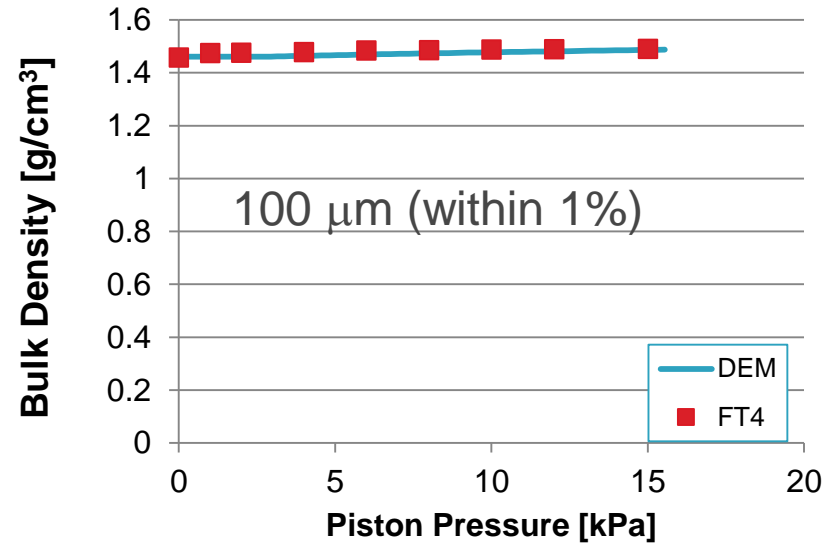
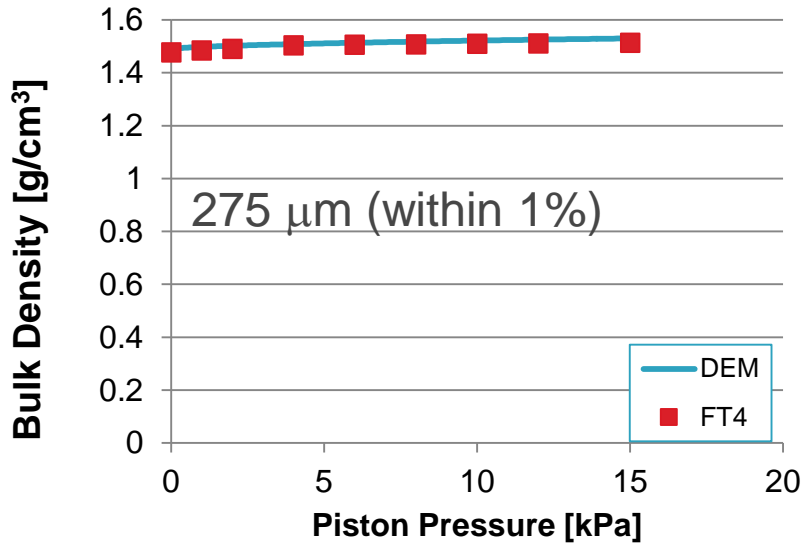


Compressibility: FT4 vs Small Scale Cup and Piston

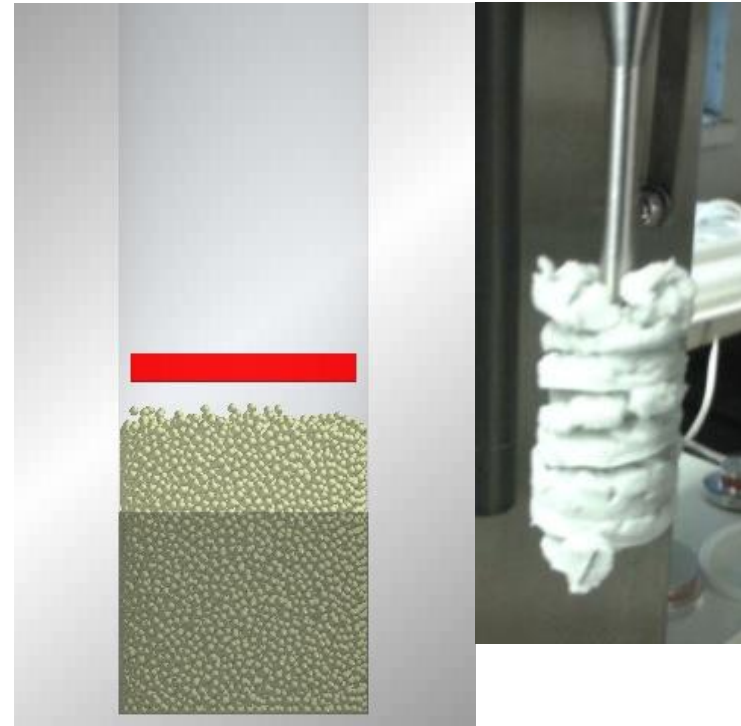
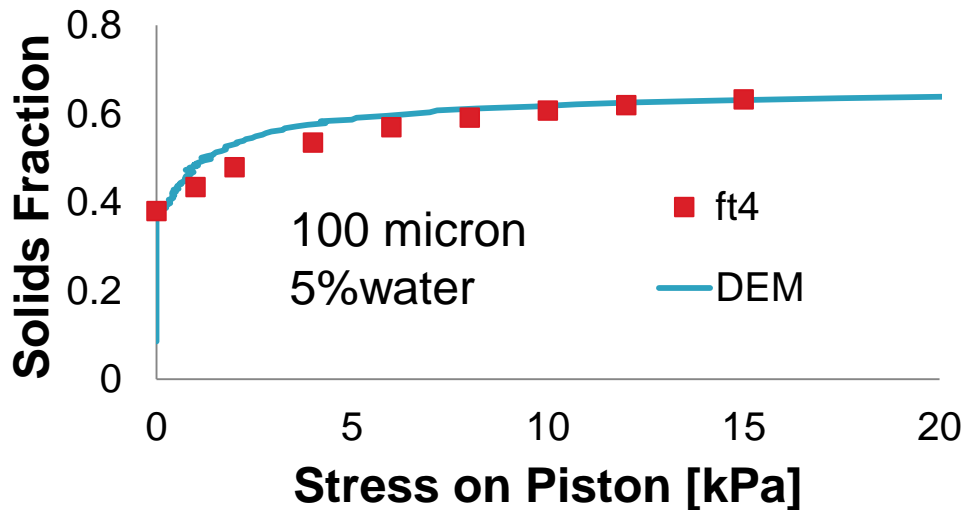
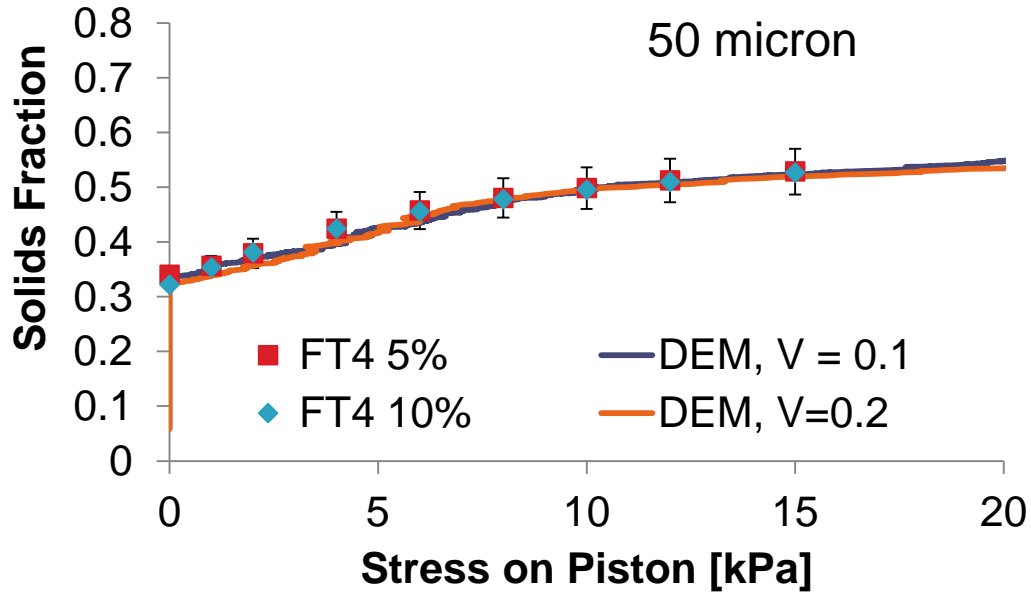


EDEM Simulations – Dry Beads

Matching Compressibility Data



EDEM Simulations – Dry Beads Matching Compressibility Data



Remarks

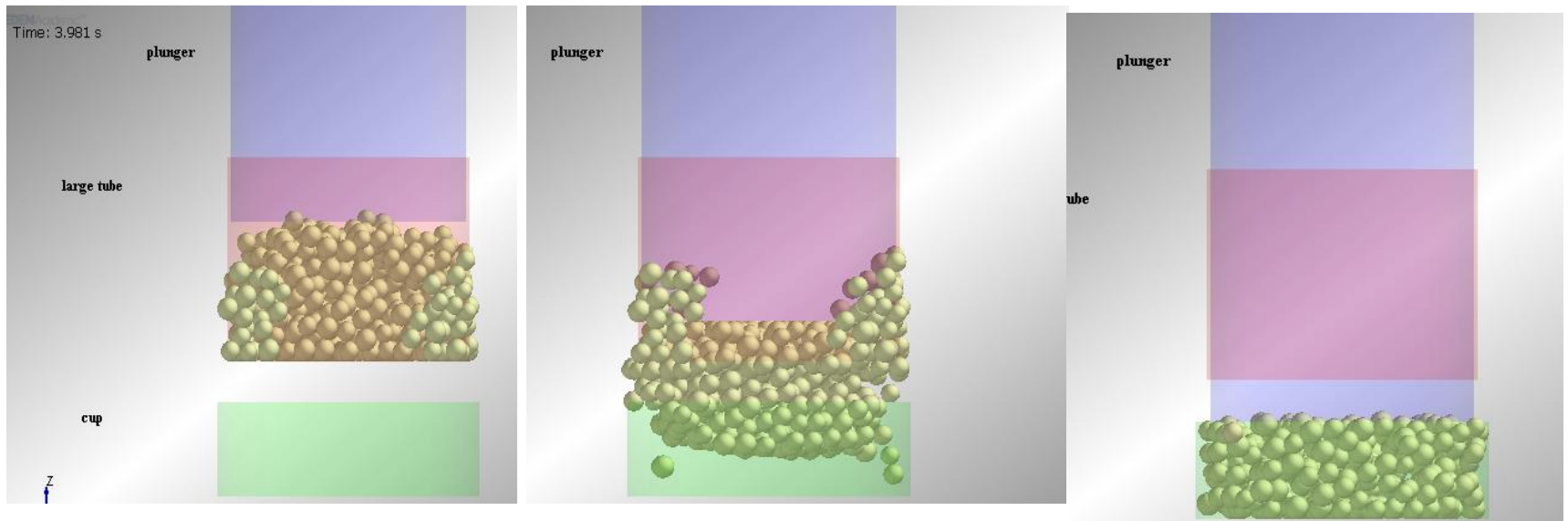
- The compressibility tests on the novel cup and piston devices show that the live material match well with multiple placebos
- Cup filling with live material will be performed at Picatinny
- Cup filling experiments at Rutgers will be carried out with the placebo material
- Simulations show comparable compressibility results and will be used to perform cup filling simulations



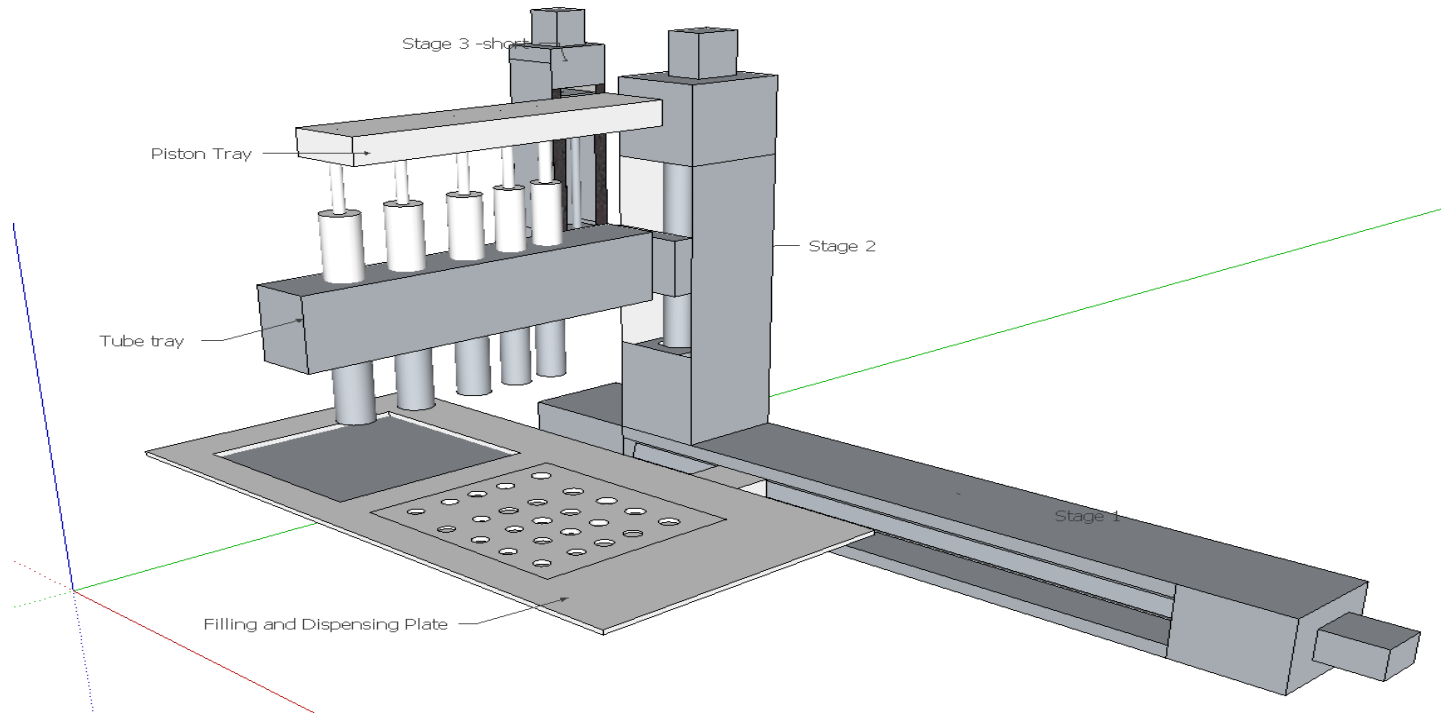
PASTE CUP FILLING

EDEM of Dosating

A model created with DEM that pushes the collected particles out of the nozzle (rose colored) by a plungers (purple) into a cup (green). The progression of the plunger pushing the sample out of the tube and into the cup can be seen from left to right for each tube size.



Placebo Cup Filling Device

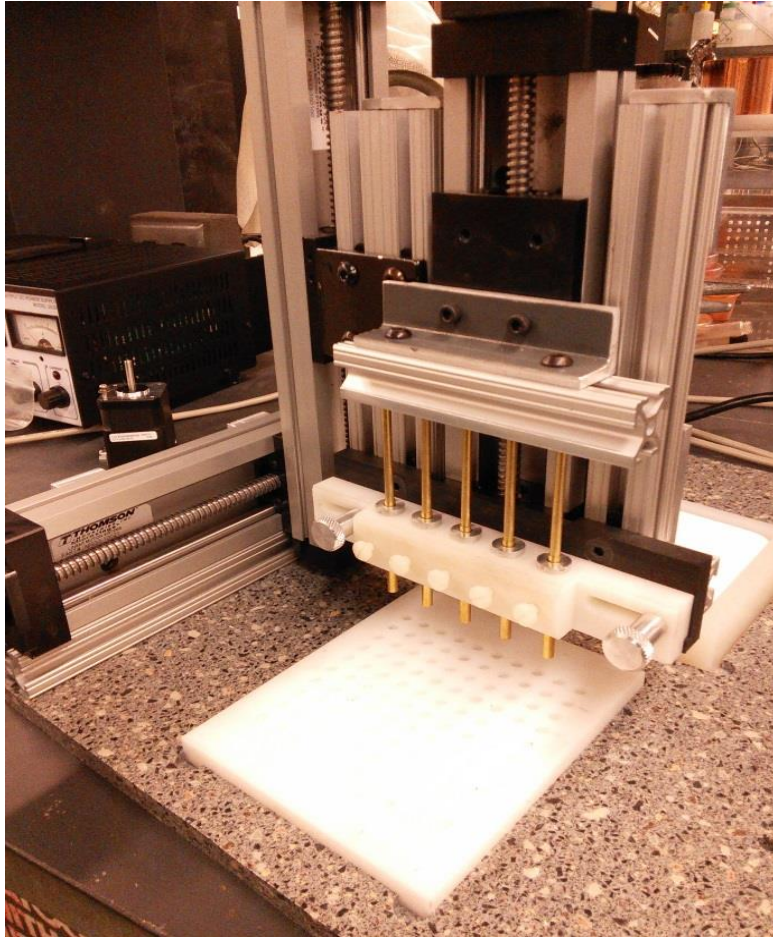


Manual tests proved feasibility.

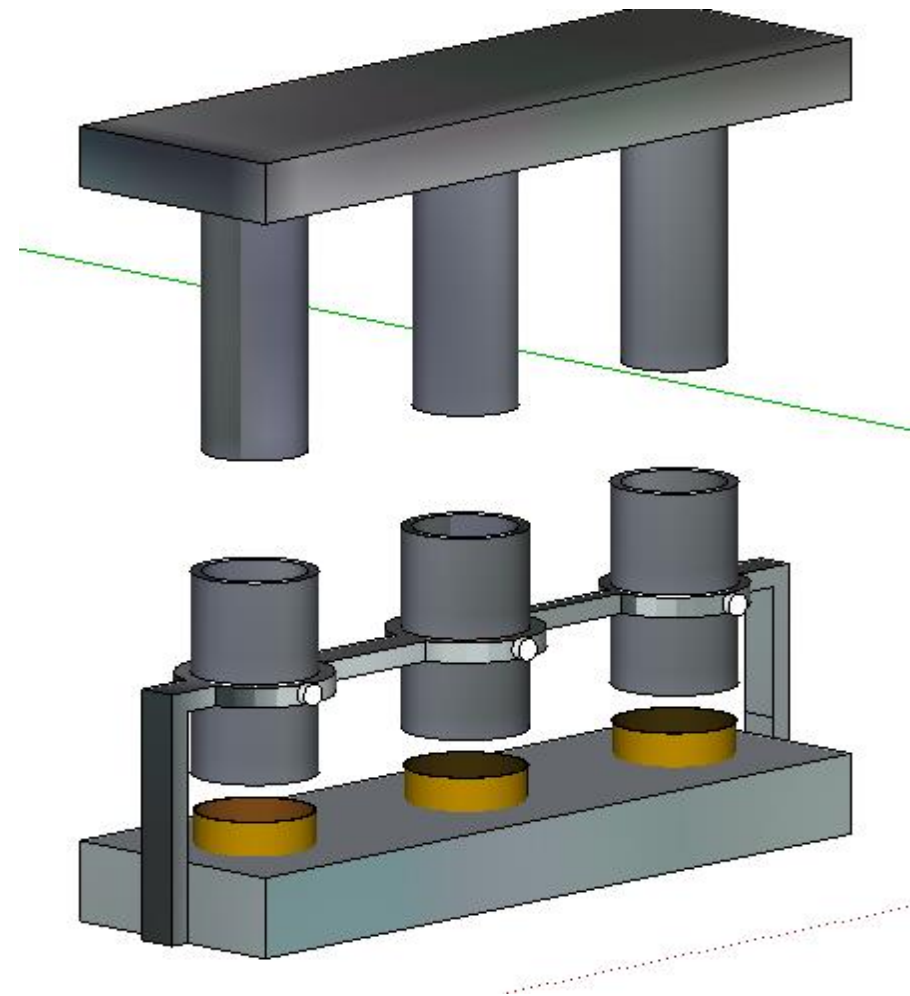
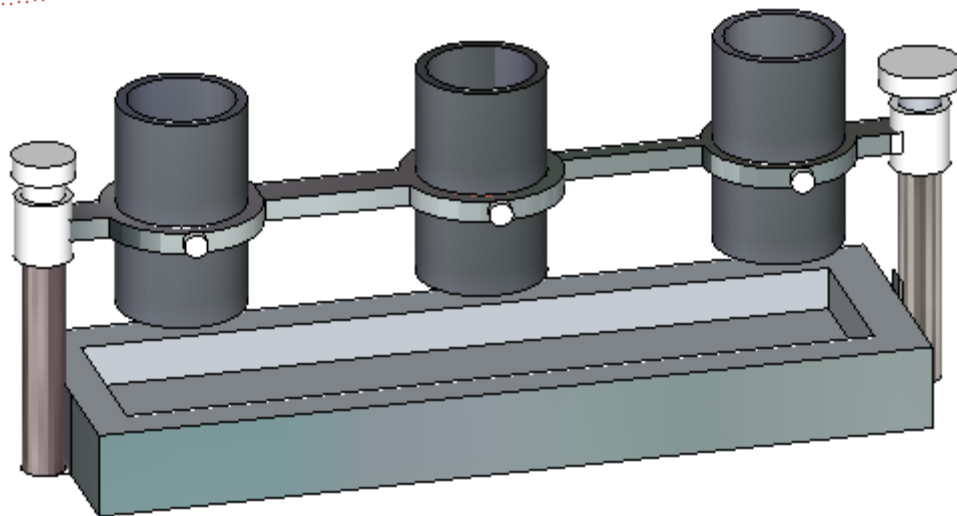
Able to fill 5 cups at a time and up to 100 cups.

Variability will depend heavily on the material properties.

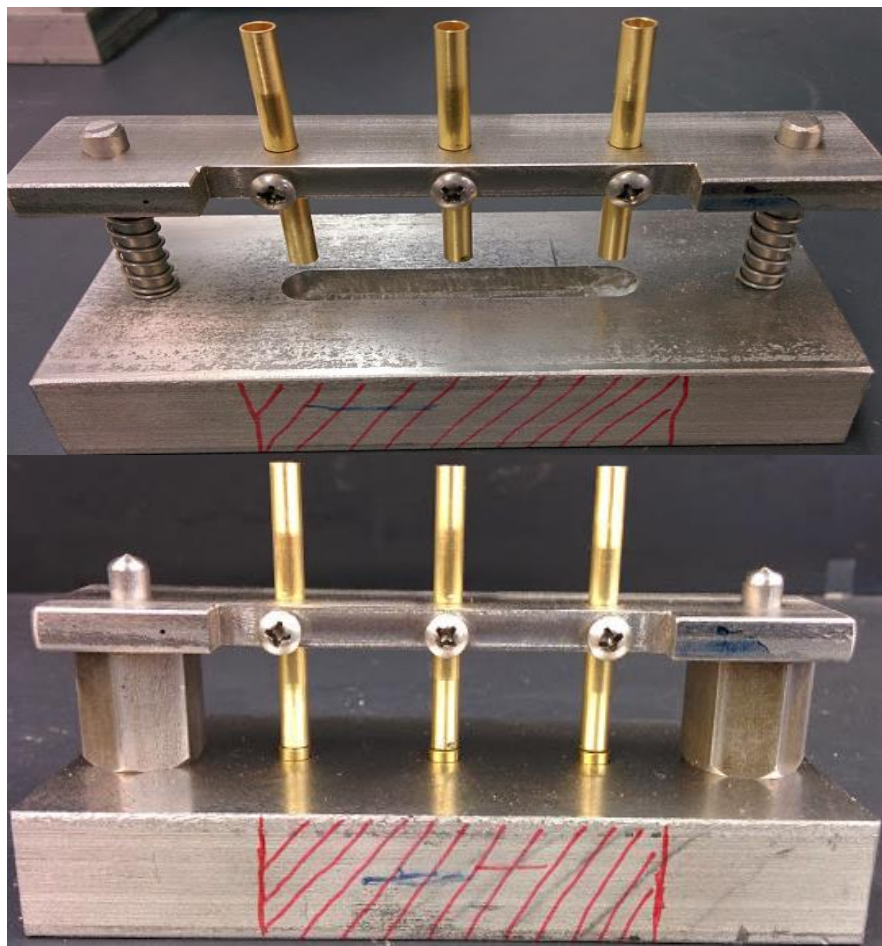
Machined dosating device



Energetic Cup Filling Device



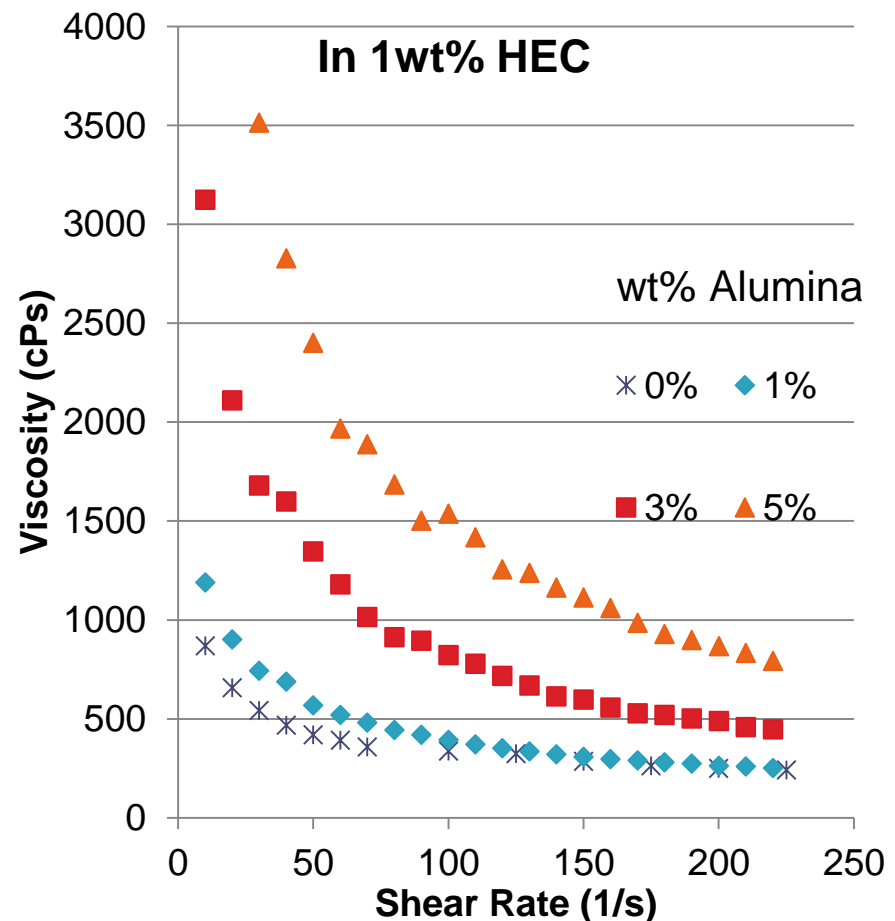
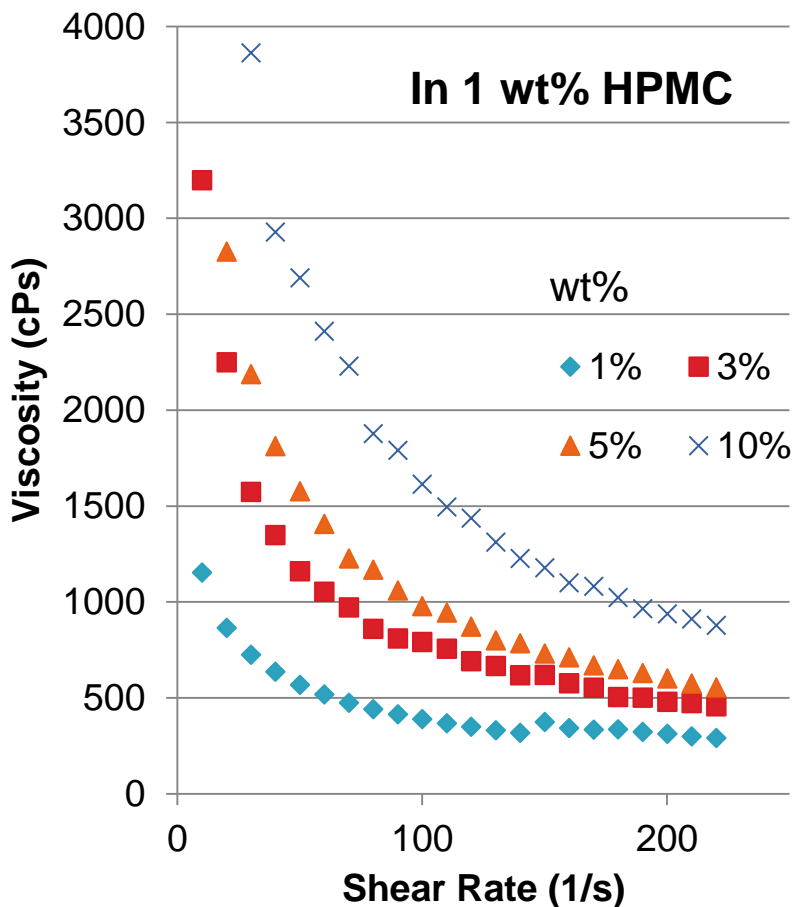
Small Scale Dosing Device



Slurry Rheology

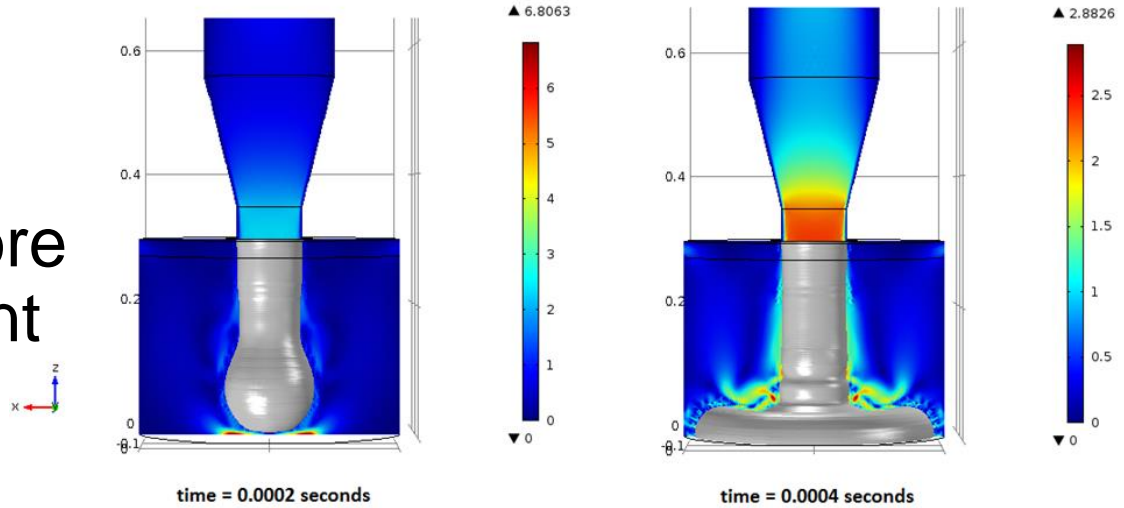
- Placebo viscosity was obtained using low and high viscosity Brookfield DV-III Rheometers
- ARES Rheometer was used to obtain viscosity measurements for MIC
- Contact angle and density were also obtained
- Using these properties, simulations can more accurately represent the system

Placebo Study: Effect of Nano-sized Alumina Loading on Polymer Solutions

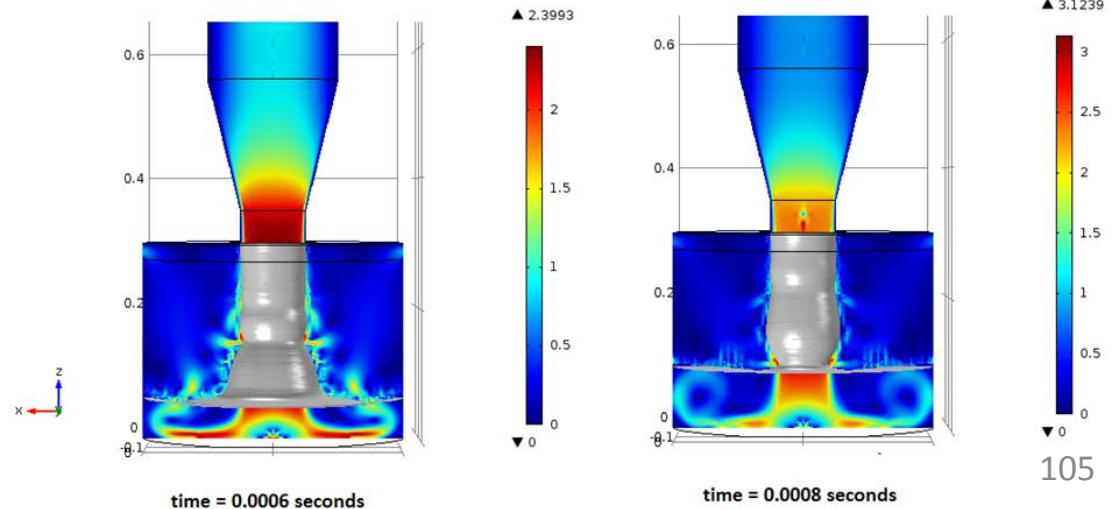


Slurry Cup Filling Simulations

- Using these properties, simulations can more accurately represent the system



- Slurry simulation velocity magnitude (m/s) (colors) and surface of slurry (gray).



Remarks

- Rutgers will be performing cup filling experiments with placebos
- MIC cup filling to be performed by Picatinny
- Cup filling of MIC has been successfully performed by Innovative Materials and Processes (IMP)

Acknowledgements

- Post-docs
 - Gang Xiong (synthesis, laser diagnostics)
 - Zhizhong Dong (nanowire, nanoparticle synthesis)
 - James Scicolone (green primer automation)
- Graduate students
 - Chris Stout (nanoparticle synthesis)
 - Hua Hong (graphene synthesis)
 - Bill Mozet (PLD)
 - Michelle Lee (MD simulations)
- Collaborators
 - Keivan Esfarjani
- Funding
 - National Science Foundation
 - Army Research Office
 - U.S. Army
 - DARPA
 - Office of Naval Research